AD-762 376

SELECTED MATERIAL FROM SOVIET TECHNICAL LITERATURE, MARCH 1973

Stuart G. Hibben

Informatics, Incorporated

Prepared for:

Air Force Office of Scientific Research
Advanced Research Projects Agency

22 May 1973

Informatics Inc

UNCLASSIFIED
Security Classification

DOCUMENT CONTROL DATA - R & D

(Security classification of title, body of abstract and indexing annotation must be entered when the overall report is classified)

1. ORIGINATING ACTIVITY (Corporate author)
Informatics Inc.
6000 Executive Boulevard
Rockville, Maryland 20852

2a. REPORT SECURITY CLASSIFICATION
UNCLASSIFIED

2b. GROUP

3. REPORT TITLE
Selected Material from Soviet Technical Literature, March 1973

4. DESCRIPTIVE NOTES (Type of report and inclusive dates)
Scientific . . . Interim

5. AUTHOR(S) (First name, middle initial, last name)
Stuart G. Hibben

6. REPORT DATE
May 22, 1973

7a. TOTAL NO. OF PAGES
196 201

7b. NO. OF REFS

8a. CONTRACT OR GRANT NO
F44620-72-C-0053, P00001

b. PROJECT NO.
1622-4

c.

d. 62701E3F10

9a. ORIGINATOR'S REPORT NUMBER(S)

9b. OTHER REPORT NO(S) (Any other numbers that may be assigned this report)
AFOSR - TR - 73 - 1041

10. DISTRIBUTION STATEMENT
Approved for public release; distribution unlimited.

11. SUPPLEMENTARY NOTES
Tech. Other

Details of illustrations in this document may be better studied on microfiche.

12. SPONSORING MILITARY ACTIVITY
Air Force Office of Scientific Research
1400 Wilson Boulevard
Arlington, Virginia 22209

13. ABSTRACT

This report includes abstracts and bibliographic lists on contractual subjects that were completed in March 1973. The major topics are laser technology, effects of strong explosions, geosciences, particle beams and material sciences. A section on miscellaneous interest is also included. A report on a Soviet tunneling rocket was published separately as the March optional topic.

Laser coverage is generally limited to high power effects. All current laser material is routinely entered in the quarterly laser bibliographies.

An index identifying source abbreviations and a first-author index to the abstracts are appended.

DD FORM 1 NOV 68 1473

UNCLASSIFIED
Security Classification

SELECTED MATERIAL
FROM
SOVIET TECHNICAL LITERATURE

March 1973

Sponsored by

Advanced Research Projects Agency

ARPA Order No. 1622-4

May 22, 1973

ARPA Order No. 1622-4
Program Code No: 62701F3F10
Name of Contractor:
Informatics Inc.
Effective Date of Contract:
January 1, 1973
Contract Expiration Date:
December 31, 1973
Amount of Contract: $343,363

Contract No. F44620-72-C-0053, P00001
Principal Investigator:
Stuart G. Hibben
Tel: (301) 770-3000 or
(301) 779-2850
Program Manager:
Klaus Liebhold
Tel: (301) 770-3000
Short Title of Work:
"Soviet Technical Selections"

This research was supported by the Advanced Research Projects Agency of the Department of Defense and was monitored by the Air Force Office of Scientific Research under Contract No. F44620-72-C-0053. The publication of this report does not constitute approval by any government organization or Informatics Inc. of the inferences, findings, and conclusions contained herein. It is published solely for the exchange and stimulation of ideas.

informatics inc
Systems and Services Company
6000 Executive Boulevard
Rockville, Maryland 20852
(301) 770-3000 Telex 89-521

INTRODUCTION

This report includes abstracts and bibliographic lists on contractual subjects that were completed in March 1973. The major topics are laser technology, effects of strong explosions, geosciences, particle beams and material sciences. A section on miscellaneous interest is also included. A report on a Soviet tunneling rocket was published separately as the March optional topic.

Laser coverage is generally limited to high power effects. All current laser material is routinely entered in the quarterly laser bibliographies.

An index identifying source abbreviations and a first-author index to the abstracts are appended.

TABLE OF CONTENTS

I. Laser Technology

A. Abstracts

Aliyev, Yu. M., O. M. Gradov, and A. Yu. Kiriy. Anomalous dissipation of powerful electromagnetic radiation and its penetration of confined plasma. ZhETF P, v. 17, no. 3, 1973, 177-179.

Stationary penetration of semi-confined plasma ($z > 0$) by a transverse electromagnetic wave is analyzed with allowance for interaction of the excited longitudinal oscillations with the inhomogeneous pumping field. Normal incidence of the transverse wave is considered, the frequency ω_o of which is close to that of the plasma (ω_p). A powerful electromagnetic field of the incident wave promotes parametric interaction of the plasma with ion-acoustic oscillations. Energy of the applied field is de-localized by the parametrically increasing plasma and ion-acoustic noises and converted to energy of longitudinal noise. Thus, the amplitude $E_o(z)$ of the transverse wave decreases with increasing distance from the parametric interaction region. The distance at which energy fluxes of the applied field and longitudinal noises are equalized determines the region of applied field localization. Accordingly, depth L of penetration by the pumping wave is given by

$$L = \frac{1}{2\kappa} \ln(S^{tr}/S^{l}), \quad S^{tr} > S^{l} \quad . \qquad (1),$$

where K is the maximum value of the increment $K_2''(\omega, k_{||})$ of parametric increase of ion-acoustic and plasma waves, $S^{tr} = k_o c^2 E_o^2 / 4\pi\omega_o$ and S^l are the energy fluxes of the transverse and Langmuir oscillations in the plasma, respectively, and $k_o = \frac{1}{c}\sqrt{\omega_o^2 - \omega_p^2}$. The formula for k is derived by solving a dispersion equation for $k_z = k_z'(\omega, k_{||}) - ik_2''(\omega, k_{||})$, where $k_{||}$ is the projection of the wave vector at the plasma boundary.

The flux S^{ℓ} is expressed as a function of the spectral energy density $W'' \approx T_e$ of plasma noise and the phase volume $\Delta^3 k$ of plasma oscillations in the $k_2 \approx k$ region. The effective conductivity σ_{eff} and collision frequency ν_{eff} corresponding to L of Eq. (1) are expressed by

$$\sigma_{eff} = \frac{\nu_{eff}}{4\pi} = \frac{k_o c^2}{4\pi\omega_o L}. \qquad (2)$$

The σ_{eff} value which may be achieved under actual experimental conditions of plasma heating by a Nd glass laser is estimated for a hydrogen plasma with density $N_e = 10^{21}$ cm^{-3}, electron temperature $T_e = 16$ keV, and $T_e/T_i \geq 12$. The laser parameters are given as $\omega_o = 1.78 \times 10^{15}$ sec^{-1} and $E_o \leq 6 \times 10^8$ v/cm. In this case, using (2) and the expressions for k and S^{ℓ}, the formula

$$\nu_{eff}/\nu_{ei} \approx 5 \cdot 10^{-6} E_o \qquad (3)$$

is obtained.

Sukhorukov, A. P., S. Ya. Fel'd, A. M. Khachatryan, and E. N. Shumilov. Stationary thermal self-focusing of laser beams. IN: Kvantovaya elektronika, no. 8, 1972, 53-60.

Thermal self-focusing of a continuous laser beam in nonlinear medium is analyzed under assumptions of geometrical optics, i.e., without allowance for diffraction. Ray propagation is described by the

equation

$$d^2f_r/(dz^2) = -\alpha \exp(-\alpha z)/|R_{нл}(r_0) f_r|, \qquad (1)$$

where $f_r = r/r_0$ is the relative ray separation from the beam axis Z, r_0 is the initial ray coordinate, α is the linear absorption coefficient, and

$$R_{нл}(r_0) = 2n_0\varkappa/|(dn/dT)\,\tilde{I}_0(r_0)| \qquad (2)$$

is the characteristic of nonlinear refraction intensity. Eq. (2) shows that $R_{НЛ}(r_0)$ is a function of the coefficient $\varkappa$ of thermal conductivity and the mean intensity in the beam guide $\tilde{I}(r_0) = P_0(r_0)/(\pi r_0^2)$, where $P_0(r_0)$ is the initial power. Hence different rays exhibit different curvatures in a thermally self-focusing medium because of nonlinear refraction, with ultimate formation of an aberration image.

Solution of (1) for different absorption coefficient $\alpha R_{НЛ}$ values enables us to plot the spherical aberration images of an axisymmetric cylindrical beam (Fig. 1) and of a two-dimensional wave with a strongly prolate

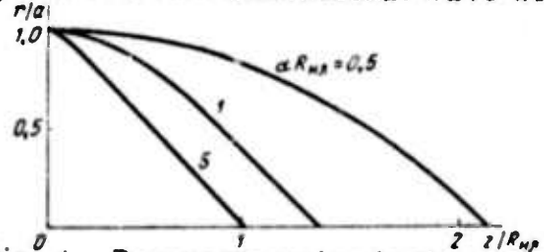

Fig. 1. Ray propagation in the case of self-focusing in media with different $\alpha R_{НЛ}$.

cross-section. Fig. 1 shows that, in the case of strong absorption ($\alpha R_{НЛ} \geq 1$), a relatively strong nonlinear refraction of rays occurs in the first layer only. Thus a strongly absorbing medium acts as a thin thermal lens with a focal length $R_{НЛ}(r_0)$. In a weakly absorbing medium ($\alpha R_{НЛ} \leq 1$), thermal self-focusing occurs over the entire nonlinear medium up to the focus ($0 < z < z_\phi$). Rays which are parallel at the medium boundary intersect the z axis at a distance

$z_\varphi = [\pi R_{H\Pi}(r_o)/\alpha]^{1/2}$. Spherical aberration images are shown in two particular cases of self-focusing: a Gaussian beam $I = I_o(0) \exp(-r_o^2/a^2)$ and a beam with intensity breakdown on the axis, $I_o = I_o(0)(r_o^4/a^4) \exp(-2r_o^2/a^2)$. The length of aberration field in the first case is comparable to that of self-focusing for a ray $r_o = a$ and rays intersect the z axis in different points. In the second case, the further the beam propagates in the medium, the thinner is the ring and the slower the contraction of its diameter.

In the case of two-dimensional wave aberrations, the beam contracts mainly along the small diameter. Qualitatively, the pattern of beam paths in a medium of arbitrary absorption is the same as that in the spherical aberrations system. Ray paths in media with $\alpha R_{H\Pi} \leq 1$ or $\alpha R_{H\Pi} \geq 1$ for the cylindrical beam and in a medium with arbitrary absorption of a two-dimensional wave can be described by formulas derived from (1).

Another type of aberration-astigmatism of a nonlinear thermal lens is analyzed for the near-axis part of the beam. This type of aberration is caused by the difference in curvature of the phase wavefront of a beam with elliptical cross-section. Assuming an invariable intensity profile, the authors show that a set of two differential equations describes the dimensionless beam radii (ellipse half-axes) $f_1(z)$ and $f_2(z)$. Introduction of the mean beam radius f into this set of equations gives a single equation

$$d^2f/(dz^2) = -\alpha \exp(-\alpha z)/(R_{H\Pi}f), \tag{3}$$

in the same form as (1). In the case of a beam parallel at the boundary entrance (the principal curvature radii of the initial wave front $R_1 = R_2 = \infty$), the elliptic cross-section in the first focal plane ($f_1 = 0$) becomes a straight line $2(a_2 - a_1)$ along the major axis a_2, and a straight line orthogonal to the first in the second focal plane ($f_2 = 0$). The elliptic cross-section of a beam with linear astigmatism ($R_1 \neq R_2$) can convert to a circular shape ahead of the

first focus. A detailed analysis is made of the optical field in the focal region, with allowance for diffraction. A correction is introduced into the equation of dimensionless width of a Gaussian beam in an aberration-free approximation. Owing to the fact that in this approximation nonlinear refraction of the beam is too high, $R_{НЛ}(a) \approx 2.3\ R_{НЛ}(0)$ is substituted for $R_{НЛ}(0)$ in the cited equation. Thus, the critical power of the beam self-channeling (f = 1) is increased by a factor of 2.3 relative to the aberration-free approximation. The Gaussian beam radius f and field axial intensity I were computed with the help of the corrected equation over a wide range of medium absorption αR_D and beam input power $R_D/R_{НЛ} = P_o/P_{cr}$, where R_D is the length of diffracted beam. A typical pattern of f and I variations in nonlinear medium (Fig. 2) shows positions of the first focus z_φ and the

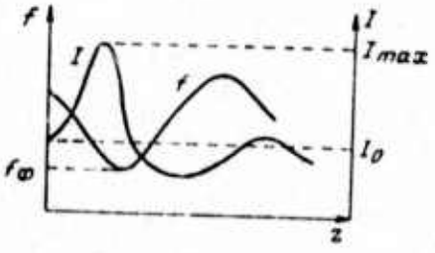

Fig. 2. Typical pattern of dimensionless beam width and beam axial intensity variations.

field intensity peak z_I.

Two criteria of self-focusing, namely beam contraction and field intensity gain, are analyzed using the cited equation of the Gaussian beam width. Interpolation of the computer data obtained for $\alpha R_D = 10^{-3}$, 1, and 5 gave the formula of the input power

$$P_0 = P_{кр}[1{,}73 + 2{,}16/(\alpha R_д)], \tag{4}$$

at which a beam contracts by half in a medium of arbitrary absorption. Eq. (4)

shows that maximum contraction (minimum f_φ) in the focus occurs for total absorption of P_o at a distance

$$z_\varphi = R_{пл}(1 + R_{пл}^2/R_д^2). \qquad (5)$$

The calculated f_φ plots (Fig. 3) show that f_φ in the focus decreases with the

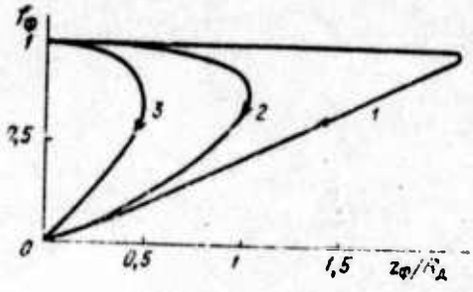

Fig. 3. Beam contraction f_φ in the focus versus its position z_φ/R_D for $\alpha R_D = 10^{-3}$ (1), 1 (2), and ≥ 1 (3). Arrows indicate directions of increase in input power.

increase in input power, while the focal point moves away from the medium boundary to a maximum distance $z_{\varphi\,max}$, which is longer in a weakly absorbing medium. Curve 3 represents a thin thermal lens. Computation of the intensity $I = \exp(-\alpha z)/f^2$ data gave the interpolation formula

$$P_0 = P_{кр}[0{,}26\alpha R_д + 2{,}17 + 1{,}44/(\alpha R_д)]. \qquad (6)$$

for a two-fold I gain ($I/I_o = 2$), which, in contrast to (4), gives $P_{o\,min} = 3.39$ P_{cr} for self-focusing in a medium with $\alpha R_D = 2.37$. The point $z_I = 0.6\ R_D$ and power extinction at that distance is $\eta = \exp(-\alpha z_I) = 0.25$.

Analysis of the incremental disturbance of the laser beam profile and phase front in a nonlinear medium indicates that the beam self-focuses faster than disturbance develops. Thus, stationary thermal self-focusing of sufficiently high-power beams proceeds without beam splitting into separate filaments, as it is the case in a locally nonlinear medium.

Baksht, R. B., Yu. I. Bychkov, and G. A. Mesyats. Feasibility of using the vapor formed on a target by a powerful electron beam as a medium for generating coherent radiation. Kvantovaya elektronika, no. 3, 1972, 89-90.

The authors propose an explosive emission technique for forming the vapor in a metal vapor laser, thereby avoiding the usual necessity of a high temperature system of vaporization. The method uses the multi-needle cathode developed by Mesyats as shown in Fig. 1, which on

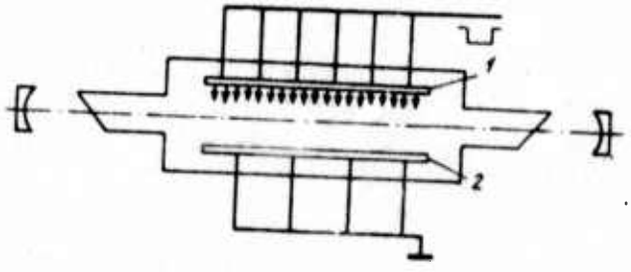

Fig. 1. Field emission technique for metal vaporization.

1 - cathode needles; 2 - anode

application of a high voltage pulse develops an extended high density current sufficient to vaporize a large area of anode surface over an interval of 1 or 2 μsec

Calculations and experiments show that the ionization of the resultant interelectrode vapor can lead to population inversion if optimum energy conditions are maintained.

The incident energy on the anode surface is given by $q = 3.67 \times 10^{-5} u_o^{5/2} d^{-2} \delta$ in w/cm^2, where u_o = diode voltage, d = diode spacing, and δ is a numerical factor on the order of unity. It is shown that an optimum q exists for given conditions, e.g. for u_o = 200-300 kv and d = 1-2 cm, q should be in the 10^7--10^8 w/cm^2 range; a higher density results in a less efficient vaporization in terms of input pulse energy.

Since the current rise time for the field emission discharge is relatively slow (10^9-10^{10} a/sec), it may be necessary to provide a fast-rise followup voltage pulse to the existing vapor region in order to obtain population inversion.

Kaliski, S. Conductive laser heating of nonhomogeneous plasma. Bulletin de l'Academie Polonaise des Sciences, serie des sciences techniques, v. 20, no. 12, 1972, 211 (963)-215 (967).

A simplified method of momentums, which was introduced by the author in the same periodical [v. 20, 1972, 1(35) and 7(41)] for spherical and cylindrical waves in single-temperature plasma, is extended to solution of the plane wave problem in a nonhomogeneous plasma heated by a laser. The method of solving averaged equations is based on assumption of the electron mechanism of heat conduction and disregards, in a first approximation, the fusion energy recovered. It is shown that the general

solution obtained by the simplified method describes weak inhomogeneities more realistically than the solution obtained by the classical method of momentums. In addition, a closed form solution was derived for linear inhomogeneities (two-temperature plasma). It is noted that a general simplified solution, but not in closed form, can be obtained for the spherical or cylindrical wave with allowance for the recovered energy of nuclear fusion. The author concludes that the cited solutions extend to some degree the range of averaged description to inhomogeneous, specifically weakly inhomogeneous media.

Volosevich, P. P., S. P. Kurdyumov, and Ye. I. Levanov. Various thermal heating regimes from interaction of intense radiation flux with matter. ZhPMTF, no. 5, 1972, 41-48.

Gas dynamic and thermal processes induced by high-power laser radiation interacting with matter are analyzed, with allowance for nonlinear electron thermal conductivity. Sublimation energy is considered to be negligible in comparison to thermal and kinetic energy of vapors formed by the interaction. Two boundary-value problems of radiation gas dynamics are treated on the following assumptions. Problem A assumes that, near the gas-vacuum or gas-piston boundary, radiation flux $q = q_0 t^g$, where q_0 and q are constants and t is time, is totally absorbed and heat transfer in the gas occurs by the heat conduction mechanism only ($q = 0$). In problem B, $q(0, t) = q_0 t^g$ flux interferes with heat transfer according to the equation

$$\partial q / \partial m = -K_0 T^{n_1} \rho^{b_1 - 1} q \qquad (1)$$

where $m>0$ is the Lagrangian mass variable, and T and ρ are temperature and

density, respectively. Additional boundary (m = 0) and initial (m>0) conditions are formulated for both problems. The condition of self-similar solution to both the A and B problems is that

$$g = 3/2\,(a-1) \tag{2}$$

The additional condition to problem B solution is

$$a_1 = 1/2 - a \tag{3}$$

where a and a_1 are dimensionless exponents of T in the expressions of the coefficients $\varkappa$ and k of thermal conductivity and absorption, respectively. Self-similar solution of the A and B problems can be obtained by solving a set of ordinary differential equations in dimensionless variables.

An extended analysis of the problem A solution at $k \to \infty$ showed the existence in a moving medium of two different heat propagation regimes: supersonic and subsonic, which are characterized by temperature waves of the first (TW-I) and the second kind (TW-II), respectively. It is shown that, in the case of completely ionized plasma (g = 1), the TW-I regime exists on condition that

$$\frac{E}{\tau^2} > \frac{1}{2}\lambda_* \frac{\rho_0^2 R^{2}}{\varkappa_0} \tag{4}$$

and TW-II regime exists on the inverse condition. E in (4) is the total radiative energy incident upon the medium during time τ, ρ_0 and $\varkappa_0$ are the initial values of ρ and $\varkappa$, and R is the gas constant. The dimensionless constant λ_* is determined by numerical self-similar solution to problem A.

In time the nonself-similar solution at an arbitrary g value changes to the self-similar one, if the TW-II regime exists in the region of heating, i.e. between the TW-II front and the vapor-vacuum boundary (Fig. 1).

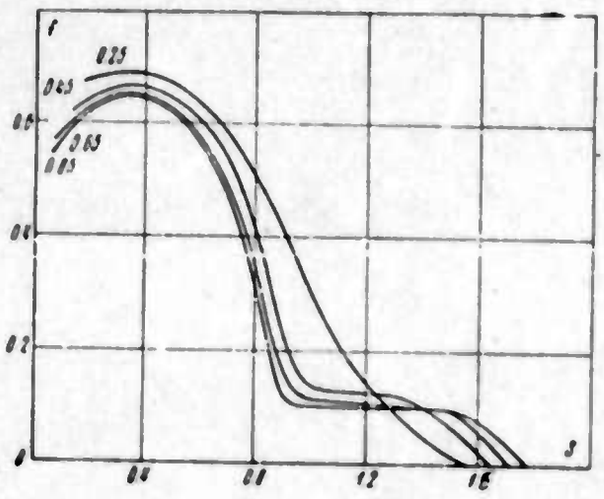

Fig. 1. Dimensionless temperature f versus self-similar variable s.

Pressure P_T at the TW-II front can be approximated by the pressure P_v at the front of shock wave propagating ahead of TW through the medium of $\rho = \rho_o$ (Fig. 2). This approximation makes it possible to connect self-similar

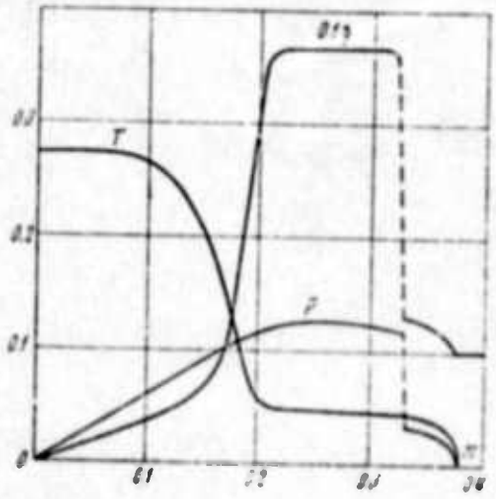

Fig. 2. TW-II propagation pattern

solution in the $0 \le m \le m_T$ region of TW propagation with the nonself-similar shock wave. Thus, the self-similar solution to problem A could be obtained in the form

$$m = s q_0^{(2n-b-1)/d} \rho^{-(2n+1)/d} x_0^{2/d} t^{n_0}$$
$$v(m,t) = u(s)\, q_0^{(1-b)/d} \rho^{(n+1)/d} x_0^{-1/d} t^{n_0}$$
$$T(m,t) = f(s)\, q_0^{2(1-b)/d} \rho^{(1+2b)/d} x_0^{-2/d} t^{2n_0}$$
$$\rho(m,t) = \delta(s)\, q_0^{2(n-1)/d} \rho^{-3(n+1)/d} x_0^{2/d} t^{n_1},$$

where $d = 2n + 1 - 2b$

$$W_i(m,t) = \omega(s) q_0 t^{\varepsilon}, \quad q(m,t) = \varphi(s)\, q_0 t^{\varepsilon}$$

where $\varphi(s) = 1$ at $s = 0$ and $\varphi(s) = 0$ at $s > 0$ (5)

$$n = 1 + \frac{\varepsilon}{3} + \frac{2n_1}{3}, \quad n_0 = \frac{\varepsilon}{3} - \frac{n_1}{3}, \quad n_1 = \frac{2(a-1)\varepsilon - 3}{2a - 3b - 1}$$

The unknown functions v(m, t) and W(m, t) given by (5) are the velocity and the heat flux due to electron thermal conductivity, respectively. The solution of (5) is self-similar at an arbitrary $g > -1$. The formulas of the heating depth m_T and P_T at the TW front, mass velocity D_v and mass coordinate m_v of the shock wave are derived from (5). By comparing the cited shock wave and TW parameters, critical time t_* of change to a self-similar regime was determined, to be

$$t_* = (1)\sqrt{0.5(\gamma+1)\beta_1}\,(g/3 + n_1/6 + 1)^{-1} s^{-1} (\rho_0^{1-a})^{2/n_1} \times$$
$$\times [(\rho^{2(a+1)} t x_0^{-2} q_0^{1-a})_2^{3}]^{2n-2a-3b} \qquad (6)$$

where γ is the ratio of heat capacities and β_1 is the dimensionless pressure at the TW front with the coordinate S_1.

It follows from (6) that a self-similar regime exists at $t > t_*$, if $2a + 1 - 3b > 0$, $a > 1$, and $g < 3(a-1)/2$. If $g > 3(a-1)/2$, the self-similar TW-II regime exists at $t < t_*$. In case of $g = 3(a-1)/2$, a self-similar regime exists in both heating and shock regions. At $g < 3(a-1)/2$, transition from the initial TW-I to TW-II regime occurs at $g < 0$ in the asymptotic phase of heating or at $g = 0$, i.e. in case of $q(0, t) = q_0 = \text{const}$. At $g > 3(a-1)/2$, the initial TW-II self-similar regime changes to a TW-I regime in the asymptotic phase. Simplified formulas are given for calculating $T(m, t)$, m_T, and t_* for a particular case of constant radiation flux at the boundary ($g = 0$) and totally ionized gas ($a = 5/2$, $b = 0$).

Ulyakov, P. I. High-temperature vaporization of metals. I-FZh, v. 24, no. 2, 1973, 256-261.

The electron component of heat capacity is taken into account in calculation of the thermodynamics of equilibrium vaporization of metals. Saturated vapor pressure is calculated as a function of temperature T:

$$p/p_0 = v^{-1/2}\exp\left[\left(\Lambda + \frac{1}{2}\right)\left(1 - \frac{1}{v}\right) - \frac{\sigma}{v}(v-1)^2\right]. \quad (1)$$

By substitution in (1), the linear rate of metal vaporization v is found:

$$v = \frac{v_k}{v}\exp\left[\left(\Lambda + \frac{1}{2}\right)\left(1 - \frac{1}{v}\right) - \frac{\sigma}{v}(v-1)^2\right], \quad (2)$$

where $v_k = p_0 V_t \sqrt{\gamma/RT_k}$.

The dependence of saturated vapor pressure p and of the linear vaporization rate v on dimensionless temperature ν, and the dependence of vaporization parameters (saturated vapor pressure p, rate v and temperature ν) on the density of the energy absorbed by the metal are shown in Figs. 1 and 2 for aluminum and copper and for iron, aluminum, copper and tin, respectively.

In high-temperature vaporization of metal without shielding of its surface, there is a certain limit which is governed only by the properties of the vaporized material. The maximum vaporization rate is reached at a somewhat lower temperature than maximum pressure.

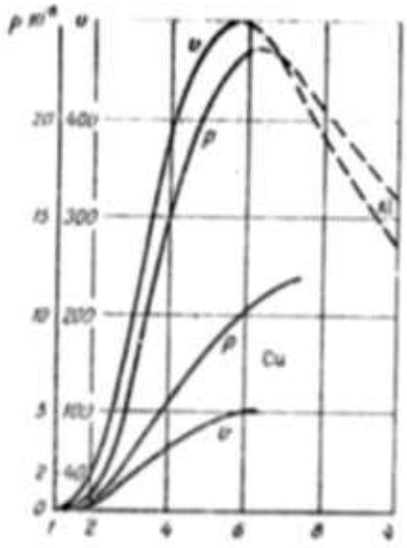

Fig. 1. Dependence of saturated vapor pressure p, N/m^2, and linear vaporization rate v, m/sec, on dimensionless temperature ν for aluminum and copper.

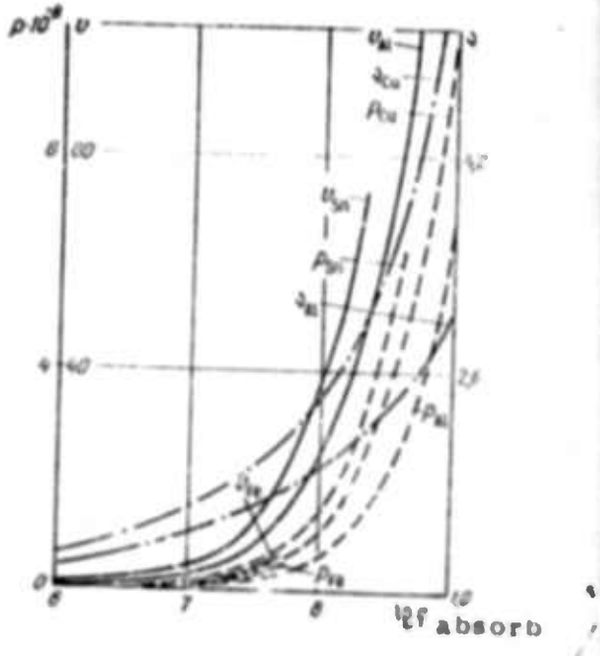

Fig. 2. Dependence of vaporization parameters of pressure p, rate v and temperature ν on the density of the power of energy q absorbed by the metal for iron, aluminum, copper and tin; p - N/m^2; v - m/sec; q - w/cm^2

Veyko, V. P., G. A. Kotov, M. N. Libenson, and M. N. Nikitin. Thermochemical effects of laser radiation. DAN SSSR, v. 206, no. 3, 1973, 587-590.

Laser-induced localized chemical reactions on the surface or within a solid material were studied in thin chromium films vacuum-deposited on a glass substrate. Free-running Nd glass laser pulses of 1-1.5 msec duration and 1-10 j energy were focused on a rectangular area of the

Cr film. Incident power density was 10^3-10^4 w/cm^2 at the surface. An slow low-grade etching of the locally-irradiated films was observed, both when they were irradiated in an oxygen atmosphere and in a 10^{-2}-10^{-3} torr vacuum. This effect is explained by the presence of an adsorbed or chemisorbed oxygen monolayer on film surfaces stored at room temperature. In disagreement with theoretical estimates, the preirradiation number of oxygen atoms adsorbed is therefore sufficient to saturate the film surface with oxygen during irradiation. The kinetics of thin chromium oxide film growth was examined by measuring the film electrical resistance during exposure. Variations in the resistance during a laser pulse were recorded by two oscilloscopes (Fig. 1). Oscilloscope traces of current variations

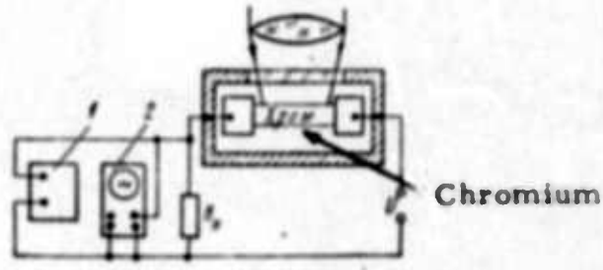

Fig. 1. Experimental circuit for study of oxidation kinetics: 1 - loop oscillograph, 2 - CRO.

show an increase in resistance of films heat-treated before irradiation in an oxygen atmosphere. This increase in R results from a decrease in conducting layer thickness owing to oxide film formation.

Thickness x(t) of Cr_2O_3 films during a pulse of τ = 1 msec and 10^4 w/cm^2 and theoretical x(t) were calculated using oscilloscope traces and the Cabrera-Mott theory of diffusion-controlled growth of very thin films, respectively. The theoretical x(t) were in good agreement with the experi-

mental x(t) data (Fig. 2) to t ≈ 0.6 msec. The divergence between the

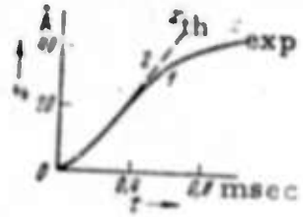

Fig. 2. Thickness of Cr_2O_3 film versus time, x(t). 1 - experimental curve, 2 - theoretical curve.

two curves after t = 0.6 msec was tentatively attributed to decay of the actual laser pulse and a consequent slower temperature increase, and an x_{exp} decrease in relation to x_{theor}. An approximate evaluation yielded values of $x_{theor} \approx 70$ Å and $x_{exp} \approx 45$ Å. The discrepancy between the two x values is acceptable in view of the uncertain x_1, diffusion activation energy, and film temperature values used in the calculations. In addition to Cr, oxidation of Fe-Ni-Co and Cr-SiO alloys, reduction of $MgO-MnO-Fe_2O_3$ ferrites, and other reactions were induced by laser radiation.

Plis, A. I., Ye. L. Tyurin, and V. A. Shchegiov. Heating of materials by short laser pulses. ZhTF, v. 17, no. 12, 1972, 2568-2576.

In connection with the use of laser energy for heating solid materials to fusion temperatures, a theoretical analysis is given of two-dimensional solid target heating by ultrashort ($\tau_p \lesssim 10^{-11}$ sec) powerful laser pulses. The heat conduction and gas dynamic unloading of the heated material are taken into account. A density profile n(x) and the optimum heating conditions of a plasma layer formed by single-pulse interaction with the target

are defined for ice, lithium deuteride, or polyethylene materials used for neutron generation.

An analytic method was developed for calculating plasma layer temperature T_{lim} and energy Q absorbed in the plasma at the pulse cut-off time t_c. Pulse reflection from the cut-off boundary x_c, where the electron density is $n_c = 10^{21}/cm^3$, is taken into account in calculations. With allowance for additional plasma heating by the reflected pulse, the approximate formulas of Q and T_{lim} for an arbitrary n(x) are, respectively,

$$Q = \left(\frac{3}{2} n_e\right)^{2/3} (3a\mathcal{E}_0)^{1/3} \int_{-\infty}^{x_c} \left(\frac{n}{n_e}\right)^{2/3} dx \text{ (erg/sq. cm)} \tag{1}$$

and

$$T_{lim} = \left(\frac{10a\mathcal{E}_0}{3n_e}\right)^{2/3} \text{(erg)}. \tag{2}$$

where $\mathcal{E}_0$ is the pulse energy density (erg/cm^2) and a is a constant. It was found that by allowing for reflection, absorption increases by 32%. The maximum Q, for a given initial thickness x_0 and electron density n of the plasma layer, is given by

$$Q \approx 1.35 n_0 x_0 \left(\frac{a\mathcal{E}_0}{n_e}\right)^{2/3} \tag{3}$$

The lifetime of the absorbing layer with optimum parameters is

$$t_{opt.} = \frac{x_0}{2n_e c_0}. \tag{4}$$

where c_0 is the initial sound velocity at $T_e = T_i$. At pulse cut-off the electronic heat-conduction wave and the unloading wave start to propagate into the target material. These processes are distinguished by the equality $T_e = T_i$ at the time t_{ei} at which a noticeable fusion reaction sets in.

Plasma heating, with allowance for the cited processes, is described by a single universal integrodifferential equation. At the dimensionless time $\bar{t} = t/\tau \to 0$ the self-similar solution of this equation, with exclusion of gas dynamic terms, is

$$\bar{T} = (9/)^{-1/3} = \bar{x}_T^{-1} \qquad (5)$$

where $\bar{T} = T/\theta$ is the dimensionless temperature, and $\bar{x}_T = x_T/\delta$ is the dimensionless coordinate of the heat wave front. Comparative T/θ and x_T/δ versus t/τ plots calculated from (5) and the universal equation, together with plots of the unloading wave coordinate x_s/δ versus t/τ, show that the unloading wave overtakes the heat wave in a finite time, and adiabatic expansion of plasma occurs. At a time $t = \tau$, separation of x_T from x_s is at a maximum ($x_s/x_T = 0.4$) and $T_e \approx T_i$. The fusion neutron yield is calculated from this time onward using the given solutions and data from the literature. The neutron yield N and the total fusion energy $Q_{f.e.}$ were accordingly calculated for solid deuterium D and a D-T mixture, respectively, and were plotted against the absorbed Q (Fig. 1 and 2). The lifetime of a hot plasma was

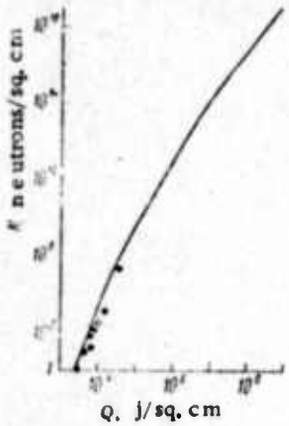

Fig. 1. N versus Q plot for a solid D target, $n_d = 5 \times 10^{22}$ cm^{-3} Dots are for literature data.

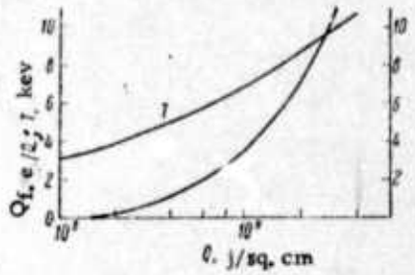

Fig. 2. Relative fusion energy yield $Q_{f.e.}/Q$ and plasma average temperature T versus Q plots for D ($n_d = 2.4 \times 10^{22}$ cm^{-3})-T ($n_t = 3.6 \times 10^{22}$ cm^{-3}) target.

calculated to be

$$\tau_{т./п.} \approx \tau = 10^7 n_0^{-1} Q^{1/2}, \qquad (6).$$

At $\tau_f = 10^{-8}$ sec, $Q = 3 \times 10^8$ j/cm^2 is required to attain a $Q_{f.e}/Q = 1$ ratio.

Aksel'rod, I. L., and A. Z. Volynets.
Development of a sublimation process
in a monochromatic e-m radiation field.
EOM, no. 5, 1972, 52-55.

A brief theoretical study is given on sublimation processes generated on a surface exposed to monochromatic radiation. The sublimation characteristics are derived in terms of the temperature stress developed in the irradiated surface, assuming a relatively thin planar target with normal incidence of the beam. The first step in the solution is to define the temperature field and then to deduce the resultant stress relationships from the field. An expression for maximum attainable temperature stress is finally obtained in terms of beam and target parameters.

A theoretical numerical example is then given for the case of fresh-water sheet ice; this shows that incident power densities on the order of 700 w/m^2 would be sufficient to generate surface cracks. However, since ice has flow properties, the derived solutions would only apply for a sufficiently thin layer in which the temperature field is rapidly established.

B. Recent Selections

i. Beam-Target Effects

Andreyev, V. , and P. I. Ulyakov. Thermoelastic stresses in a plate from a cylindrical source with an arbitrary time-intensity characteristic. FiKhOM, no. 1, 1973, 27-31.

Bykovskiy, Yu. A., V. Ya. Gamlitskiy, N. I. Gribov, and I. N. Nikolayev. Moessbauer effect in iron films deposited by thermal and laser methods. IVUZ Fiz, no. 2, 1973, 146-148.

Dzhaksimov, Ye. Calculation of intensive light absorption coefficient by charge carriers in semiconductors. FTT, no. 2, 1973, 644-645.

Grigor'yev, B. A. Simplification of one-dimensional problems of thermal conductivity from pulsed radiative heating of flat bodies. TVT, no. 1, 1973, 133-137.

Gurevich, G. L., and V. A. Murav'yev. Effect of laser irradiation on thin films. FiKhOM, no. 1, 1973, 3-8.

Lariokhin, B. Lasers in 1973 (Survey of foreign technology). Krasnaya zvezda, 15 February 1973, p. 3.

Libenson, M. N., and M. N. Nikitin. Diffusion of atoms from film to substrate under laser irradiation. FiKhOM, no. 1, 1973, 9-14.

Lisitsa, M. P., and I. V. Fekeshgazi. Laser irradiation damage on the surface or within transparent glass. IN: Sb. Kvantovaya elektronika, no. 5 (11), 1972, 86-88.

Marin, O. Ye., N. F. Pilipetskiy, and V. A. Upadyshev. Formation of laser-initiated cracks. MP, no. 1, 1973, 82-89.

Mirkin, L. I. Mechanical deformation and destruction of metals from effects of a laser beam with a 10^{-3} second pulse duration. FiKhOM, no. 1, 1973, 31-33.

Mirkin, L. I. Feasibility of displacement of atoms in a solid from the effects of a pulsed laser. IVUZ Fiz, no. 2, 1973, 106-108.

Mirkin, L. I. Contact melt zone on a ferrite-graphite interface from the effect of laser pulses. FiKhOM, no. 1, 1973, 143-145.

Rubinshteyn, A. I., and V. M. Fayn. Theory of avalanche ionization in transparent dielectrics from the effects of a powerful electromagnetic field. FTT, no. 2, 1973, 470-478.

Teslenko, V. S. Optico-hydrodynamic parameters of laser breakdown in liquids. IN: Sb. VI Vsesoyuznaya konferentsiya po nelineynoy optike, Minsk, 1972, 81. (RZhRadiot, 2/73, no. 2Ye213)

Vlasov, R. A., K. P. Grigor'yev, I. I. Kantorovich, and G. S. Romanov. Mechanism of shock ionization from optical breakdown of transparent dielectrics. FTT, no. 2, 1973, 444-448.

Zverev, G. M., V. S. Naumov, and V. A. Pashkov. Self-focusing of ultrashort laser pulses in solid dielectrics. FTT, no. 2, 1973, 575-576.

ii. Beam-Plasma Interaction

Aksenov, V. V., V. M. Yeroshenko, A. A. Mushinskiy, and L. N. Pyatnitskiy. Collective scattering of laser radiation in a plasma. TVT, no. 1, 1973, 1-5.

Alekseyev, V. A., S. D. Zakharov, P. G. Kryukov, and Yu. V. Senatskiy. Feasibility of using a dense plasma jet as a target in studies of laser heating. KSpF, no. 7, 1972, 57-61.

Aliyev, Yu. M., O. M. Gradov, and A. Yu. Kiriy. Anomalous dissipation and penetration of electromagnetic radiation into a confined plasma. ZhETF P, v. 17, no. 3, 177-179.

Basov, N. G., A. R. Zaritskiy, S. D. Zakharov, O. N. Krokhin, P. G. Kryukov, Yu. A. Matveyets, Yu. V. Senatskiy, and A. I. Fedosimov. Generation of powerful light pulses at 1.06 and 0.53 μ and its application to plasma heating. 1. Experimental studies of radiation reflection during laser plasma heating at two wavelengths. IN: Sb. Kvantovaya elektronika, no. 5 (11), 1972, 63-71.

Kaliski, S. Concentric conduction-type laser heating of D-T plasma. Bulletin de l'Academie Polonaise des Sciences, Serie des sciences techniques, no. 1, 1973, 1 (37)-7 (43).

Kaliski, S. Laser concentric conduction heating of two-temperature D-T plasma. Bulletin de l'Academie Polonaise des Sciences, Serie des sciences techniques, no. 1, 1973, 9 (45)-15(51).

Kolerov, L. N., G. D. Petrov, and P. A. Samorskiy. Laser methods in heterogeneous plasma diagnostics. IN: Sb. Ukrainskaya respublikanskaya nauchno-tekhnicheskaya konferentsiya, prosvyashch. 50-letiyu metrologicheskoy sluzhby UkrSSR, 1972, Khar'kov, 1972, 57. (RZhMetrolog, 2/73, no. 2.32.1007)

Kurbatov, Yu. A., and V. F. Tarasenko. Time characteristics of spark discharges initiated by laser bursts. PTE, no. 1, 1973, 142-144.

Lemberg, Ye. A., Yu. V. Tkach, I. I. Magda, N. P. Gadetskiy, and V. U. Abramovich. Commutation of discharges using a pulsed ultraviolet gas laser. PTE, no. 1, 1973. 140-142.

Rodichkin, V. A., and G. Ya. Rusakova. Effect of electrode-target polarity and lens focal plane position on laser-ignited discharge characteristics. ZhTF, no. 2, 1973, 345-348.

Vinogradov, A. V., B. Ya. Zel'dovich, and I. I. Sobel'man. Effect of saturation on stimulated scattering from laser heating of plasma. ZhETF P, v. 17, no. 5, 1973, 271-274.

Volobuyev, I. V., B. V. Granatkin, and A. I. Isakov. Liquid scintillator detector for recording neutron irradiation in a laser plasma. KSpF, no. 7, 1972, 69-72.

Volyak, T. B., S. D. Kaytmazov, A. M. Prokhorov, and Ye. I. Shklovskiy. Effect of magnetic field on soft x-radiation in a laser plasma. ZhETF, v. 64, no. 2, 1973, 481-484.

Vyskrebentsev, A. I., and Yu. P. Rayzer. Simple theory of breakdown in monatomic heavy gases in fields from low to optical frequency ranges. ZhPMTF, no. 1, 1973, 40-47.

2. Effects of Strong Explosions

A. Abstracts

Korobeynikov, V. P., and Yu. M. Nikolayev. Shock waves and magnetic field configuration in interplanetary space. Cosmic Electrodynamics, v. 3, no. 1, 1972, 3-24. (RZhF. 10/72, no. 10G83). (Translation)

The propagation of shock waves generated by chromospheric solar flares in interplanetary space is analyzed. Plasma motion is described using a gas dynamics approximation. Four models of the plasma perturbation source are examined: blast wave, piston, point explosion followed by piston motion, and concentrated perturbation with energy and mass input. The magnetic field configuration in the shock wave wake was determined from the freezing-in condition. Theoretical data are compared with data obtained by observation of plasma parameters.

Ivanov, K. G. Depth of an interplanetary shock wave. Kosmicheskiye issledovaniya, no. 5, 1972, 788-789.

Earlier published experimental magnetic profiles of interplanetary shock waves in solar wind were used to calculate shock front velocity D and transit time τ; front depth $\Delta = D\tau$; magnetosonic Mach number M_m; the local mean free path behind the front; the front inclination in the magnetic field; and the most probable value of the parameter $\beta_2 = 8\pi p_2 / F_2^2$, where p_2 is the solar-wind plasma pressure and F_2 is the magnetic field intensity. The data are tabulated. The magnetic profiles are vibrational (V) or step (S) types. The calculated Δ values are in the 3×10^3 - 27×10^4 km or ~(75-4300) ranges of the Larmor ionic radii r_{L2}. Thus, Δ is 10^2-10^5 times

greater than the usually observed depths of the forward magnetospheric wave front. The V-profile wave-front is 10-100 times wider than that of the S-profile waves. At $\beta \geq 1$ in the solar wind, the theory and analysis of the cosmic probe data for V-profile waves yield $\Delta \sim 10^9$-10^{10} cm. These calculations, however, are not applicable to the solar wind at $\beta \approx 1$.

Kuz'micheva, A. Ye., L. I. Dorman, and N. S. Kaminer. Velocity of shock wave propagation from geomagnetic storms and Forbush decreases. GiA, no. 5, 1972, 918-920.

The velocity was studied of shock wave propagation determined from the delay time Δt from the start of a magnetic storm and the incident Forbush decrease relative to a chromospheric flare. The Δt dependence on the chromospheric flare heliographic longitude λ is examined using solar activity and geomagnetic distribution data from the literature. For the period 1957 to 1969, 76 events with a Forbush decrease amplitude of $F \gtrsim 3\%$ and 41 $F = 1$ to 3% events were used. The plot in Fig. 1 shows a weak relationship between Δt and λ.

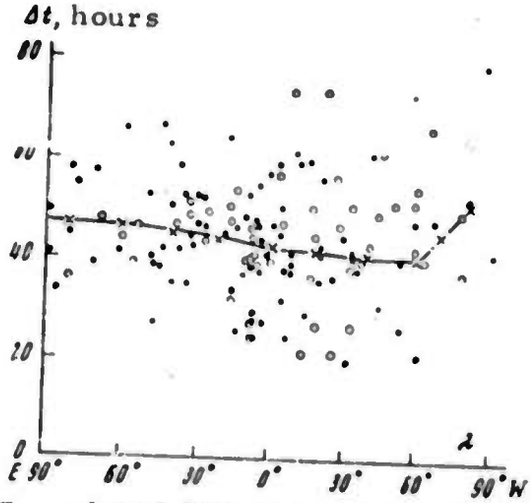

Fig. 1. Correlated dependence of Δt versus λ. Dark circles - events of $F \gtrsim 3\%$; light circles - events of $F = 1$ to 3%. The crosses in the broken line connect Δt values calculated at 20° intervals of $\Delta \lambda$.

The relationship of Δt to the diurnal K_p index sums preceding magnetic storms was studied for Forbush decreases with amplitudes of $F \gtrsim 1$ and $\gtrsim 3\%$, both for all flares and for central ones ($\lambda = 30^\circ$ E - 30° W). A rise in Δt was observed in all cases with decreased ΣK_p. Fig. 2a shows Δt versus λ for all flares, and Fig. 2b shows this dependence for the central flares only.

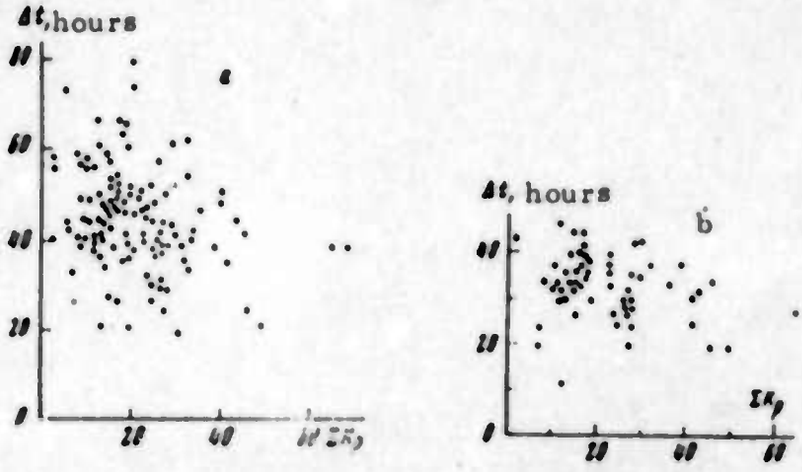

Fig. 2. Δt versus ΣK_p.
a- all flares, b- central flares only.

Variations in Δt as a function of λ were calculated for a spherical shock wave generated by a plasma bunch radially ejected from the flare region. The dependence shown in Fig. 3 assumes the shock waves are generated at a distance a from the sun.

A comparison reveals that a model which assumes shock wave generation in a flare region disagrees with experimental data. Results of the study Δt in terms of solar flare conditions show that the plasma bunch radially ejected from the flare area generates a quasi-spherical shock wave at

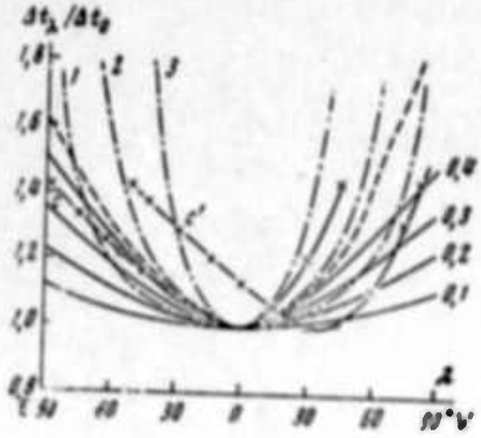

Fig. 3. Relationship of $\Delta t_\lambda / \Delta t_o$ to λ. Δt_λ and Δt_o - delay of shock waves generated by plasma bunches ejected from flares at longitudes of λ and $\lambda = 0^o$. Curves are calculated for distances of 0.1, 0.2, 0.3 and 0.4 a.u.

distances of ~0.3 to 0.4 a.u. from the sun. The velocity of this wave decreases with distance from the solar central meridian.

Pelinovskiy, Ye. N., and V. Ye. Fridman.
Statistical phenomena of shock wave generation.
Akusticheskiy zhurnal, no. 4, 1972, 590-594.

Statistical characteristics of shock wave discontinuity formation length are analyzed under the assumption that quasiharmonic initial disturbances with a random envelope generate the waves. The initial disturbance probabilistic distribution is considered for: 1) a normal initial disturbance velocity distribution, and 2) a uniform distribution of the incident wave amplitude or frequency.

The one-dimensional probability density $W(x_s,t)$ of the discontinuity formation length is used to formulate an expression for the normal distribution of the initial disturbance velocities:

$$W(y)=\frac{1}{\sqrt{2\pi}\,y^2}\left\{2\delta y\, e^{-1/2y^2}+\sqrt{\pi/2}\,[1+\Phi(1/\sqrt{2}\,\delta y)]\,e^{-1/2y^2}\right\}. \tag{1}$$

where y, δy are dimensionless variables and Φ is an integral Laplace function. For large and small values of δy, simpler asymptotic expressions for W(y) are formulated. The graphically represented W(y) had a maximal value at $y = 1/\sqrt{3}$. Based on the graph and derived formulas for W(y), various properties of the probability density of the shock wave discontinuity formation length are indicated. Other statistical characteristics such as the mean length $\langle y\rangle$ of shock wave generation and variance δy of the shock wave generation coordinate are also derived. In the case of a uniform distribution of the amplitude and frequency, corresponding statistical characteristics of $W(x_s)$, $\langle x_s\rangle$, σx_s are calculated. Results are valid for nonlinear sound waves in a homogeneous medium, and the study of noise transmission through regular weakly-nonhomogeneous media. A similar approach would be feasible for nonstationary media.

Pelinovskiy, Ye. N., A. I. Saychev and V. Ye. Fridman. Shock wave generation in statistically-nonuniform gas. Akusticheskiy zhurnal, no. 4, 1972, 627-629.

Continuing the analysis described in the preceding abstract, the authors studied the statistical characteristics of shock wave formation length in a medium with large-scale density fluctuations. One-dimensional

sound waves in a stationary isothermic gas are analysed under the assumptions that the incident wave is nonuniform and the reflected wave is neglected. The solution of sound equations is given as:

$$t - \frac{x}{c} + \frac{(1+\gamma)v}{2c^2}\sqrt{\rho(x)}\int_0^x \frac{dx'}{\sqrt{\rho(x')}} = F(x)\sqrt{\rho(x)}. \qquad (1)$$

where c - sound velocity, v - gas particle velocity, γ - isentropic exponent, ρ - gas density, randomly dependent on the coordinates, and F is a function determined from boundary conditions. The solution is valid to the point x_s, where the discontinuity is formed. Then velocity at which the discontinuity is formed is established, and an equation for x_s is formulated. The equation indicates that the shock wave formation length is a function of gas density with a probability distribution that can be determined for Markov processes only. The functional can be considered as Markovian when the correlation length l is small compared to the length R_* of the discontinuity formation. The probability density $W(x_s)$ is consequently determined by solving the initial Kolmogorov equation with certain boundary and initial conditions. For a homogeneous medium, $W(x_s)$, mean $\langle x_s \rangle$, and variance σx_s are given in explicit form. A graph of $W(x_s)$ is presented. The authors conclude that the results have application in such astrophysics problems as the calculation of chromospheric turbulence during nonlinear wave propagation in the solar atmosphere.

Kuskov, A. M. Calculating diffraction from weak shock wave interactions on a plate. VLU, no. 19, 1972, 95-102.

An incident triangular shock wave is assumed to be perpendicular to a rectangular plate edge; the other plate edge is rigidly fixed. A basic integro-differential equation, containing diffractional terms and describing the motion of a plate is derived under the simplifying conditions of shock wave total reflection and plate rigidity before the shock wave arrival.

The particular case of a plate rigidly built into an infinite wall is studied. The simplest version is initially analyzed when the transient processes of diffraction propagation over the entire plate surface are completed. The integro-differential equation describing the plate motion is an ordinary differential equation with constant coefficients. An equation of motion of a plate for an arbitrary time interval is described, based on approximate diffraction terms and the interpolation of the equation corresponding coefficients. From the basic equation, an approximate equation is derived which allows for the diffractional effect of an arbitrary time interval. The more complicated case of a plate which is one of an infinite number of identical plates is also considered. Under various conditions for the diffraction terms, an equation of motion is formulated for such a plate subjected to a weak shock wave.

The derived equations are nonlinear with variable coefficients. The final equation can be substantially simplified assuming that the coefficient are sums of $2t_1$ and $2t_{11}$ periodic functions and the ratio of these periods is a rational number. The nonlinear differential equations with constant and variable coefficients are integrated by ordinary numerical methods. In the computational process, it is necessary to select mesh points of the computation net such that the coefficients of the equation lose their analytical properties.

Kutateladze, S. S., A. P. Burdukov, V. V. Kuznetsov, V. Ye. Nakoryakov, B. G. Pokusayev, and I. R. Shreyber. Structure of a weak shock wave in a gas-liquid medium. DAN SSSR, v. 207, no. 2, 1972, 313-315.

Experimental results are given to verify theoretical findings on shock waves propagating in a gas-liquid medium.

A piezoelectric pressure sensor measured the shock wave structure. The sensor had a flat response from 20 to 50 kHz and a 6.3 v/bar sensivity. The experimental installation consisted of a vertical transparent plexiglass tube with an ID = 6 cm and length = 100 cm. The gas-liquid mixture was obtained by injecting nitrogen into the liquid through a porous plate in the lower part of the tube. By applying plates of varying porosity, bubbles with diameters of 0.02, 0.3, and 0.6 cm were produced. Volumetric gas content varied from 0.01 to 0.15.

The perturbation pulse was generated by rupturing the diaphragm, which was composed of one or more cellophane sheets, at a rupturing rate of $\sim 2 \times 10^{-5}$ sec. The piezoelectric pressure sensors were arranged along the shock tube length inside the wall. Sensor signals were fed into a cathode-ray oscillograph for photographing. The "noise" levels of surfacing bubbles were measured and the effect of elastic waves developing at the shock tube wall during the diaphragm rupture was evaluated. Oscillograms of pressure oscillations in a shock wave front propagating in water-nitrogen and water-glycerine mixtures are presented in Figs. 1 and 2 where t_r is the time of rupture, a_o is the volumetric gas content, R_o is the bubble equilibrium radius, ν is the liquid cinematic viscosity, and M is the Mach number.

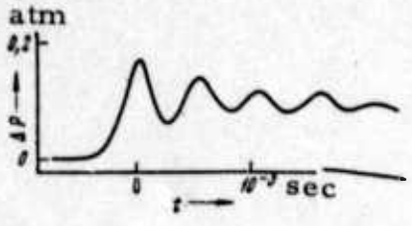

Fig. 1. Shock wave profile for a water-nitrogen mixture, R_o = 0.15 cm, a_o = 0.06, $\nu = 10^{-2}$ cm^2/sec, t_r = 3 msec, M = 1.08.

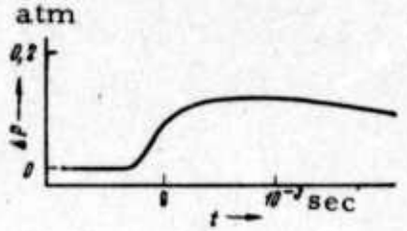

Fig. 2. Shock wave profile for 40% water-glycerine mixture. R_o = 0.15, a_o = 0.06, $\nu = 4 \cdot 10^{-2}$ cm^2/sec, t_r = 3 msec, M = 1.06.

The experimental results agree qualitatively with the theoretical data.

Naugol'nykh, K. A. Conversion of shock waves into acoustic waves. Akusticheskiy zhurnal. no. 4, 1972, 579-583.

The conversion of a weak shock wave into an acoustic wave is analyzed. Expressions for the discontinuity length and width, and the impulse length of a spherical shock wave are presented. Conditions under which these expressions are invalid and the shock wave converts into an acoustic wave are examined. By equating the shock wave width with that of the impulse, the expression for the distance r_1 at which the shock wave width is equal to the impulse length is derived as:

$$r_1/r_0 = \frac{\alpha v_0 \rho l_0}{b} = \mathrm{Re} \qquad (1)$$

where $\alpha = n + 1/2$, n is the isentropic exponent, v_o is a discontinuity value, ρ is the density of the medium, c is the sound velocity, $b = \frac{\alpha}{2 \rho c^3}$, and Re is the Reynolds number. The conditions of Eq. (1) are sufficient but not necessary, since in certain cases they are inapplicable for distances smaller than r_1, owing to the slowness of dissipative processes. For the latter case,

the impulse with discontinuity value v and the characteristic acoustic length l are calculated.

An example of shock wave propagation from the explosion of trotyl in water is analyzed. Using the derived formulas, the distances at which shock waves convert into acoustic waves are calculated. Results show that transition of a weak shock wave into an acoustic one occurs gradually and asymptotically. The formulas indicate only the distances at which the nonlinear and dissipative effects are comparable.

Kmonicek, V., F. Slepicka, O. Sifner, and V. Hoffer. Universal method for calculating the state of a real gas behind primary and reflected shock waves. Acta technica CSAV, no. 5, 1972, 542-567.

A universal method was devised for computing the equilibrium states of any real gas, at temperatures in the 1000-6000° K range, behind primary and reflected shock waves. The method is intended for preparation of tables and accurate and rapid evaluation of individual shock tube experiments. The method is universal in the sense that it is applicable to diverse gases and gas mixtures within a broad range of state parameters, while taking into account chemical reactions behind the shock wave. The computation requires solving equations of mass, momentum, and energy conservation, together with a thermodynamic expression of pressure p. The equations can only be solved by iteration, which is done in successive steps, first for the state behind the primary wave (denoted by subscript 2), then for the state behind the reflected wave (subscript 5). Each iteration step is of a successive refinement of a preset value of the density ratios ϱ_1/ϱ_2 and ϱ_2/ϱ_5 using

the starting set of equations. Fluctuations of the computed data are within the error of the computational procedure in the $(293.15 \pm 5)^{\circ}$ K range of initial temperatures T_1. Convergence of the iteration procedure is fast, since usually only three steps of the outer iterative cycle are required when the initial tolerance in the inner cycle is 0.05 and that of the outer cycle is 0.0005 in the 500-8000° K range.

The computed equilibrium state parameters are tabulated for CO_2, CO, H_2O, and H_2 at $T_1 = 293.15^{\circ}$ K, $p_1 = 1$-100 torr, and $M_1 = 3.5$-15. The relative deviations Δy from

$$y \in \left(T_2, z_2, \frac{h_2}{h_1}, \frac{p_2}{p_1}, \frac{\varrho_1}{\varrho_2}, T_5, z_5, \frac{h_5}{h_2}, \frac{p_5}{p_2}, \frac{\varrho_2}{\varrho_5} \right) \qquad (1)^{*}$$

are small in the computed states, e.g. in CO_2, behind the primary wave. A considerable (up to 20%) Δy, particularly at p_5/p_2 and ϱ_2/ϱ_5, appears for states behind the reflected wave. Maximum computation errors T_2, p_2, h_2, ϱ_2, T_5, p_5, h_5, ϱ_5 are estimated to be 15° K, 0.3%, 0.1%, 3%, 35° K, 1.5%, 0.1% and 2%, respectively. Computation of one point for a gas and a combination of p_1, T_1, and M_1 takes about as many seconds as there are components in the gas. The computing times and error rates are well within acceptable limits.

Gel'fand, B. Ye., S. A. Gubin, S. M. Kogarko, and S. P. Komar. Shock wave destruction of cryogenic liquid drops. DAN SSSR, v. 206, no. 6, 1972, 1313-1316.

Atomizing of cryogenic liquid propellants was studied at higher than critical temperatures and pressures. The effect on cryogenic liquid drops of the gas flow behind a shock wave is considered with reference

---

* where z is the compressibility factor and h is the enthalpy

to modelling of drop injection in a combustion chamber. Tests were made in the rectangular cross section shock tube diagrammed in Fig. 1.

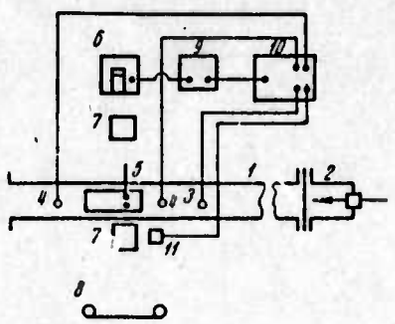

Fig. 1. Test apparatus. 1 - low pressure chamber, 2 - high pressure chamber, 3 - viewing windows, 4 - pressure sensors, 5 - liquid nitrogen drop generator, 6 - flare lamp, 7 - targets, 8 - fixed film, 9, 11 - delay circuit, 10 - oscillator trigger.

Parameters were: internal boiling point temperature of liquid nitrogen drop generator, 77° K; liquid density, 0.82 kg/m^3; viscosity, $2 \cdot 10^{-4}$ kg/(mxsec); surface tension, 15×10^{-3} n/m; low pressure chamber temperature and pressure, 293° K and 1 atm; and liquid nitrogen critical temperature, T^* 126° K, representing a relative supercritical temperature T/T^* in the medium of 2.23. Liquid drop breakup was studied for d_o = 40 to 500 μ nitrogen drops in shock waves with rectangular and triangular pressure profiles. Shock wave Mach numbers varied between M = 1.06 to 1.2 and the duration of triangular wave positive pressure phases was δt = 800 to 950 μsec. Rectangular pressure profile waves had a flow duration with constant parameters of $t > 2.5$ μsec. Pressure sensors measured wave parameters at an error rate of 20 to 25%. Microphotograph measurements of drop size and the time calculations were accurate within 10%.

Tests results show that breakup factors are a negligible function of the ambient temperature. Earlier findings on the characteristics of liquid breakup at $T/T^* \approx 0.5$ to 0.7 are also valid at $T/T^* \approx 2$. Increased ambient temperatures affected only the vaporization of an atomized liquid.

At ambient temperatures $T/T^{*}>1$, liquid vaporization is basically a factor of liquid breakup dynamics, since at a critical Weber number, We^{*}, the vaporization rate of the developing particles greatly exceeded the destruction rate of the source drops. Drop vaporization at $We>We^{*}$ only slightly affects the initial mass. Pressure of saturated vapor p_v approaching the ambient pressure did not affect the liquid drop breakup. Tests also show no variation in the destruction time from abrupt liquid boiling at $p_v>p$.

The authors conclude that destruction and vaporization of fuel drops at an ambient supercritical temperature occurs in a time t^{*} analogous to that under atmospheric conditions.

Gogosov, V. V., and V. A. Polyanskiy. Structure of electrohydrodynamic shock waves. PMM, no. 5, 1972, 851-865.

Electrohydrodynamic shock waves structures are analyzed for small Prandtl numbers ($P<<1$) when the temperature of the medium can be considered constant, and large Prandtl numbers ($P>>1$), when heat conduction processes can be neglected.

It is shown that when the sign of the electric field component E_I^{*} at the shock wave front is normal to the front and coincides with the sign of the velocity component u_I^{*} normal to the shock wave front (i.e., $u_I^{*} E_I^{*}>0$), the shock wave maintains a structure and an electric field component normal to the front. When $u_I^{*} E_I^{*}<0$, and the current density $j^{*}>0$, the shock wave structure does not exist for all parameters at wave front. The structural analysis reveals that in this case the electric field value behind the wave front

is either equal to that at the wave front ($E_{II}^{*}=E_{\perp}^{*}$) or is connected with velocity u_{II} by the relation $u_{II}^{*} + bE_{II}^{*} = 0$, where b is the coefficient of motion. Parameters for the first and second cases of shock wave fronts are determined. A non-structured class of evolution waves is indicated. Results of analysis of structures and the evolution of waves show that the shock waves in electrohydrodynamics are always compression waves.

When the velocity and the electric field behind the shock wave are correlated by the relation $u_{II} + bE_{II}^{*} = 0$, the system of shock wave front equations can be reduced to a cubic equation in u_{II}. When the least of three possible real roots of this equation is larger than the sound velocity behind the wave, the shock wave is unstructured and nonevolutionary. When the least real root is smaller than sound velocity, a range of parameters at the shock wave front is revealed, corresponding to a structured shock wave. The two other real roots of the cubic equation correspond to nonevolutionary, unstructured shock waves. When the cubic equation has only one real root, the shock wave is structured if the value of the root is less than the sound velocity behind the shock wave front, but is unstructured in the opposite case.

When $u_I^{*}E_I^{*}<0$, current density is $j^{*}<0$, and $u_I^{*} + bE_I^{*} \neq 0$, the shock wave structural analysis indicates that the electric field at the wave front is continuous. The field at the shock wave front may have discontinuities when $u_I^{*} + uE_I^{*} = 0$. To determine the flow parameters behind the wave front, $E_{II_*}^{*}$ (or any other front parameter) must be defined. Bounds within which E_{II}^{*} can be defined are indicated. If $u_{II}^{*} + bE_{II}^{*} \neq 0$ in such shock waves, the u_I^{*} is larger and u_{II}^{*} is smaller than the velocity of sound. If $u_{II}^{*} + bE_{II}^{*} = 0$, the velocity of the medium at the front and behind the shock wave front is supersonic.

Semenova, I. P. and A. Ye. Yakubenko. One-dimensional electrohydrodynamic flow with shock waves. PMM, v. 36, no. 5, 1972, 866-873.

One-dimensional stationary electrohydrodynamic flow in a channel with shock waves is analyzed. It is assumed that the shock wave location and all parameters already of the shock wave are known. Based on these parameters and shock wave relations derived using integrals of electrohydrodynamic equations, the authors calculate dimensionless parameters S, R_q, M_1 and V_g, and a cubic equation in V is formulated. For $R_q^{-1} \leq V_g$, the electric field behind the shock wave is continuous. When $R_q^{-1} > V_g$, the electric field displays a discontinuity on the shock wave. V is determined from the cubic equation, with roots from the interval $V_g < V < R_q^{-1}$. When $R_q^{-1} < \sqrt{V_g}$, the cubic equation has only one solution, which corresponds to the transition from a supersonic to a subsonic regime. It is possible for $R_q^{-1} > \sqrt{V_g}$ to formulate a criterion for the existence of a root in the subsonic regime. This criterion is expressed as:

$$R_q^2 > \frac{P_g(\sqrt{V_g}) + S\sqrt{V_g}}{SV^{1.5}} \qquad (1)$$

When the interaction parameter S is small, this inequality is always satisfied. If condition (1) is not satisfied, all three roots of the cubic equation are located in a supersonic domain; and, at such S, R_q and M_1, a stationary flow with shock waves evidently does not occur. In the plane (E,v), an electrical field versus velocity diagram is constructed which aids in flow analysis based on electrical field and velocity values at the shock wave front. An electrohydrodynamic shock adiabat is also constructed for the perfect gas.

Chushkin, P. I. Method of characteristics for three-dimensional supersonic flow. AN SSSR, Vychislitel'nyy tsentr, Moskva, 1968, 122 p (RZhMekh, 11/72, no. 11B340 K) (Translation)

A numerical method of characteristics is presented to solve problems of supersonic stationary three-dimensional flow around a body. Other numerical methods of calculation are discussed briefly, and development of the three-dimensional method of characteristics is reviewed. Basic equations of characteristics are derived in three independent variables. The main part of the study is devoted to four numerical programs of the three-dimensional method of characteristics which are efficiently used to calculate three-dimensional supersonic gas flow. The programs are: forward tetrahedral, backward tetrahedral with interpolation throughout and those using bicharacteristic directions only or two-dimensional characteristic correlations. The programs are initially formulated for a perfect gas, then extended to a real gas with allowance for equilibrium and nonequilibrium physicochemical conversions. Numerical data are given for three-dimensional supersonic flows, including nonequilibrium flow.

Gorskiy, V. B. Eddy-free relativistic gas flow. DAN SSSR, v. 207, no. 2, 1972, 309-312.

The isentropic vortex-free, steady-state flow was analyzed of an ideal gas based on relativistic theory. Since the Bernoulli integral for the entire gas volume is satisfied, the two conditions for vortex-free flow are formulated. Adding the isentropicity condition to these equations and representing the continuity equation for the steady-state flow in velocity components, a closed system of four equations is derived describing the flow

in an ordinary Euclidean space. Assuming that the sound velocity and enthalpy have a specific form, exact equations of motion in velocity components and equations for the potential and stream functions are initially derived for plane and axisymmetric flow. The flow equations are simplified using the theory of small perturbations in the subsonic, supersonic and hypersonic ranges. Approximate equations for subsonic, supersonic and hypersonic flow in plane, axisymmetric and three-dimensional cases are described. Based on the relativistic flow equations, the similarity laws are generalized, and in an analogous manner, approximate equations and similarity laws for three-dimensional flow are established. All calculated results within the nonrelativistic limit ($c \longrightarrow \infty$, c - light velocity) are precisely convertible into corresponding formulas and equations of normal gas dynamics.

Koshelev, E. A. Energy dissipation from an underground explosion. ZhPMTF, no. 5, 1972, 184-187.

The initial temperature field from an underground explosion is analyzed along with the relationship between the energy used for heating the ground, the energy dissipated in the plastic flow behind the shock wave-front, and the residual energy in the detonation products when the motion of the cavity boundary stops. The solution is based on the ground model of Kompaneyets (DAN SSSR, 109, 1, 1956) is used. According to the model, the equation of the ground state for a spherical symmetry is formulated as:

$$\rho\left(\frac{\partial u}{\partial t} + u\frac{\partial u}{\partial r}\right) = \frac{\partial \sigma_r}{\partial r} + \frac{2(\sigma_r - \sigma_\theta)}{r}, \frac{\partial}{\partial r}(r^3 U) = 0 \qquad (1)$$

with the plasticity condition

$$\sigma_r - \sigma_\theta = k + m(\sigma_r + 2\sigma_\theta) \qquad (2)$$

and the cavity boundary and shock wave front conditions

$$\sigma_r(a) = -P(a)$$
$$\sigma_r(R) = -\rho\xi\dot{R}^2 - P_* \qquad (3)$$

where R - the shock wave front radius, a - the cavity radius; σ_r, σ_θ - components of the stress tensor, r - a coordinate, u - mass velocity of particles, P(a) cavity pressure, P_* - the pressure of irreversible compression, k and m - plasticity parameters. From Eq. (1), conditions (2, 3) and the relation between R and a based on the mass conservation law, a second order differential equation for the shock wave front radius R is derived which is reduced to a dimensionless form in y ans x variables. This equation was solved by computer for the values: $P_0 = 7.97 \times 10^4$ kg/cm^2; $P_* = 6$ kg/cm^2 and k = 1.41 kg/cm. Integral curves are represented graphically for four sets of ξ ($\xi = 1 - \frac{\rho}{\rho_0}$; ρ_0 - initial density) and m values. Expressions for the compression, energy e, and plastic flow energy l_2 are formulated and graphically represented for $\xi = 0.05$ and m = 0.233. Formulas for total compression energy, E_1, plastic flow energy E_2 are derived. Quantitative relations between E_1, E_2 and residual energy E_3 given in percentages for various ground characteristics are tabulated.

Results indicate that the largest part of explosion energy is in the plastic flow behind the shock wave. The initial temperature field in the ground after an explosion has a delta shaped character, with maximum temperatures on the cavity boundary and very rapid decay with distance.

Zhubayev, N., and K. Zhunusov. Study of the effectiveness of an air-cushion charge. IN: Sbornik. Problemy voprosov mekhaniki gornykh porod, Alma-Ata, Izd-vo Nauka, 1972, 166-182 (RZhMekh, 11/72, no. 11B265)

A theoretical analysis is given of the effectiveness of a borehole air cushion charge, placed at a distance above the borehole bottom. Charge detonation products parameters (pulsation, pressure, and the duration of the detonation products effect on the borehole walls) and the tamping material motion rate are compared with those of a standard core charge. Assumptions are that the explosive charge converts instantly to a high-pressure gas; wave effects on the detonation products are negligible; the velocity of the detonation products rock interface is low relative to the axial dispersion rate of detonation products in the borehole; and the detonation products propagation along the boundary is consequently one-dimensional. The tamping material is considered to be nondeformable and rigid. The tamping material propagation rate is determined by applying Newton's law to the entire material mass. It is assumed that the detonation products of an air-cushion charge expand instantly in the air-cushion to a pressure equal to that given by a polytropic relation. For a conventional core charge, detonation products expand according to a polytropic equation with exponent $n = 1.25$. The theoretical plots show that application of an air-cushion contributes to a substantial deceleration of the tamping material, an increase in the duration of the detonation products effect on the borehole walls, and a decrease of the initial peak pressure of detonation products.

Kandyba, M. I., O. B. Bakhtin, and E. V. Chudutov. Effect of total explosion delay gap on reduction in seismic oscillation velocity. IN: Sbornik. Akustika v stroitel'stve, Kiyev, Izd-vo Budivel'nik, 1972, 63-67 (RZhMekh, 11/72, no. 11V119)(Translation)

Surveying data are examined on the seismic effect of short delay borehole charge explosions on buildings and installations located on irrigated ground with a complex geology. It was established that prolongation of the blast effect decreases the vibration velocity of the buildings and installations. Formulas are given for calculating earthquake-proof ranges and the weight of explosive charges.

Kandyba, M. I., and A. S. Zhmudenko. Effect of the number of short delay explosion stages on seismic wave generation. IN: Sbornik. Akustika v stroitel'stve, Kiyev, Izd-vo Budivel'nik, 1972, 57-62 (RZhMekh, 11/1972, no. 11V791)(Translation)

A study is presented of the seismic wave interference and damping from the explosion of charges in rocks, based on the selection of the number of delaying stages between groups of simultaneously exploding charges. The results are applicable to protection techniques for objects located within the seismically dangerous zone of a blasting operation.

Lebedev, T. S., D. V. Korniyets, V. I. Shapoval, and V. A. Korchin. Uprugiye svoystva gornykh porod pri vysokikh davleniyakh (High-pressure eleastic properties of rocks). Kiyev, Izd-vo Naukova dumka, 1972, 184 p. (RZhMekh, 11/72, no. 11V802 K). (Translation)

This monograph is divided into two parts. Part I is a study of elast properties of rocks under high hydrostatic pressures; and Part II, a study of elastic constants of rocks under high quasiuniform pressurec and temperatures.

Drukovanyy, M. F., V. G. Kozlov, and I. A. Semenyuk. Experimental investigation of fracturing in stressed media. IN: Sbornik. Termomekhanicheskiye metody razrusheniya gornykh porod, Kiyev, Izd-vo Naukova dumka, part b, 1972, 11-14 (RZhMekh, 11/72, no. 11V607). (Translation)

An experimental study of crack formation was made in rock (salt, marble) and transparent material (plexiglas, glass) specimens, uniaxially compressed by exploding charges of different sizes. Qualitative crack disposition patterns are identified for various compressive load values.

Komir, V. M., L. M. Geyman, V. S. Kravtsov, and N. I. Myachina. Modelirovaniye razrushayushchego deystviya vzryva v gornykh porodakh (Modelling of destruction in rocks from blasting). Moskva, Izd-vo Nauka, 1972, 216 p. (RZhMekh, 11/72, no. 11V803 K). (Translation).

Basic postulates of dimensional analysis and similarity theory are examined. Methods of rock blasting simulation are initially generalized for application in the study of the explosion mechanism. New similarity criteria, with allowance for the distribution of decreased strength zones, are introduced in the destruction simulation process.

Korsakov, P. F. Effect of rock anisotropy on delay gap during short-delay explosive charge blasting. Fiziko-tekhnicheskiye problemy razrabotki poleznykh iskopayemykh, no. 2, 1972, 49-56 (RZhMekh, 11/72, no. 11V784)(Translation).

A method is introduced for calculation of a delay gap during short-delay blasting, allowing for anisotropic rock characteristics. Anisotropy is defined as the ratio of longitudinal wave propagation velocity in the direction of the least resistance to the velocity in a normal direction. Formulas are derived for the optimum delay gap of limestone, dolomite, and granite. Experimental data support the admissibility of the derived formulas in delay gap calculations.

Zapol'skiy, A. K., V. B. Rozanov, and I. V. Kholin. Initial stage of discharge development from an electric explosion of a wire in vacuum. KSpF, no. 5, 1972, 3-8.

The initial stage of discharge development from an electric explosion of a wire was investigated in vacuum in a 200 mm diameter steel chamber at pressures to (2 --3)x10^{-4} torr (Fig. 1). A 0.38 mm copper wire

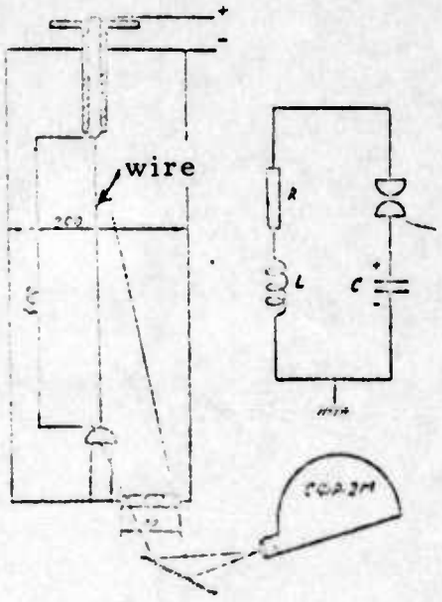

Fig. 1. Exploding wire experiment. Dimensions in mm.

was stretched between two stainless steel electrodes, and a 120 μf capacitance condenser battery, charged to 25 kv, was used as a power source. A Rogovski belt measured the discharge current through the wire, and a high speed camera photographed the discharge at 5x10^{5} frames/sec. Tests were conducted first at a discharge chamber and busbar inductance of L = 320 nh and battery voltages U from 7 to 25 kv (which corresponded to an energy storage of 2.9 ~37.5 kj); and then with L increased to 600 nh. In the first

case, the discharge development pattern did not vary significantly. The wire was preheated by current and breakdown subsequently occurred in the vapors forming near the surface. After about 24 μsec, the discharge column disintegrated and current started flowing in the chamber space, during which the copper wire maintained its initial form and location. In the second case, at battery voltages U > 23 kv, the wire evaporated simultaneously over the entire volume, but only the external part of the gaseous clouds glowed, through which most of the current passed. The glow region width varied negligibly with time. The internal diameter of the cold region increased at the rate of 1.4 km/sec. Fig. 2 illustrates discharge

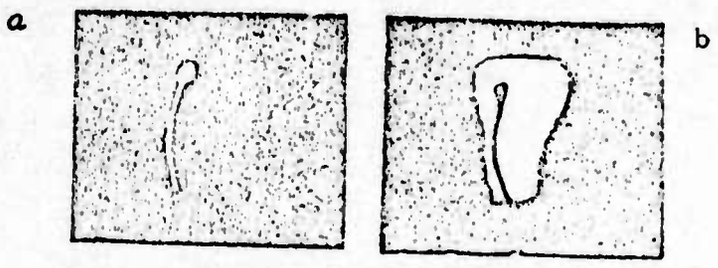

Fig. 2(i). Discharge development at L = 320 nh. a) after 2 μsec; b) after 16 μsec.

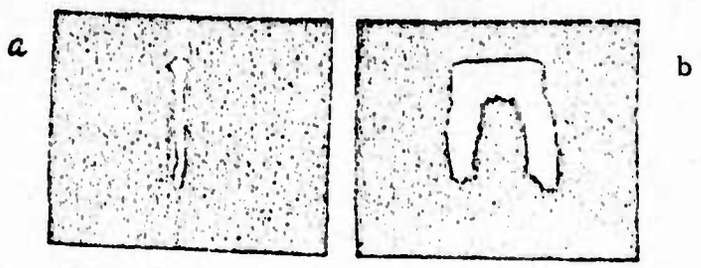

Fig. 2(ii). Discharge development at L = 600 nh. a) after 2 μsec; b) after 14 μsec.

development. At 320 and 600 nh, and 22 and 24 kv, respectively, the sublimation time was identical, amounting to ~4 μsec; but discharge characteristics differed substantially. The authors conclude that phase transition in the wire material does not necessarily occur simultaneously over the whole wire length, and that the transient dynamics are a complex function of circuit parameters.

Vorob'yev, V. S., and A. L. Khomkin. Characteristics of Debye shielding and the equation of state for a partially-ionized plasma. TVT, no. 5, 1972, 939-949.

A modified hamiltonian, derived from an ordinary coulomb electron-ion hamiltonian with the aid of canonical transformation, is used to describe a partially ionized plasma. After canonical transformation, the hamiltonian has the form

$$\begin{aligned} H = &\sum_{\alpha}(\varepsilon_{\nu}-\mu_{\nu})a_{\nu}^{+}a_{\nu}+\sum_{\alpha}(E_{\alpha}\sin^{2}f_{\alpha}+T_{\alpha}\cos^{2}f_{\alpha})Q_{\alpha}^{+}Q_{\alpha}- \\ &-\sum_{\alpha\nu\omega}\sin f_{\alpha}\cos f_{\alpha}(E_{\alpha}-T_{\alpha})\varphi_{\alpha}(\nu\omega)(a_{\nu}^{+}a_{\omega}^{+}Q_{\alpha}+ \\ &+Q_{\alpha}^{+}a_{\omega}a_{\nu})+\sum_{\nu\omega,\omega'\nu'}\Big[(\nu\omega|V|\omega'\nu')-\sum_{\alpha}\sin^{2}f_{\alpha}(E_{\alpha}-T_{\alpha})\times \\ &\times\varphi_{\alpha}(\nu\omega)\varphi_{\alpha}(\nu'\omega')\Big]a_{\nu}^{+}a_{\omega}^{+}a_{\omega'}a_{\nu'}+H', \end{aligned} \tag{1}$$

where E_{α} is the eigenvalue of the Schroedinger energy equation for fermions ν and ω, interacting with the potential V. The electron-ion potential after canonical transformation is shown in Fig. 1.

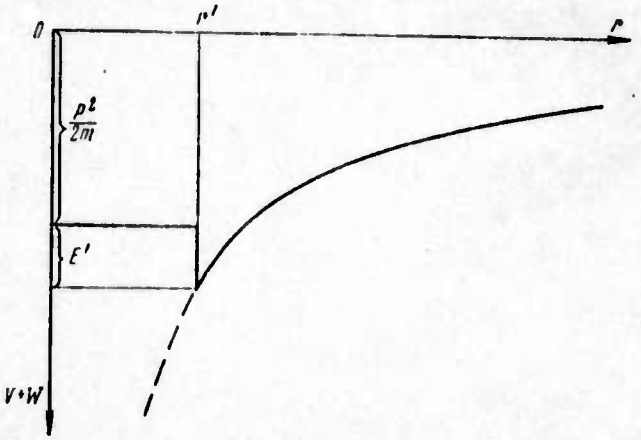

Fig. 1. Form of electron-ion potential after canonical transformation $r' = e^2/\frac{p^2}{2\mu} + |E'|$. The dashed line is the Coulomb potential e^2/r.

The correction for electron and ion energy is calculated by taking into account the non-Coulomb part of the interaction W in the Hartree-Fock approximation. The Debye correction of thermodynamic potential (Ω), corresponding to the hamiltonian $\tilde{H}$, is found from the ring approximation

$$-\frac{\beta\Lambda\Omega_D}{V}=\frac{2\sqrt{\pi}\,e^2\beta^{1/2}}{3}(\tilde{n}_e+\tilde{n}_i)^{3/2}. \tag{2}$$

Numerical solution of the equation of state for Ω has the final form

$$-\frac{\beta\Omega}{V}=\frac{e^{\beta\mu_e}}{\Lambda_e^3}+\frac{e^{\beta\mu_i}}{\Lambda_i^3}+\frac{2\sqrt{\pi}e^2\beta^{1/2}}{3}\left(\frac{e^{\beta\mu_e}}{\Lambda_e^3}+\frac{e^{\beta\mu_i}}{\Lambda_i^3}\right)^{3/2}\zeta(\gamma^3)+\frac{e^{\beta(\mu_e+\mu_i)}}{\Lambda_i^3}\Sigma_a, \tag{3}$$

where $\zeta(\gamma^3)$ is the correcting function for the Debye term, whose graph is shown in Fig. 2.

Fig. 2. Dependence of ϵ, ζ, ζ_1 on γ^3. The dashed line is the asymptotic expression (38) for ϵ.

As follows from (3), ζ_1 reduces the Debye term at high densities. This decrease is physically related to the fact that the electrons whose kinetic energy is less than or on the order of the average energy of interaction are probably captured by the ions to form atoms. In fact, these electrons do not take part in Debye shielding, but their fraction increases as density increases.

Vetchinin, S. P., A. G. Khrapak, and I. T. Yakubov. Equation of state for a plasma of dense metal vapors and electron mobility. TVT, no. 5, 1972, 954-960.

A low-temperature, weakly-ionized plasma of dense metal vapors (e.g., Hg) is analyzed with allowance for electron (ion)-neutral atom interactions and, in the first approximation, paired atom-atom interactions. The equations of state and ionization equilibrium are derived. The equation of state of the nonideal plasma could not be reduced to a Van-der-Waal equation, because the pressure difference $(p-p_o)$ between the nonideal and ideal plasma increases exponentially with the atom concentration N. An electron mobility μ formula which was derived without allowance for interatomic reactions, indicates an exponential decrease of μ with an increase in N. The theoretical expressions for a nonideal plasma are explained in terms of the atomic cluster formation around an electron. A comparison with literature experimental data on a plasma of pure Hg and Hg with small Cs additions generally confirmed the authors' basic theoretical premises.

Sevast'yanov, R. M and N. A. Zykov. Equation of state for a dense gas. TVT, no. 5, 1972, 979-987.

The authors propose a semi-empirical equation of state with principal terms obtained theoretically and in the same form as the Van der Waal equation. A statistical mechanics equation of state of a dense fluid composed of spherical, nonpolar molecules is used as an initial equation.

By splitting and evaluating the integral in the right-side of the initial equation and using expansions of certain functions in series, a new equation of state for dense gas is derived. The equation contains the "compressibility" term Z(y) for a dense gas composed of rigid spheres. An approximate form for Z(y) is obtained and the equation of state is revised and applied to the calculation of the compressibility of argon and methane. Calculation results compared with experimental data in the literature are presented in four tables. Verification of 302 experimental points, including a solidification curve for argon, indicates that the mean deviation calculated from experimental results was 0.47% and the maximum deviation was 2.82%.

Fortov, V. Ye., and B. N. Lomakin.
Interpolated equation of state for tungsten.
TVT, no. 5, 1972, 1118-1119.

An interpolated equation of state for tungsten at intermediate pressures is derived using the method of the author Fortov and Krasnikov (ZhETF, 59, 1970, 1645) and in the form of the polynomial

$$E(p, V) = \sum_{k+l \leq q} \sum a_{kl} V^k p^l, \qquad (1)$$

where E-internal energy, p - pressure, V - specific volume. The l_{KL} coefficients were determined from experimental data in the literature on shock compression of the continuous and porous tungsten. Tungsten shock adiabats for $p \gtrsim 100$ mbar were calculated according to Thomas-Fermi theory at the finite temperature $T \neq 0$. Coefficients of the equation polynomial (1) at q = 3 are tabulated. Shock adiabats for various initial porosity were formulated from the numerical solution of the equation

$$\tfrac{1}{2}(p + p_0)(V_0 - V) = E(p, V) - E_0. \qquad (2)$$

Hugoniot adiabats for various porosities calculated using Eqs. (1) and (2) are plotted in Fig. 1.

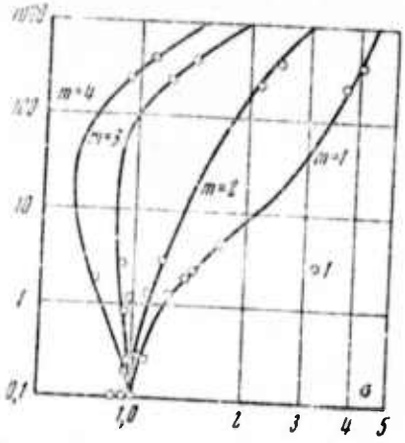

Fig. 1. Hugoniot adiabats of various initial porosity, $m = \rho_o^*/p_o$ (ρ_o - initial density in the medium, ρ_o^* - density of continuous material), calculated using equations (1) and (2). 1 - points used in deriving the equation of state (1). X - axis = p (Mbar), Y - axis = compression level $\sigma = \rho$.

Denisova, N. D., and O. N. Bystrova. Gas phase compressibility of zirconium and hafnium tetrachlorides. Moskva, 1972, 7 p. (RZhKh 19ABV, 20/72, no. 20B586 DEP). (Translation)

P-V-T relationships were obtained for $ZrCl_4$ and $HfCl_4$ vapors using constant capacity piezometers. Equations of state in virial form describe the behavior of gaseous $ZrCl_4$ and $HfCl_4$. The virial coefficients were determined from compressibility data. The volatility coefficients of the compounds are less than unity. Deviation from the perfect state was greater for $ZrCl_4$ because of stronger intermolecular interactions in the $ZrCl_4$ vapor.

Geller, V. Z., A. Ya. Kreyzerova, I. A. Paramonov, and Ye. G. Porichanskiy. Equation of state and thermodynamic properties of liquid F - 113. IAN B, Seryya fizika-enorgetychnykh navuk, no. 4, 1972, 65-68.

The equation of state of liquid freon F-113,

$$P = A(T)\rho + B(T)\rho^3 + C(T)\rho^5, \quad (1)$$

where ρ is the density, was formulated from previously obtained P-V-T experimental data using the procedure of Vasserman and Kreyzerova (ZhPMTF no. 2, 1972). The procedure allows the use of experimental data for an arbitrary T value. Expressions for A(T), B(T), and C(T) are given. Equation (1) is valid in the 240-460° K temperature and 0.1-300 bar pressure ranges at reduced density $\rho/\rho_{cr} > 1.8$. The rms deviation of ρ calculated from (1) was 0.05% for 134 experimental values, and within the experimental error level. The calculated ρ values are in good agreement (within 0.1-0.2%) with earlier data, and deviated by 0.3% from the data for a liquid under pressure. Density, enthalpy, and entropy of liquid freon F-113 in the 240-460° K temperature and 25-300 bar pressure ranges were calculated using Eq. (1). The tabulated enthalpy and entropy data for pressures to 35 bar deviate from the earlier published data by no more than 0.5 kj/kg and 0.002 kj/kg x °K, respectively. The thermodynamic data at pressures above 35 bar is published for the first time.

Mukhitdinov, Dzh. Calculating heat capacities of monatomic gases. IN: Uchenyye zapiski Tashkentskogo gosudarstvennogo pedagogicheskogo instituta, v. 90, 1971, 71-78 (RZhKh, 22/72, no. 22B571)(Translation)

An expression, previously derived by the author for statistical sums of monatomic gases and liquids, is used to calculate equilibrium properties of argon gas. Internal energy, pressure, C_v and C_p heat capacities, enthalpy, and ultrasound velocity are calculated. A comparison of theoretical and experimental data indicates that the theory adequately describes the true evolution of the cited physical parameters. The numerical method introduced, despite its simplicity, is applicable for calculations of the equilibrium properties of homogeneous monatomic gases.

Shamko, V. V. TNT equivalence of a high-power underwater spark discharge. EOM, no. 5, 1972, 16-19.

A theoretical analysis is made of underwater spark discharges and chemical explosions to establish which power source is more advantageous for technological processes such as stamping, lamination, and rock crushing. Allowance was made for wide ranging fluctuations in underwater spark discharge parameters, since only a limited range of parameters have been analyzed in previous studies. The shock wave pressure amplitude P_m was selected as a term of comparison. The energy equivalence factor

$$\zeta = 1{,}8 \cdot 10^{-10} \frac{I^{4/3}}{L^{4/3} C^{2/3}} \qquad (1)$$

(where L is the inductance and C is the capacitance of the spark discharge circuit, and l is the discharge channel length) was introduced as the power equalizing factor. The unknown correlation between the spark discharge P_m and the initial parameters of the spark generator and the water medium was determined. In an acoustic approximation, a cylindrical shock wave P_m at distances $r \leq 2.5\ l$ from the discharge channel was given by

$$P_m = P_a^m \sqrt{\frac{a(\tau_m)}{r}}. \tag{2}$$

where $a(\tau_m)$ is the channel radius at the time τ_m of peak power and P_a^m is the channel maximum pressure at or near τ_m. The discharge channel is assumed to be a plasma cylinder with a uniform l and cross-section.

Correlations between P_m and the discharge and medium parameters were derived from the equation of energy balance in the channel and data in the literature on channel expansion. The correlations

$$P_m = \frac{0{,}16A^{1/4} \rho_0^{3/8}}{\sqrt{r}} \frac{U_0^{3/4} C^{1/8}}{l^{1/8} L^{1/2}}, \tag{3}$$

$$P_m = \frac{0{,}21\,(1 - 0{,}1\,r/l)\,A^{1/4} \rho_0^{3/8}}{\sqrt{r}} \frac{U_0^{3/4} C^{1/8}}{l^{1/8} L^{1/2}} \tag{4}$$

and

$$P_m = \frac{0{,}22A^{1/4} \rho_0^{3/8}}{r^{1.13}} \frac{U_0^{3/4} C^{1/8} l^{1/2}}{L^{1/2}}, \tag{5},$$

(where $A = 0.25 \times 10^5\ V^2 \cdot sec/m^2$ is the spark constant, ρ_0 is the initial

water density, and V_o is the initial voltage) were obtained for the cylindrical ($a(r_m) < r \leq 2.5\ell$), intermediate ($2.5\ell < r \leq 7\ell$), and spherical ($r > 7\ell$) symmetric regions, respectively. A comparison of P_m data calculated from eqs. (3)-(5) with experimental P_m data obtained by the author or taken from the literature (Table 1) indicates that the calculated P_m data are reasonably accurate.

Table 1. Comparison of experimental pressure amplitude data and that calculated from eqs (3)-(5).

Sequence No.	U_o, kV	C, μf	L, μH	l, mm	r, cm	P_m^{exp}, atm	P_m^{exp}, atm	$\lvert\Delta P\rvert$, %
1*	80	0,76	4	320	12	280	370	32
2*	50	6,7	3	264	26,1	210	276	31
3	50	2,87	13,5	121	30,4	110	128,5	17
4	50	2,87	13,5	121	13,7	225	173	30
5	32	2,87	13,5	80	26,5	63	82,5	31
6*	29	3,1	16	40	20	75	67	11
7*	29	3,1	3,2	40	20	200	226	13
8*	29	3,1	8	40	20	115	143,5	25
9*	25	1	15	80	20	80	75,6	6
10	25	2,87	2,25	40	8,3	405	374	8
11*	25	1	0,8	0,5	10	35	43	23
12*	21,6	0,24	3	50	5	230	267	16
13*	19	3,1	3,2	40	20	150	167	11,3
14*	19	3,1	8	40	20	85	105,5	24
15**	15	1	0,8	5	10	63	92	46
16**	15	1	0,8	0,5	6	51	52	2
17**	15	1	0,8	0,5	50	5	4,8	4
18**	10	1	0,8	0,5	10	22	21,6	2
19**	5	1	0,8	0,5	10	14	14	0

The experimental P_m measurements were made in the middle of a plane perpendicular to the discharge channel axis. Eqs.(3)-(5) may be applied in the design of hydroelectric power plants.

---

* Data of I. Z. Okun' (ZhTF, v. 41 no. 2, 1971, 292-301).

** Data of L. Bjorno (Amer. Soc. Mech. Eng., 1969, 111).

Using Eq. (5), the P_m of a spherical shock wave generated by an underwater spark discharge was compared to the P_m of a TNT explosion. The latter was expressed by the Cole formula as a function of the energy E_T of the TNT charge. The spark discharge P_m was expressed by a similar formula as a function of discharge energy $E_d = CU_o^2/2$ multiplied by the equivalence factor (1). It follows from this factor that variable U_o discharges or those with ζ equal to that of the TNT explosion are the only ones which are similar in energy to TNT explosions. A set of differing explosives with the equivalent weight $G_e = \zeta E_d/Q$ (where Q is the specific energy of the explosive charge) is required to match the underwater spark discharge power. Since ζ is often > 1 or $\zeta = 7.45$ for the no. 1 type of discharge in Table 1, the use of high-power under water spark discharges in engineering operations is frequently more advantageous energetically than chemical explosive charges.

Antonov, E. A., and A. M. Gladilin. Amplification of detonation waves in secondary reaction zone of a two-phase medium. MZhiG, no. 5, 1972, 92-96.

A numerical solution is obtained to a problem on the non-stationary one-dimensional flow of a gas plus solid particle mixture, with secondary chemical reactions between particle vapor and detonation products. It is assumed that an $H_2 + 1/2\ O_2$ mixture detonates in a half-space $X > O$ yielding a detonation H_2O product which reacts exothermically, behind the detonation wave front with element A vapors. Under certain conditions, the heat Q of this secondary reaction is transferred to and amplifies the primary detonation front. To determine the amplification conditions, the flow of each phase of the two-phase medium is described by separate sets

of differential equations with allowance for phase transitions and chemical reactions. The two sets of equations are solved simultaneously by the movable net method. The method of characteristics with iteration is applied to numerically integrate the set describing the solid phase.

Results were used to map flow profiles behind the detonation wavefront at 50 cm from the origin. The profiles (Figs. 1, 2, and 3) were

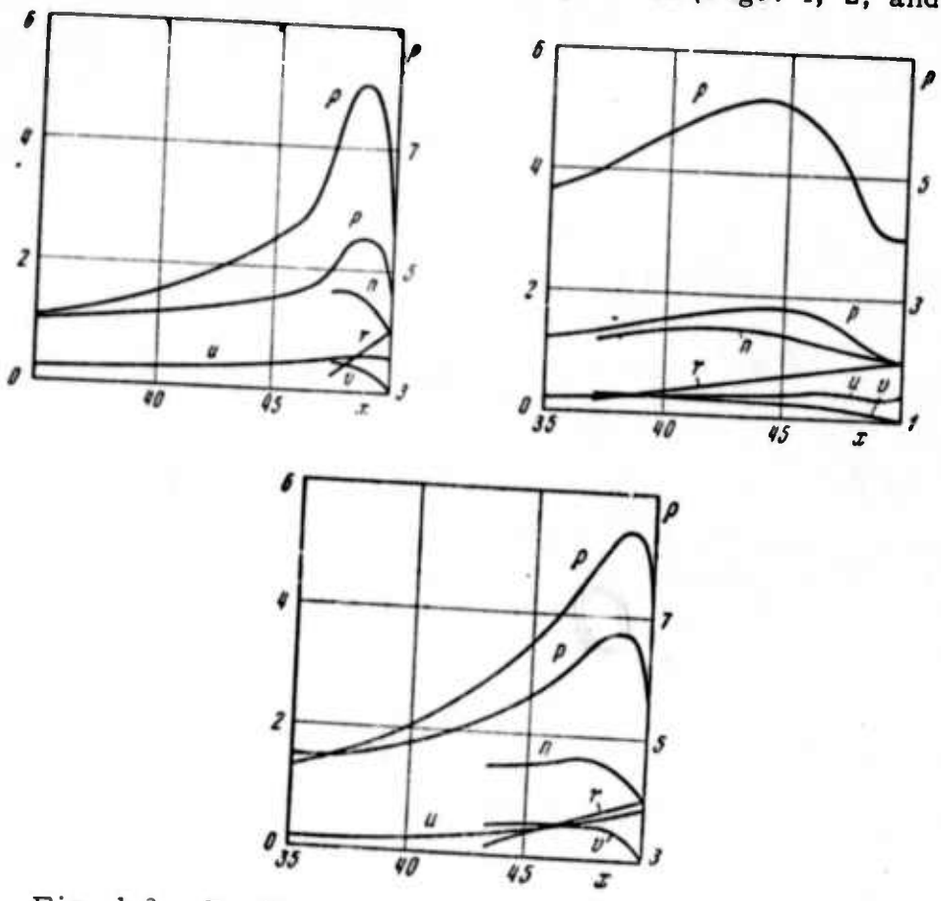

Fig. 1-3. Profiles of gas velocity u, pressure p, density ρ, particle number n/unit volume, particle radius r, and particle velocity V behind a detonation wave. The scale of ρ is at the right; the scale of the other parameters is at the left. Fig. 1: $r = 2.5 \times 10^{-6}$ m, Q = 150 kcal/mol; Fig. 2: $r = 5 \times 10^{-6}$ m, Q = 150 kcal/mol; Fig. 3: $r = 5 \times 10^{-6}$ m, Q = 250 kcal/mol.

calculated for a detonation wave front initially propagating at D_o = 2,500 m/sec. All of the parameters plotted in ordinates of the Figs. 1-4 are dimensionless and the distances x are in cm. Under the conditions illustrated in Figs. 1 and 3, D increased by 85 and 575 m/sec., respectively. The pressure p in these cases increased behind the wave front owing to increases in ρ, from intensive vaporization. Notwithstanding the sharp slope of the p profiles, a shock wave was not formed and the thermodynamic function profiles behind the detonation wave were stable. The D profile in Fig. 4 shows that the detonation front is perturbed at 8 cm from

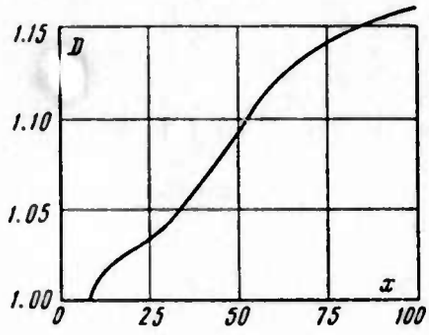

Fig. 4. Detonation front velocity vs. distance from the origin of detonation: $r = 5 \times 10^{-6}$ m, Q = 200 kcal/mol.

the origin. The amplification is explained by the increases in temperature immediately behind the front and the gas velocity in the interval between the p hump and the front. The D (x) profile levels at x > 100 cm. D does not increase, even at Q = 300 kcal/mol., in the presence of particles with $r > 10^{-5}$ m.

Kiyashko, S. V., M. I. Rabinovich, and V. P. Reutov. Observation of explosive instability of parametrically-guided waves. ZhETF P, v. 16, no. 7, 1972, 384-387.

Results are described of experimental observations of the explosive instability of electromagnetic waves. Experiments were conducted in a nonlinear medium in the RF range on a two-wire transmission line with nonlinear leakage and a current and voltage relationship $j = \sigma_H U^2$. Tunnel diodes were used as nonlinear leakage components with operating points at the characteristic maximum. A monochromatic wave with a frequency of ω_1, ω_2, or ω_3 was generated in the test system, in which linear dissipation was introduced independent of the tunnel diodes; the wave attenuated exponentially during line propagation. A pair of waves, with frequencies ω_i and ω_j was subsequently applied, and a third, combined frequency wave was generated as a result of synchronism; the amplitudes of all waves increased simultaneously. The growth rate was dependent on the amplitude boundary values. When synchronism did not occur, both waves decayed independently. A similar experiment was conducted for a degenerating case: the interaction of fundamental waves with second harmonics, which yielded similar results. Fig. 1 shows the attenuation of the

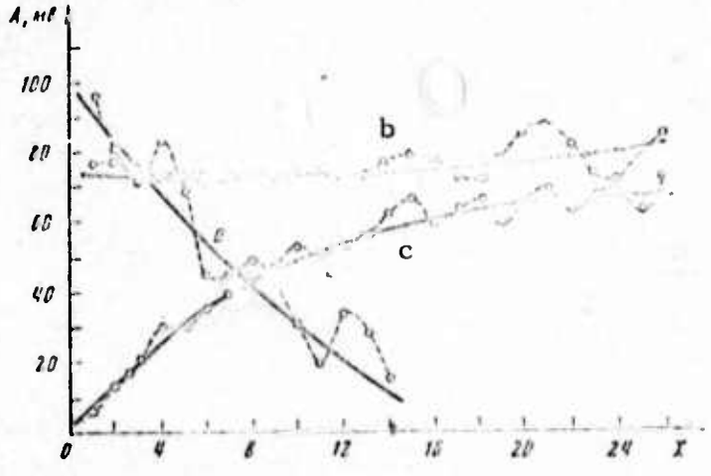

Fig. 1. Attenuation of ω and 2ω waves.

ω and 2ω waves without interactions (curve a); and with a nonlinear interaction (curves b and c). It is seen that under synchronism the wave amplitudes simultaneously increase, attesting to the presence of explosive instability. The results were also valid in the absence of linear dissipation.

B. Recent Selections

i. Shock Wave Effects

Adadurov, G. A., O. N. Breusov, V. N. Drobyshev, and S. V. Pershin. Effect of shock waves on materials: phase and chemical reactions in niobium pentoxide. IN: Sb. Goreniye i vzryv, Moskva, Nauka, 1972, 540-543. (RZhKh, 5/73, no. 5B823)

Adadurov, G. A., V. I. Gol'danskiy, and P. A. Yampol'skiy. Chemical transformations of condensed materials from shock wave effects. Zhurnal Vsesoyuznogo khimicheskogo obshchestva im. Mendeleyeva, v. 18, no. 1, 1973, 80-89.

Belyakov, V. D. Quantitative analysis of stress waves in an elastic medium under short-duration dynamic effects. IN: Sb. Gornoye davleniye i gornyye udary, Leningrad, VNIMI, sb. 85, 1972, 133-138. (RZhMekh, 2/73, no. 2V108)

Cherepanov, G. P., and V. B. Sokolinskiy. Impact fracturing of brittle bodies. Eng. Fract. Mech, v. 4, no. 2, 1972, 205-214. (RZhMekh, 2/73, no. 2V571)

Danilin, G. A. Asymptotic solution to shock layer equations close to the critical point of a sphere under intensive blowing. MZhiG, no. 1, 1973, 164-168.

Danilov, V. A., G. G. Chernyshov, and A. I. Akulov. Drop impact deformation of liquid films. FiKhOM, no. 1, 1973, 52-58.

Dunayev, Yu. A., G. K. Tumakayev, T. V. Zhiknareva, and V. R. Lasovskaya. Kinetics of ionization and excitation of mercury atoms ahead of and behind a shock front. IN: Shock tube res. Proc. 8th Int. Symp., London, 1971, London, 1971, 33/1-33/12. (RZhMekh, 2/73, no. 2B178)

Gel'fand, B. Ye., S. A. Gubin, S. M. Kogarko, and S. T. Komar. Liquid drop breakup in gas flow behind shock waves with triangular profiles of gas velocity variation. IN: Sb. 11-ya Vsesoyuznaya konferentsiya po voprosam ispareniya, goreniya i gaz. dinamiki dispersnykh sistem, 1972, Odessa, 1972, 58-59. (RZhMekh, 2/72, no. 2B534)

Gendugov, V. M., and I. N. Zverev. Surface temperature of thermally-conductive liquids behind a shock wave with mass transfer and chemical reactions in the boundary layer. VMU, no. 1, 1973, 110-113.

Gladyshev, M. K., and V. A. Gorelov. Experimental determination of ionization time behind a powerful shock wave in air. MZhiG, no. 1, 1973, 171-173.

Ibragimova, L. B. Excitation mechanism of the electron state of a cyanogen molecule in shock waves. IN: Nauchnyye trudy. Institut mekhaniki Moskvoskogo universiteta, no. 18, 1972, 70-87. (RZhKh, 5/73, no. 5B115)

Ivanov, K. G. Configuration of interplanetary shock waves from powerful chromospheric flares (based on space probe measurements). Astronomicheskiy zhurnal, v. 50, no. 1, 1973, 146-149.

Klimishin, I. A., and O. F. Novak. Theory of nonstationary shock waves in a moving gravitational atmosphere. Visnyk L'viv. un-tu, Ser. fiz, no. 7(15), 1972, 20-24. (RZhMekh, 2/73, no. 2B175)

Kubenko, V. D. Constructing step functions in problems of weak shock wave interactions with cylindrical and spherical surfaces. DAN UkrSSR, Ser. A, no. 2, 1973, 148-152.

Mar'yasin, I. L., and Z. A. Nabutovskiy. Kinetics of soot formation from thermal pyrolysis of benzole and acetylene in a shock wave. III. KiK, no. 1, 1973, 175-181.

Nigul, U. K., and Yu. K. Engel'brekht. Shock wave initiation in an elastic half space from one-dimensional nonlinear intermediate wave processes excited by continuous interactions. MTT, no. 1, 1973, 69-82.

Novak, O. F., and I. A. Klimishin. Generalization of the Brinkley-Kirkwood method for the case of nonadiabatic shock waves. Visnyk L'viv un-tu, Ser. fiz., no. 7)15), 1972, 25-27. (RZhMekh, 2/73, no. 2B187)

Pleshanov, I. V. Calculating parameters of a chemically-reacting gas behind incident and reflected shock waves. IN: Sb. Teplofizicheskiye svoystva i gazodinamika vysokotemperaturnykh sred, Moskva, Izd-vo Nauka, 1972, 41-44. (RZhMekh, 2/73, no. 2B184)

Salamandra, G. D. Formation of shock waves before a flame front. IN: ibid., 130-135. (RZhMekh, 2/73, no. 2B167)

Sechenov, V. A., O. Ye. Shchekotov, and O. S. Batsukov. Cesium condensation from an incident shock wave in cesium vapor. TVT, no. 1, 1973, 198-200.

Sinkevich, O. A. Stability of a plane ionized shock wave in a magnetic field. IN: Sb. Fizika nizkotemperaturnogo plazmy, Tr. III Vsesoyuznaya konferentsiya po dinamike razrezh. gazov, VI sekts., Novosibirsk, 1971, 6-11. (RZhMekh, 2/73, no. 2B23)

Tyunyayev, Yu. N., Yu. V. Lisitsyn, Ye. Z. Novitskiy, A. G. Ivanov, and V. N. Mineyev. Electrical conductivity of alloyed and gamma-irradiated NaCl behind shock wave fronts. IN: Sb. Goreniye i vzryv, Moskva, Izd-vo Nauka, 1972, 591-596. (RZhKh, 5/73, no. 5B563)

Wlodarczyk, E. Propagation of a plane loading shock wave in a bilinear elastic rod. Biul. WAT J. Dabrowskiego, v. 21, no. 8, 1972, 49-59. (RZhMekh, 2/73, no. 2V114)

Wlodarczyk, E. Formation and propagation of plane shock waves in an elastoplastic bilinear material. ibid., 61-70. (RZhMekh, 2/73, no. 2V115)

Yaushev, I. K. Decay of an arbitrary discontinuity in branched channels. IN: Sb. Chislovyye metody mekhanicheskogo sploshnogo sredy, Novosibirsk, v. 3, no. 3, 1972, 92-107. (RZhMekh, 2/73, no. 2B169)

Yurmanov, Yu. A., A. B. Ryzhik, B. S. Limonov, and V. S. Makhin. Ignition of dispersed magnesium in oxygen behind shock waves. IN: Sb. II-ya Vsesoyuznaya konferentsiya po voprosam ispareniya, goreniya, i gazovoy dinamike dispersnykh sistem, 1972, Odessa, 1972, 58. (RZhMekh, 2/73, no. 2B1005)

Zubov, Ye. N., and A. F. Sidorov. Solution to a single boundary value problem for unsteady, three-dimensional gas flow and propagation of weak spherical shock waves. IN: Sb. Chislovyye metody mekhanicheskog sploshnogo sredy, Novosibirsk, v. 3, no. 3, 1972, 32-50. (RZhMekh, 2/73, no. 2B156)

ii. Hypersonic Flow

Artonkin, V. G., P. G. Leutin, K. P. Petrov, and Ye. P. Stolyarov. Aerodinamicheskiye kharakteristiki ostrykh i prituplennykh konusov pri dozvukovykh i sverkhzvukovykh skorostyakh (Subsonic and supersonic aerodynamic characteristics of sharp and blunt cones). Tr. Tsentral'nyy aerogidrodinamicheskogo instituta im. Zhukovskogo, Moskva, 1972, 93 p. (KL, 7/73, no. 4768)

Atanov, G. A. Numerical analysis of supersonic flow in a hydrojet. MZhiG, no. 1, 1973, 155-158.

Barantsev, R. G., A. I. Yerofeyev, Yu. D. Nagornykh, A. A. Pyarnpuu, and D. S. Strizhenov. Rarefied gas interaction with solid surfaces. IN: Sb. Vzaimodeystviye goza s poverkhnost'yu tverdogo tela, Novosibirsk, 1971, 1-38. (RZhMekh, 2/73, no. 2B269)

Bochkarev, A. A., N. I. Kislyakov, V. A. Kosinov, A. K. Rebrov, and R. G. Sharafutdinov. Supersonic flow of rarefied gas around a porous plate. IN: Sb. Eksperimental'nyye issledovaniya i voprosy modelirovaniy techeniy razrezhen. gaza i plazmy, Novosibirsk, 1971, 94-99. (RZhMekh, 2/73, no. 2B260)

Burmistrov, A. I., and V. S. Talyzina. Calculating flow regimes of gratings with supersonic profiles using correlated data on blowing of plane subsonic compressor gratings. IVUZ Mashinostroyeniye, no. 2, 1973, 168-169.

Kalinina, S. V., and V. I. Kornilov. Effect of sweep angle and unit Reynolds number on boundary layer transition at supersonic speeds. ZhPMTF, no. 1, 1973, 159-162.

Kapustin, Ye. A., R. D. Kuzemko, A. Ya. Trunov, and V. D. Pugach. Characteristics of transonic and supersonic jets during two-phase flow discharge. IN: Sb. Intensifikatsiya metallurgicheskikh protsessov vduvaniyem poroshkoobraznykh materialov, Moskva, Izd-vo Metallurgiya, 1972, 207-215. (RZhMekh, 2/73, no. 2B393)

Kislyakov, N. I., A. K. Rebrov, and R. G. Sharafutdinov. Diffusion processes in the mixing zone of a low density supersonic jet. ZhPMTF, no. 1, 1973, 121-127.

Korobeynikov, V. P., P. I. Chushkin, and L. V. Shurshalov. Two-dimensional nonstationary problems of volumetric dispersion of compressed gases. IN: Sb. XIII Mezhdunarodnyy kongress po teoreticheskoy i prikladnoy mekhanike, 1972, Moskva, Izd-vo Nauka, 1972, 63. (RZhMekh, 2/73, no. 2B285)

Lapygin, V. I., and N. A. Ostapenko. Supersonic gas flow around the leeward side of a conical wing. MZhiG, no. 1, 1973, 112-121.

Luk'yanov, G. A. Scatter of hypersonic flow on a supersonic gas jet from interactions in a free molecular regime. MZhiG, no. 1, 1973, 176-179.

Omelik, A. I. Gas dynamic molecular source with ohmic preheating. IN: Sb. Vzaimodeystviye gaza s poverkhnost'yu tverdogo tela, Novosibirsk, 1971, 81-86. (RZhMekh, 2/73, no. 2B268)

Polyanskiy, O. Yu. Modelling hypersonic air flow using differing gases. IN: Sb. Eksperimental'nyye issledovaniya i voprosy modelirovaniya techeniy razrezhen. gaza i plazmy. Novosibirsk, 1971, 118-122. (RZhMekh, 2/73, no. 2B485)

Prikhod'ko, V. D., and A. M. Sizov. Approximation of flow parameters from supersonic jet interactions. MZhiG, no. 1, 1973, 168-170.

Provotorov, V. N. Viscous interaction on a plate in hypersonic unsteady dissociative gas flow. IN: Sb. Eksperimental'nyye issledovaniya i voprosy modelirovaniya techeniy razrezhen. gaza i plazmy, Novosibirsk, 1971, 83-87. (RZhMekh, 2/73, no. 2B273)

Shaykhutdinov, Z. G., A. M. Rusak, V. M. Klevanskiy, I. S. Saburov, and Ch. A. Yarullin. Effect of flow model on calculation characteristics of vaporization and afterburning in supersonic high temperature gas flow. IN: Sb. 11-ya Vsesoyuznaya konferentsiya po voprosam ispareniya, goreniya i gazovoy dinamiki dispersnykh sistem, 1972, Odessa, 1972, 64. (RZhMekh, 2/73, no. 2B1008)

Yermolayev, I. K., A. I. Leont'yev, V. A. Fadeyev, and B. N. Yudayev. Convective heat transfer in a zone of supersonic overexpanded jet interaction with an oblique obstacle. TVT, no. 1, 1973, 207-209.

Zavarzina, I. F., A. A. Vasil'yev, and N. V. Prokopenko. Local heat transfer during supersonic rarefied gas flow around a finite length cylinder. IN: Sb. Eksperimental'nyye issledovaniya i voprosy modelirovani techeniy razrezhen. gaza i plazmy, Novosibirsk, 1971, 47-52. (RZhMekh, 2/73, no. 2B868)

Zavarzina, I. F., and A. A. Vasil'yev. Experimental study of local heat transfer of axisymmetric bodies with spherical bluntness in rarefied gas flow. IN: ibid., 112-117. (RZhMekh, 2/73, no. 2B872)

Zusman, V. B., A. O. Koreysha, and V. M. Shkuropatov. Generating high speed molecular beams by ion supercharging in a plasma flow. IN: Sb. Vzaimodeystviye gaza s poverkhnost'yu tverdogo tela, Novosibirsk, 1971, 93-98. (RZhMekh, 2/73, no. 2B262)

Zusman, V. B., and Yu. D. Nagornykh. Generating high speed molecular beams by supercharging an ion beam. IN: ibid., 87-92. (RZhMekh, 2/73, no. 2B263)

Zuyev, N. D., V. M. Kalugin, and M. V. Prochukhayev. Rarefied gas flow around a flat plate with a sharp leading edge. IN: Sb. Eksperimental'nyye issledovaniya i voprosy modelirovaniya techeniy razrezhen. gaza i plazmy, Novosibirsk, 1971, 3-9. (RZhMekh, 2/73, no. 2B267)

iii. Soil Mechanics

Blyumin, M. A. Photogrammetric measurement of ejecta scattering range. IVUZ Gorn, no. 1, 1973, 35-37.

Bodoky, T., G. Korvin, I. Liptal, and J. Sipos. Analysis of initial seismic pulses near an underground explosion. Geofizikai kozlemmenyuk, v. 20, no. 3-4, 1972, 7-27. (RZhMekh, 2/73, no. 2V731)

Borovikov, V. M. Feasibility of using piezoceramics for high pressure measurements (during rock blasting). Fiziko-teknicheskiye problemy razrabotka poleznykh iskopayemykh, no. 3, 1972, 121-123.

Dergunov, V. P., A. V. Steshenko, and V. A. Shumilo. Test measurements of deformation and stress from blasting of inclined (borehole) charges under laboratory conditions. IN: Sbornik nauchnykh trudov Noril'skogo vechernogo industrial'nogo instituta, no. 8, 1970, 61-66. (LZhS, 6/73, no. 18733)

Dmitriyev, A. P., and Yu. I. Protasov. New methods of rock crushing. IVUZ Gorn, no. 12, 1972, 24-33.

Dremin, A. N., K. K. Shvedov, Ye. G. Baranov et al. Study of detonation of industrial explosives: detonation characteristics of 80/20 grain granulite and AS-8 granulite (rock crushing). Fiziko-tekhnicheskiye problemy razrabotka poleznykh iskopayemykh, no. 4, 1972, 41-44.

Drukovanyy, M. F., E. I. Yefremov, V. F. Dzhos, and L. G. Pereyaslavskiy. Effect of charge configuration on explosive pulse parameters during crushing of friable media. IVUZ Gorn, no. 1, 1973, 62-64.

Dudkin, N. K. Protective properties of water-filled charge casings. IN: Sbornik nauchnykh trudov Noril'skogo vechernogo industrial'nogo instituta, no. 8, 1970, 54-60. (LZhS, 6/73, no. 18734)

Firstov, P. P., and V. A. Shirokov. Seismic observations of ground micromotions at the Bol'she-Bannaya deposit of thermal waters. Geologiya i geofizika, no. 7, 1972, 112-115.

Gurin, A. A., and V. L. Grammakov. Attenuation of air shock waves from collisions during blasting in underground mines. IN: Sb. Razrabotka rudnykh mestorozhdeniy, no. 14, 1972, 80-83. (RZhMekh, 2/73, no. 2B172)

Kalinin, A. A., and B. V. Kozlovskiy. Increasing the effectiveness of crushing blast-resistant rock with a large-block structure. IN: Sbornik nauchnykh trudov Noril'skogo vechernogo industrial'nogo instituta, no. 8, 1970, 67-72. (LZhS, 6/73, no. 18737)

Kasumov, F. K. Physical characteristics of explosive crushing of fissured rock and methods of controlling the lump size of rock masses. Za tekhnicheskiy progress, no. 2, 1973, 31-33.

Kravets', V. G., O. O. Vovk, and V. V. Postnov. Allowance for physico-chemical properties of soils in calculating confined and cratering charges. DAN UkrSSR, A, no. 3, 1973, 274-277.

Lemesh, N. I., and B. V. Pozdnyakov. Role of tamping in control of blast effects. Gornyy zhurnal, no. 2, 1973, 45-47.

Lemesh, N. I., and B. V. Pozdnyakov. Kinematic factors of explosive displacement of rock in the demolition zone. Fiziko-tekhnicheskiye problemy razrabotki poleznykh iskopayemykh, no. 4, 1972, 36-40.

Lysenko, Yu. I., V. Ye. Bichuk, and V. Z. Semeshin. Contour blasting in tunnelling. Shakhtnoye stroitel'stvo, no. 10, 1972, 14-16. (LZhS, 7/73, no. 22168)

Plakhotnyy, P. I., I. P. Sadovoy, and V. I. Savityuk. Effect of caving rock pressure on the stress generated in a rock mass from detonation of explosive core charges. IN: Sb. Razrabotka rudnykh mestorozhdeniy, no. 14, 1972, 72-77. (RZhMekh, 2/73, no. 2V735)

Popov, V. Opposed explosions (delayed double charge method for controlled mine-tunneling). Sotsial'isticheskaya industriya, 13 March 1973, p. 2.

Rideshich, I. Feasibility of defining optimum blast parameters from seismic measurement data. Vojnotehnicki glasnik, no. 12, 1972, 1142-1157.

Rideshich, I. Determining destruction parameters using blast wave theory and similarity methods. Vojnotehnicki glasnik, no. 11, 1972, 1040-1053.

Shen'shakov, V. S. Tamping: an important element of blasting. Gornyy zhurnal, no. 2, 1973, 47.

Smirnov, A. A. Search for effective parameters of drilling and blasting in systems with gob flushing using concrete. IN: Sbornik nauchnykh trudov Noril'skogo vechernogo industrial'nogo instituta, no. 8, 1970, 168-176. (LZhS, 6/73, no. 18753)

Tseytlin, Ya. I., N. I. Smoliy, and M. I. Ganopol'skiy. Effect of borehole tamping on the intensity of air shock waves. Gornyy zhurnal, no. 2, 1973, 42-44.

Usov, O. Ya., D. I. Betin, A. Z. Podorvanov, V. P. Barbalyuk, P. A. Ryabov, and A. P. Yakimenko. Use of ammonium nitrate explosives under complex hydrogeological conditions. Gornyy zhurnal, no. 2, 1973, 38-41.

Zabudkin, I. L., Yu. G. Kuznetsov, G. I. Tambiyev, and G. P. Ayshenova. Shaped charge method of detonating a granular explosive charge. Fiziko-tekhnicheskiye problemy razrabotki poleznykh iskopayemykh, no. 4, 1972, 126-127.

iv. Exploding Wire

Aleksandrov, V. M., A. P. Baykov, V. A. Ivanov, A. M. Iskol'dskiy, L. S. Krotman, Yu. Ye. Nesterikhin, and A. A. Nesterov. Modelling and optimizing the parameters of a magnetic-explosive generator with a current breaker. Avtometriya, no. 1, 1973, 46-50.

Industrial applications of an exploding wire device (Impulse-2M). Sctsialisticheskaya industriya, 15 February 1973, p. 4.

Chachin, V. N., V. K. Rakhuba, and N. N. Stolovich. Energy balance during electrical explosive stamping of tubular parts. IAN B, Seriya fiziko-tekhnicheskikh nauk, no. 1, 1973, 80-86.

Shneyerson, G. A. Theory of electric explosion of a skin layer in an ultra-powerful magnetic field. ZhTF, no. 2, 1973, 419-428.

v. Equations of State

Avdeyeva, G. M. Expansion of an equation of state in the $(4-\epsilon)$-dimensional Heisenberg model. ZhETF, v. 64, no. 2, 1973, 741-755.

Borisov, M. I., and P. G. Maslov. Methods of calculating thermodynamic properties of real gases. ZhPK, no. 2, 1973, 351-355.

Malyshenko, S. P. Thermodynamic properties of liquid parahydrogen. IN: Sb. Teplofizicheskiye svoystva veshchestv pri nizkikh temperaturakh, Moskva, 1972, 14-30. (RZhKh, 4/73, no. 4B712)

Pridatchenko, Yu. V., and Yu. I. Shmakov. Rheological equations of state for weakly-concentrated suspensions of rigid ellipsoidal particles. ZhPMTF, no. 1, 1973, 141-145.

Timoshenko, N. I., Ye. P. Kholodov, and A. L. Yamnov. Determining the secondary virial coefficient of compressibility and the secondary refractometric virial coefficient, based on dispersion of refractive index values. ZhFKh, no. 2, 1973, 431-432.

vi. Miscellaneous Effects of Explosions

Aksel'rud, G. A., A. D. Molchanov, I. N. Fiklistov, and V. P. Kosyk. Mass transfer in a solid-liquid system from effects of high voltage spark discharges in a tube. (Deposited in VINITI, 8/25/72, no. 4762-72), Minsk, 1972, 13 p. (RZhMekh, 2/73, no. 2B1044 DEP)

Andreyeva, N. V., L. A. Kursheva, F. B. Moshkovich, V. A. Muradyan, and I. I. Strizhevskiy. Explosive properties of monovinyl acetylene in divinyl acetylene. IN: Sb. Doklady IV Vsesoyuznoy konferentsiy po khimii atsetilena, Alma-Ata, v. 3, 1972, 384-390. (RZhKh, 4/73, no. 4B992)

Aslanov, S K. Stability in combustion of liquid explosives. IN: Sb. 11-ya Vsesoyuznaya konferentsiya po voprosam ispareniya, goreniya i gazovoy dinamiki dispersnykh sistem, 1972, Odessa, 1972, 68-69. (RZhMekh, 2/73, no. 2B1011)

Baranayev, M. K., V. M. Vitelis, and K. M. Shumov. Shell effects on the initial parameters of an underwater explosion of a cylindrical explosive charge. ZhPMTF, no. 1, 1973, 165-168.

Cherepanov, G. P., V. V. Rzhevskiy, and L. V. Yershov. Explosion in a brittle body. Eng. Fract. Mech, v. 4, no. 2, 1972, 215-218. (RZhMekh, 2/73, no. 2V569)

"Exploding" icebergs. Trud, March 15, 1973, p. 4.

Fogel'zang, A. Ye., V. Ya. Adzhemyan, B. S. Svetlov, S. M. Kolyasov, and M. B. Gandel'man. Relationship of explosive compounds combustion rate to initial temperature. IN: Sb. 11-ya Vsesoyuznaya konferentsiya po voprosam ispareniya, goreniya i gazovoy dinamiki dispersnykh sistem, 1972, Odessa, 1972, 38-39. (RZhMekh, 2/73, no. 2B978)

Kostina, Ye. S. Role of hydrogen in ignition of powdered titanium hydride. IN: ibid., 26. (RZhMekh, 2/73, no. 2B958)

Kozlov, V. Effect of an underwater explosion on fish, and determination of the danger zone radius. Rybnoye khozyaystvo, no. 2, 1973. 18.

Lebedev, M. A., and M. M. Rusakov. Detonating an explosion with a high energy density. ZhPMTF, no. 1, 1973, 168-170.

Mel'nikova, N. S. Explosions in detonation media with variable initial densities. PMM, no. 1, 1973, 172-177.

Moisheyev, I. N. Flow parameters behind a stabilized detonation wave under balanced heat and mass transfer. IN: Uchenyye zapiski TsAGI, v. 3, no. 5, 1972, 104-109. (LZhS, 8/73, no. 24740)

Ordzhonikidze, S. K., A. D. Margolin, and Ye. Yu. Skuridin. Combustion of liquid explosives in an inertial force field. IN: Sb. 11-ya Vsesoyuznaya konferentsiya po voprosam ispareniya, goreniya i gazovoy dinamiki dispersnykh sistem, 1972, Odessa, 1972, 43. (RZhMekh, 2/73, no. 2B988)

Potap'yev, S. V., A. N. Sinyukov, and V. G. Korneyev. Method of field seismic surveying using bombing. Geologiya i geofizika, no. 7, 1972, 82-90.

Sagomonyan, A. Ya., and V. A. Kulikov. Explosion of a spherical charge in a compressed plastic medium. VMU, no. 1, 1973, 85-92.

Trofimov, N. I. Effects of an explosion in an elastoplastic space. Condition of repeated loading. IN: Trudy nauchno-issledovatel'skogo instituta matematiki VGU (Voronezh universitet), no. 6, 1972, 28-33. (LZhS, 7/73, no. 21573)

Wolski, W., and A. Burewicz. Ferromagnetic products of an explosive reaction between $Co(NO_3)_2$ and $(NH_4)_4[Fe(CN)_6]$. Acta chimica. Academia scientiarum Hungarica, v. 72, no. 1, 1972, 25-32. (RZhKh, 5/73, no. 5B1020)

3. Geosciences

A. Abstracts

Tokarev, P. I., S. A. Fedotov, A. A. Godzikovskaya, and V. M. Zobin. Earthquakes in Kamchatka and the Commander Islands. IN: Akademiya nauk SSSR. Institut fiziki Zemli. Zemletryaseniya v SSSR v 1967 godu (Earthquakes in the USSR in 1967). Moskva, Izd-vo Nauka, 1970, 188-215.

Detailed observations of earthquakes in Kamchatka and the Commander Islands, begun in 1961, were continued in 1967. A network of 14 seismographic field stations operated in 1967, including the reopened Ozero station which expanded the area of reliable recording of earthquakes with $E \geq 10^8$ j. The stations were equipped with VEGIK seismograph system with T_s = 1.2 sec and M_{max} = 10,000 at 1-20 Hz, except for the station at Esso which has an SKM seismograph system with T_s = 1.2 sec and T_{max} = 30,000. A catalog listing of the following data on 806 earthquakes with $E \geq 10^9$ j occurring in Kamchatka and the Commander Islands in 1967 is given: date, origin time (GMT), epicenter coordinates, focal depth, energy class K = lgE(j), accuracy class in determination of the epicenter, accuracy class in determination of the focal depth, and the name of the region where the earthquake originated. The distribution of all 1481 recorded earthquakes with respect to energy is as follows:

Earthquake energy (in joules)	10^7	10^8	10^9	10^{10}	10^{11}	10^{12}	10^{13}	10^{14}	10^7-10^{14}
No. of earthquakes	198	477	386	242	122	45	9	2	1481

Two epicenter maps are given, one for earthquakes with $E \geq 10^9$ j (Fig. 1) and the other for earthquakes with 10^7 j $\leq E \leq 10^8$ j (Fig. 2).

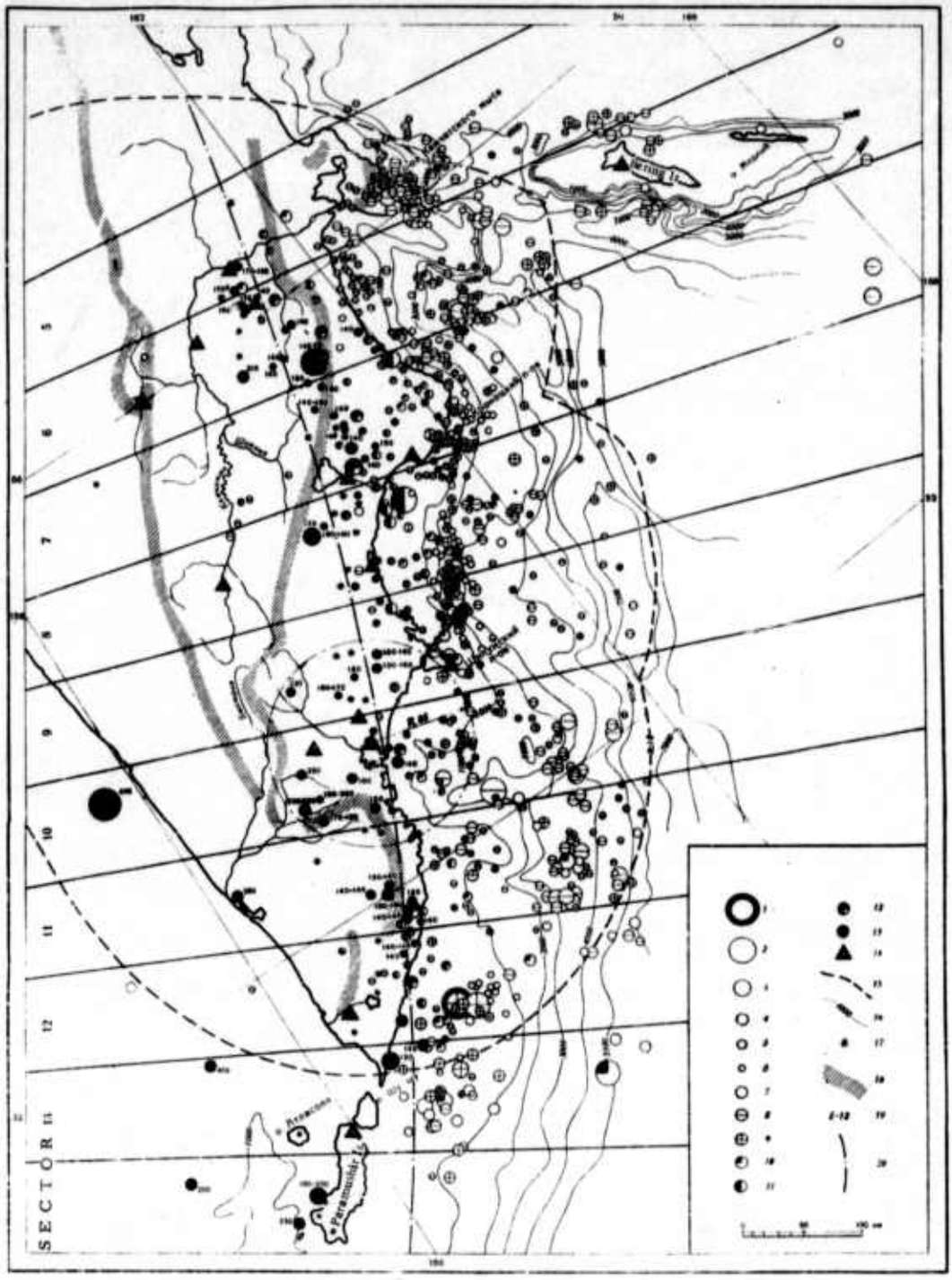

Fig. 1. Epicenter Map of Earthquakes with $E \geq 10^9$ j in Kamchatka and the Commander Islands in 1967.

Earthquake energy (in joules): 1- 10^{14}, 2- 10^{13}; 3- 10^{12}; 4- 10^{11}; 5- 10^{10}; 6- 10^9. Focal depth (in km): 7- unclassified with respect to focal depth; 8- 0-25; 9- 26-50; 10- 51-75; 11- 76-100; 12- 101-125; 13- > 125; 14- seismographic stations; 15- boundary of region with reliable recording of earthquakes with $E \geq 10^{10}$ j; 16- isobaths; 17- active volcanos; 18- major mountain ridges; 19- sectors; 20- volcanic arc.

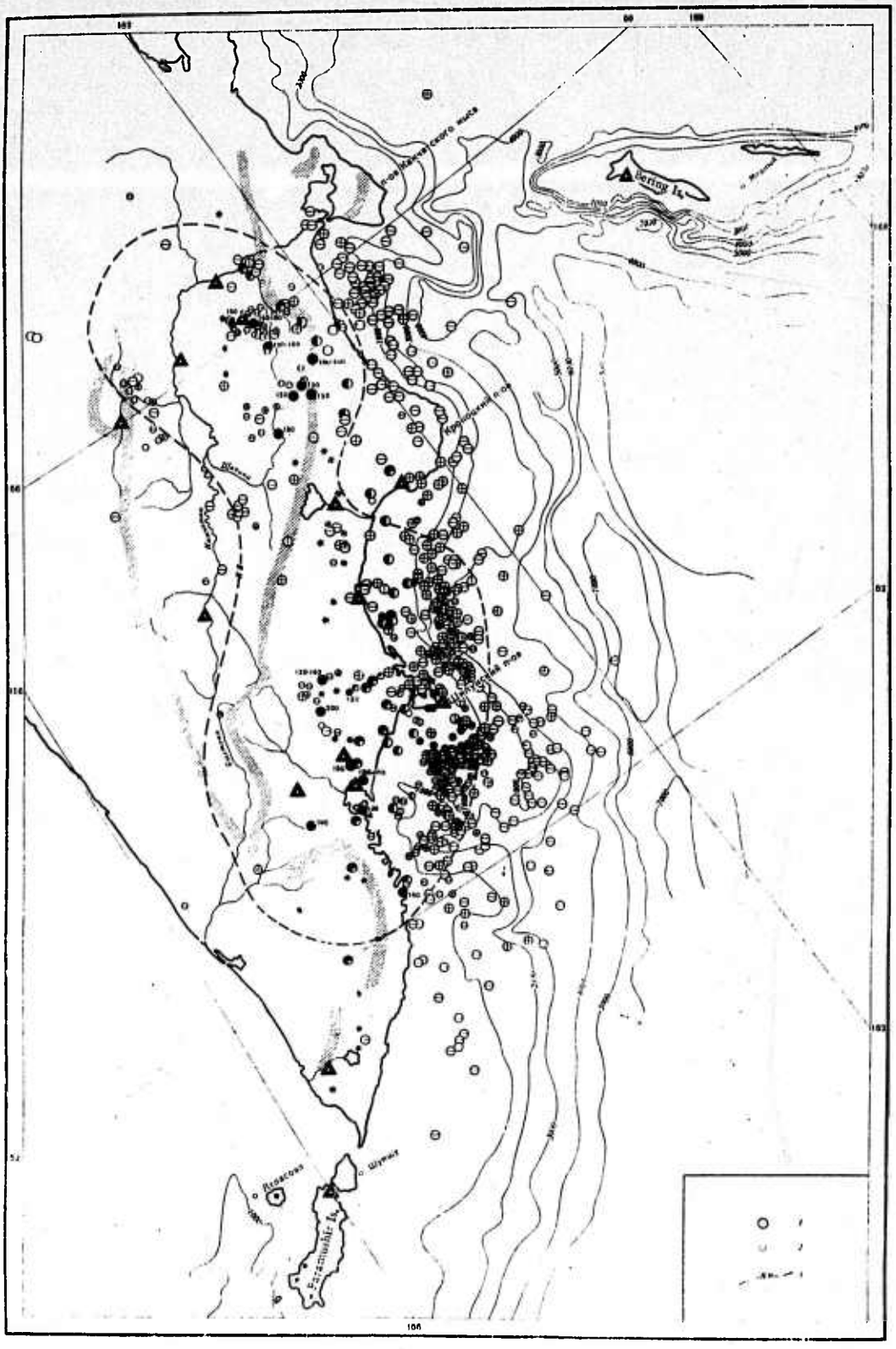

Fig. 2. Epicenter Map of Weak Earthquakes in Kamchatka in 1967.

Earthquake energy (in joules): 1- 10^8; 2- 10^7; 3- boundary of region of reliable recording of earthquakes with E = 10^3 j; Other designations the same as in Figure 1.

The slope of the recurrence graph* $\gamma = -0.56$ for earthquakes with H = 0-110 km in the area of reliable recording earthquakes with $E \geq 10^{10}$ j; $\gamma = -0.37$ for earthquakes with H = 101-200 km in the area of reliable recording of earthquakes with $E \geq 10^{9}$ j.

A seismic activity map compiled for earthquakes with $H \leq 100$ km is shown in Figure 3. A_{10} was calculated using, as the averaging area, a 8800 km^2 ellipse with 150-km-long major axis parallel to the Kurile-Kamchatka and Aleutian trenches in the Kamchatka and Commander Islands regions, respectively. In the areas of weak earthquakes with $10^{8} \leq E < 10^{10}$ j the area used for averaging was a circle with a 30-km radius.

The distribution of hypocenters in the entire seismic zone and its sectors (indicated in Fig. 1) is shown in Figure 4a in the form of their projections onto a vertical plane transverse to the axis of the Kamchatka - Kurile - Hokkaido volcanic arc. Most of the hypocenters are concentrated within a focal layer. As can be seen on the composite transverse section (Fig. 4b), the focal layer has a thickness of 78 km and dip angle of 48°. The layer is confined to the contact of the blocks of continental and oceanic crust and upper mantle. The distribution of hypocenters of earthquakes within a 100-km wide strip along Kamchatka is shown in Figure 5. Earthquake hypocenters are distributed uniformly, and the focal layer extends continously along Kamchatka.

The majority of the epicenters of earthquakes in 1967, similar to previous years, lies within two strips: the main strip, along the Kamchatka coast confined to the emergence of the Pacific Ocean focal zone onto the earth's surface; the other strip, southward from the Kronatskiy Zaliv along the lower part of the continental slope of the Kurile-Kamchatka trench.

---

* $\lg N = f(K)$ where $K = \lg E(j)$

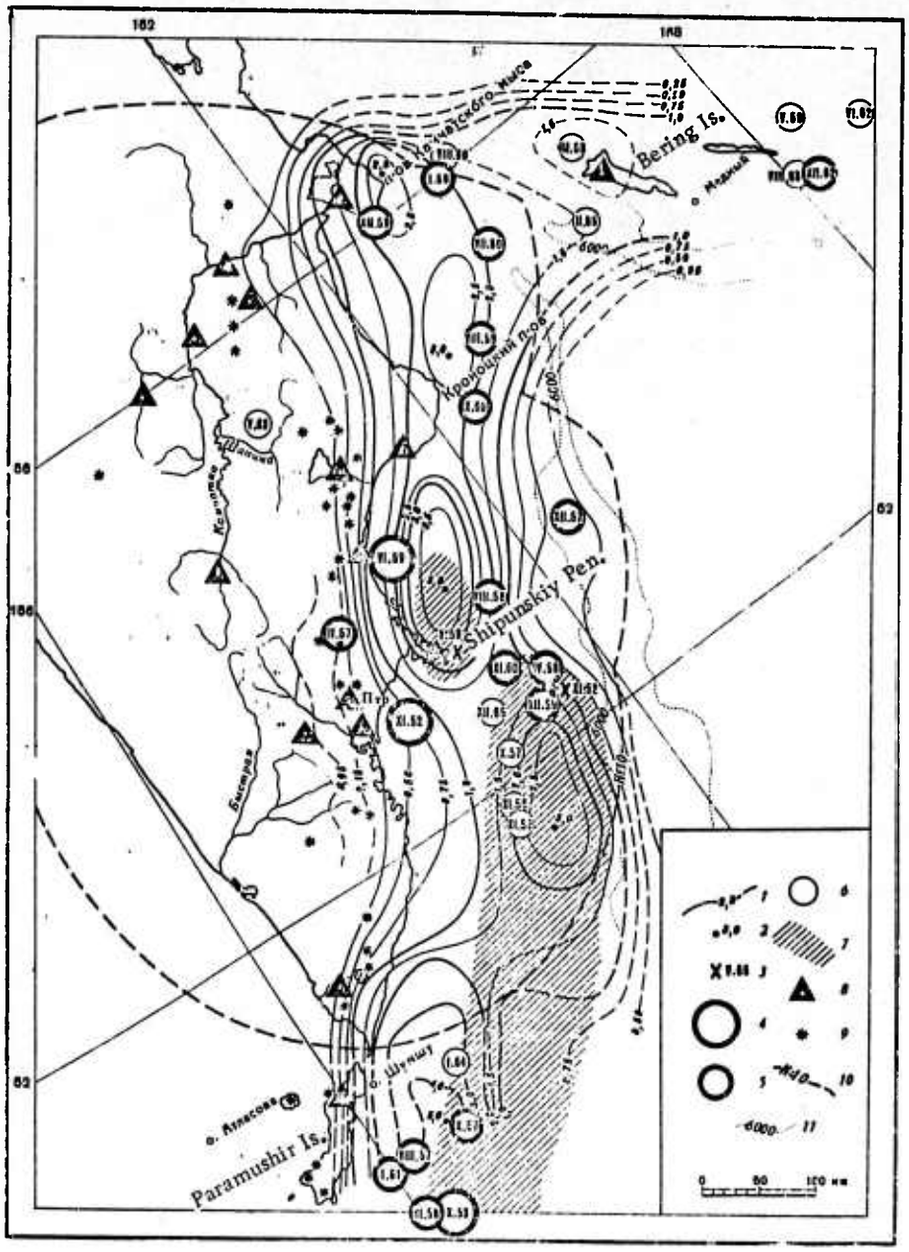

Fig. 3. Seismic Activity Map for Kamchatka and the Commander Islands for 1967.

1- Seismic activity isolines in units of A_{10}: 2- seismic activity maxima in units of A_{10}. Epicenters of strong earthquakes during 1951-65 (H = 0-100 km): 3- $M \geq 7\ 3/4$; 4- M = 7-7 1/2. Epicenters of earthquakes during 1956-65: 5- M = 6 1/4- 6 3/4; 6- M = 6; 7- hypocentral regions of the earthquakes of 4 November 1952 with M = 8.5 and 5 May 1959 with M = 7 3/4 (9); 8- seismographic stations; 9- active volcanos; 10- boundary of region of reliable recording of earthquakes with $E \geq 10^{10}$ j; 11- isobaths.

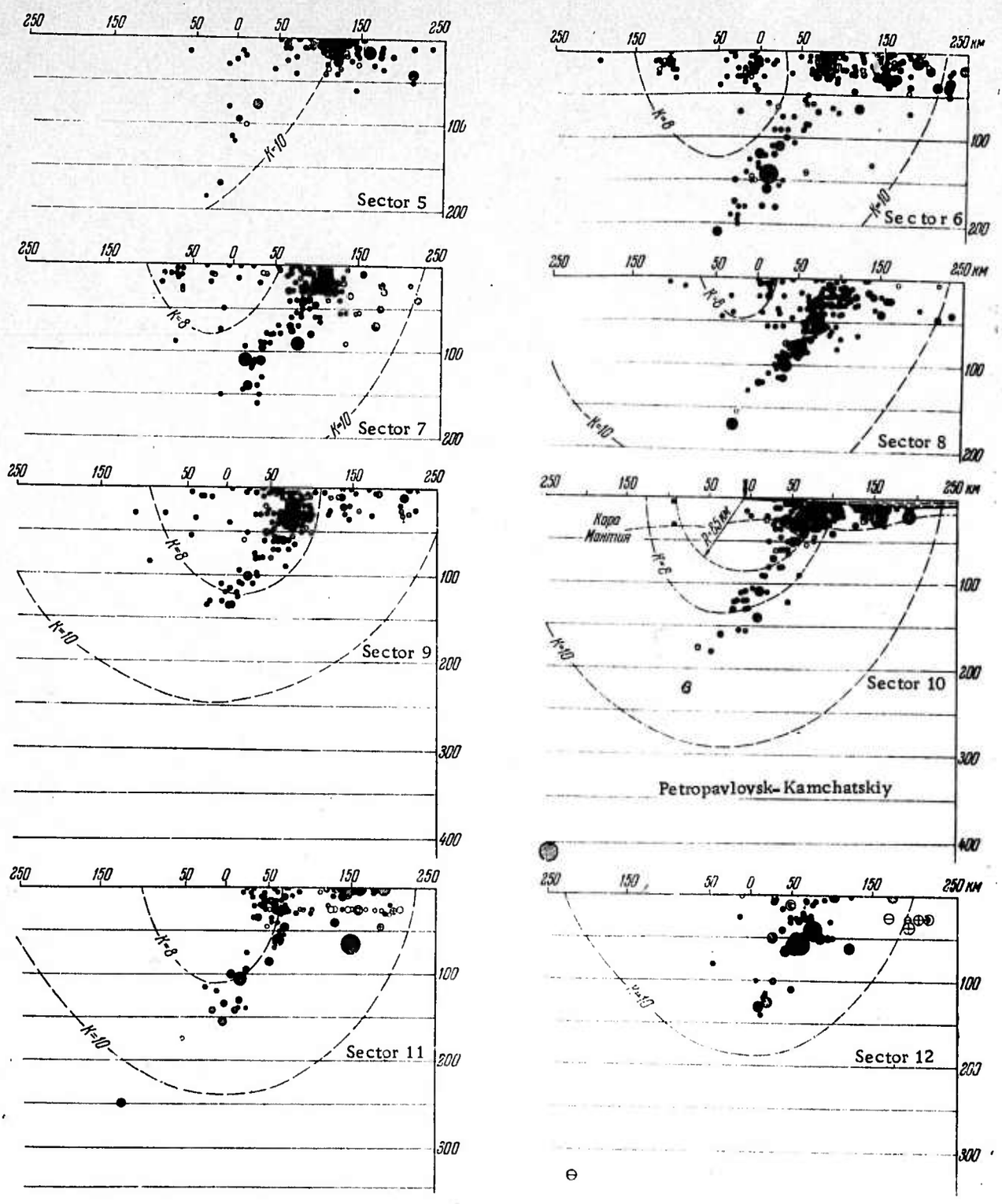

Fig. 4a. Transverse Sections of Hypocenters of Earthquakes in 1967 within Sectors 5-12 (a), and Composite Section (b).

Earthquake energy: 1 thru 6 - the same as in Fig. 1. Accuracy class; 7 - a (±5 km); 8 - b (± 10 km); 9 - c (± 15 km); 10 - n/c (± 16-25 km); 11 - assumed epicenter (error greater than 25 km); 12 - boundary of focal layer with a thickness of 74 km.

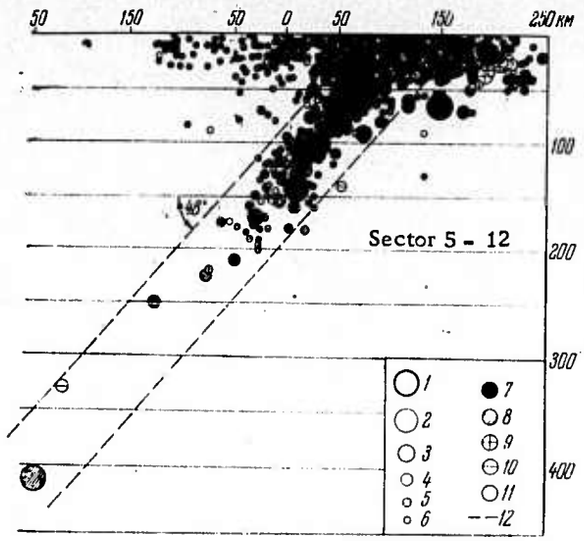

Fig. 4b. (Same as 4a).

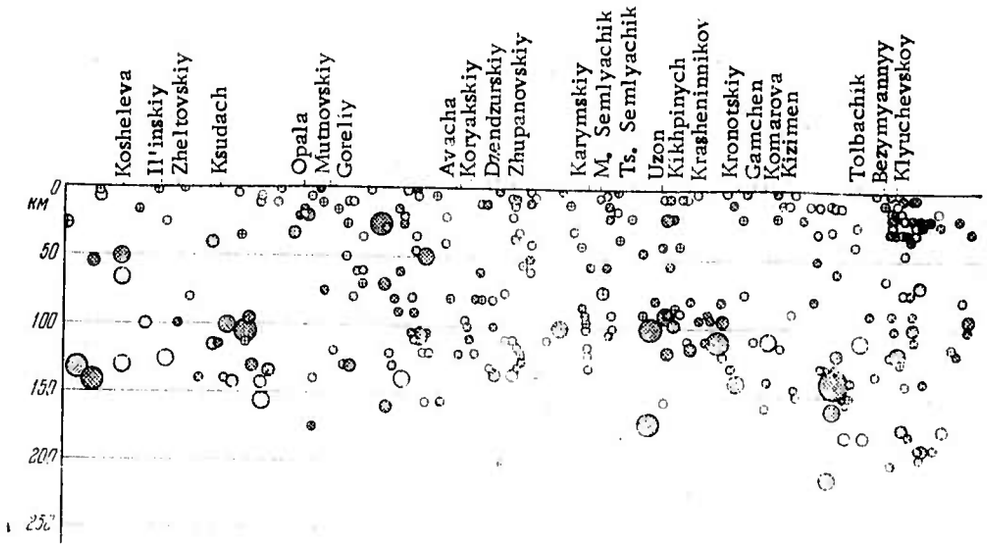

Fig. 5. Longitudinal Section of Hypocenters of Earthquakes in 1967 within the 100-km Wide Strip (± 50 km from the volcanic arc, see Fig. 1). Designations the same as in Figure 4a.

Seismic activity in the Kamchatka coastal zone (the two epicentral bands) in 1967 was at the same level as in the 1961-66 period ($A_{10} \sim 0.7$ to $A_{10} = 3.3$). The most intense earthquake swarms occurred in the Kamchatka Zaliv (49 shocks with $E = 10^9$-10^{13} j on 8-18 January and 25 shocks with $E \geq 10^9$ j between 12 January and 8 February). The maxima of seismic activity ($A_{10} \geq 2.5$) in Kamchatka Proliv migrated toward the peninsula.

The majority of earthquakes with $E \geq 10^9$ j originating in the peninsula of Kamchatka are concentrated within the focal layer. The space between the crust and focal layer, beneath the volcano chain, appeared to be seismic, not aseismic as was considered prior to 1967. The seismic activity of the folded structures of Kamchatka in 1967 was the same as in 1964-65. Epicenter concentrations are confined to the Kozyrevskiy ridge, East-Kamchatka ridge and the Klyuchi volcano group. The Kamchatka volcanos were not active in 1967.

As in previous years, earthquakes in the Commander Islands in 1967 originated along the northern and southern slopes of the islands. The seismic activity of the Aleutian Trench was lower than that of the slope facing the Bering Sea.

Rakhimov, A. R., R. D. Nepesov, and N. Annamukhamedov. Depths of strong earthquakes in the Kopet-Dag seismic zone. IN: AN TurkSSR. Izvestiya. Seriya fiziko- tekhnicheskikh, khimicheskikh i geologicheskikh nauk, no. 1, 1973, 27-29.

An attempt is made to determine focal depths of earthquakes with $M \geq 4$, originating in the Kopet-Dag seismic zone, using P- waves recorded at nearby seismographic stations. Focal depth is determined from the station discrepancies in the travel time $f_i = t_{pi} - t^*_{pi}$, where t_{pi} is observed travel time, t^*_p is travel time according to the Jefferies-Bullen tables for different presumed focal depths. The true focal depth of an earthquake is accepted as corresponding to the presumed focal depth for which f_i values change their signs. If the mean station discrepancy f_i does not change its sign, the focal depth can be determined from the station discrepancies in origin time. The true focal depth of an earthquake is accepted as corresponding to the presumed focal depth for which the mean square value of the station discrepancies in origin-time reaches the minimum.

A more accurate determination of the focal depth of an earthquake is made by comparing epicentral coordinates, calculated from the observations of distant seismographic stations, with the set of epicentral coordinates calculated using observations from nearby seismographic stations, for different presumed focal depth. The focal depths of strong earthquakes in the Ashkhabad region determined by this method are, mainly, 20-30 km. The following table gives focal depths of the Kopet-Dag earthquakes, determined by the latter method.

Focal Depths of Earthquakes in the Kopet-Dag Seismic Zone

Date	Time, hour	h, km	M
September 17, 1961	5	45	4.2
March 19, 1962	23	50	4.5
November 12, 1964	8	20	5.2
December 3, 1964	22	50	4.5
May 7, 1965	1	45	4.5
December 6, 1965	14	5	4.0
January 18, 1966	20	30	4.5
November 26, 1966	13	30	4.5
January 26, 1969	2	45	5.0
November 23, 1969	11	10	4.7
November 25, 1969	9	20	4.5
January 9, 1970	9	10	4.9
July 30, 1970	0	25	6.7
July 30, 1970	2	10	4.0
July 30, 1970	2	15	4.0

Kharitonov, O. M. Solution of a wave equation for a heterogeneous medium with a vertical velocity gradient. IN: AN UkrSSR. Geofizicheskiy sbornik, no. 49, 1972, 81-84.

The motion equation for a heterogeneous medium

$$(\lambda+\mu)\ \mathrm{grad\ div}\ \bar{u}+\mu\Delta\bar{u}+\mathrm{grad}\,\lambda\ \mathrm{div}\ \bar{u}+\mathrm{grad}\,\mu\sum_{i=1}^{3}\left(\frac{\partial\bar{u}}{\partial l_i}+\mathrm{grad}\,u_{l_i}\right)\bar{l}_i=\rho\frac{\partial^2\bar{u}}{\partial t^2}, \qquad (1)$$

where l is a generalized symbol for the coordinate axes and $\bar{l}$ represents their unit vectors, is presented in the form of a system of two independent differential equations in the terms of scalar potential φ and components of vector potential Ψ_l:

$$\Delta\varphi=\frac{1}{v_p^2(x,y,z)}\cdot\frac{\partial^2\varphi}{\partial t^2}, \qquad (2)$$

$$\Delta\psi_l=\frac{1}{v_s^2}\cdot\frac{\partial^2\psi_l}{\partial t^2}. \qquad (3)$$

The solution of equations (2) and (3) is reduced to the solution of a linear homogeneous partial differential equation of the second order with the variable coefficient

$$\Delta q(x,y,z,t)=\frac{1}{v^2(x,y,z)}\cdot\frac{\partial^2 q(x,y,z,t)}{\partial t^2}. \qquad (4)$$

A particular case of an axially symmetrical medium with a vertical velocity gradient is considered. Expressions are given for total displacement representing a particular and general solution of equation (1).

Shadrin, L. Nuclear explosions produce oil. Nauka i zhizn', no. 2, 1973, 14-19.

The use of nuclear explosions to stimulate the discharge of oil and gas wells, as well as for providing storage facilities for oil and gas, is reviewed. The effects of a confined explosion on rocks are illustrated in text, as is a gas storage facility.

Two examples of Soviet use of nuclear explosions for the stimulation of oil well discharge are briefly described. In one case, three charges totaling about 13 kilotons were fired at a depth of 1350 m. The crack propagation zone was observed within an area having a radius of 300-400 m, while individual cracks were observed at distances of 800 m. The overall production of 20 nearby oil wells increased by more than one third. In another case two charges of 8 kilotons each were fired in an oil deposit consisting of dolomite and limestone. The productivity of 7 oil wells within a distance range of 800 m increased by a factor of 1.5. The problems of radiation hazard are discussed.

Yepinat'yeva, A. M. Determination of the thickness of a refraction layer. IN: AN UkrSSR, Geofizicheskiy sbornik, no. 50, 1972, 3-12.

An approximate method is proposed for the determination of the thickness of a refraction layer using time-distance curves of head waves from the layer's surface and reflected waves from its basement. A formula for thickness is developed for a three-layered homogeneous medium, assuming that the travel paths of the considered waves through the first layer coincide The errors in the thickness determined by this method are discussed.

An example is given of the determination of thickness using field data and the thickness derived is compared to that determined by ultrasonic well logging and vertical seismic profiling. The errors in the thickness determined by the proposed method are found to be up to 25%.

Chesnokov, Ye. M., and A. O. Gliko. Elastic characteristics of a homogeneous transversely isotropic model of the upper mantle. IN: AN SSSR. Izvestiya. Fizika Zemli, no. 3, 1973, 20-28.

Formulas are developed for the elastic coefficient of a homogeneous transversely isotropic model of the upper mantle. Anisotropy of P- and S-waves is estimated for a model of the upper mantle composed of olivine crystals oriented in different ways (according to the hypothesized mechanisms of the generation of elastic anisotropy of the upper mantle beneath continents and oceans). The results are compared with experimental data for continents and oceans.

The elastic coefficients (see Table 1) are determined for the following orientations of olivine crystals:

Oriented axis	$\overline{C}_{11}$ V	$\overline{C}_{11}$ H	$\overline{C}_{12}$ V	$\overline{C}_{12}$ H	$\overline{C}_{13}$ V	$\overline{C}_{13}$ H	$\overline{C}_{33}$ V	$\overline{C}_{33}$ H	$\overline{C}_{44}$ V	$\overline{C}_{44}$ H
a	22.05	21.89	8.10	8.01	6.9	6.8	32.4	32.3	8.01	8.01
b	27.5	27.2	9.14	9.04	6.85	6.83	19.8	19.7	7.30	7.27
c	25.02	24.27	6.98	6.68	7.85	7.82	24.9	24.89	7.38	7.3

Table 1. Elastic Moduli of a Transversely Isotropic Medium Composed of Olivine Crystals ($C_{ij} \sim 10^{11}$ dyne/cm^2).

Note: calculations were made using elastic moduli for olivine monocrystal according to Verma, 1960.

a) the c- axis is oriented in the direction of the OZ - coordinate axis, while the a- and b-axes are arranged arbitrarily and form an isotropy plane (the upper mantle beneath continents); b) the b-axis is oriented, while the c- and a-axes form an isotropy plane (the upper mantle beneath oceans, hypothized by Hess, 1964); c) the a-axis is oriented, while the b- and c-axes form an isotropy plane (the upper mantle beneath oceans, hypothesized by Frencis, 1969).

Velocities of P and S waves and corresponding coefficients of anisotropy determined using calculated elastic moduli are given in Table 2.

Oriented axis	$V_{P\parallel}$, km/sec		$V_{P\perp}$ km/sec		V_{SV}, km/sec		V_{SH}, km/sec		a_P, %		a_S, %	
	V	H	V	H	V	H	V	H	V	H	V	H
a	8.17	8.14	9.91	9.90	4.93	4.92	4.60	4.58	21.2	21.5	7.1	7.1
b	9.03	9.18	7.74	7.70	4.70	4.69	5.29	5.09	17.8	17.3	12.5	10.0
c	8.70	8.58	8.69	8.68	4/73	4.71	5.23	5.10	0.0	0.1	10.5	8.80

Table 2. Velocities of Elastic Waves in a Transversely Isotropic Medium Composed of Olivine Crystals.

Note: velocities are calculated using formulas according to Anderson (1961) and Fedorov (1965).

As can be seen from the above tables, if the c-axis represents a symmetry axis, anisotropy of P waves is absent while that of S-waves is significant. This is in agreement with observed data on the dispersion of the phase velocity of surface waves. If the b-axis represents a symmetry axis, anisotropy of P-waves exists, while that of S-waves is high. This fact is in agreement with experimental data on P-waves in the upper mantle beneath ocean and Hess'concept of the mechanism of the generation of elastic anisotropy. If the a-axis represents a symmetry axis, anisotropy of P-waves exists, while that of S-waves is small.

Chekunov, A. V. Symposium on the physical properties, composition, and structure of the upper mantle. IN: UkrSSR. Geofizicheskiy sbornik, no. 50, 1972, 77-80.

The papers presented at the symposium held during 19-21 April, 1971 at the Institue of Physics of the Earth in Moscow are reviewed. Twenty five papers dealing with the results of geochemical and geophysical studies of the upper mantle were presented.

Composition

It was pointed out in a number of papers that the criteria for identification of mantle material are not sufficiently unique. For example, B. G. Lutts reported the existence of at least two types of eclogites, i.e., mantle and crustal. Crustal eclogites differ from those of the mantle by the composition of rock-forming minerals, and occur only locally. The results of experiments carried out by M. P. Volarovich and his group showed that the elastic properties of crustal and mantle eclogites differ greatly. Thus, at pressures of 10-20 kbar, the velocity of compressional waves in mantle eclogites varies from 8.0-8.5 to 9.0 km/sec, while in crustal eclogites, it varies from 7.5 to 7.8 km/sec. Yu. S. Genshaft emphasized that in the modeling of the mineralogical composition of the lower crust and upper mantle, one should study mineral assemblages rather than monomineral systems. The explanation is given that the absolute stability of a mineral differs significantly from its relative stability in paragenesis. It was also pointed out that the velocity of elastic waves in minerals may decrease with an increase of their density (such as with obsidian, silver chloride, etc.). V. A. Zharikov, I. P. Ivanov, Yu. A. Litvin and M. P. Epel'baum pointed out that in studying mineral assemblages under deep-seated physicochemical conditions, attention should be paid to the partial pressure of water, carbon

dioxide, etc. Thus, the depth of the generation of granitic magma changes by a factor of two, if determined taking into account partial pressures. According to V. S. Sobolev, the composition of the upper mantle immediately beneath oceans corresponds to the stability field of plagioclase and olivine, with respect to pressure, and to the stability field of green schist facies of epidote amphibolites, with respect to temperature. At greater depths, it corresponds to spinel peridotites and, at 50-60 km, to garnet peridotites. The composition of the upper mantle immediately beneath continents corresponds to the stability field of spinel peridotites and, in places, of garnet peridotites. At greater depths, it corresponds to diamond ferrous garnet peridotites and eclogites. According to B. P. Zolotarev and S. F. Sobolev, the mantle is composed mainly of garnet and spinel peridotites, and eclogites. S. M. Kravchenko presented the results of geochemical studies of basalts from assumed mantle sources. He came to the conclusion that the upper mantle is composed of basalt achondrites and, at greater depths, of chrondites.

Magmatism and Metamorphism

It was unanimously accepted that basalt magma originates in the mantle. B. G. Lutts and other authors supporting the hypothesis of an eclogite mantle (developed by A. A. Yaroshevskiy), consider the transformations eclogite $\rightleftarrows$ basalt to be possible. While opinions with regard to the depth of the generation of basalt magma did not differ considerably, the mechanism of magma emanation was argued. The hypothesis of the zonal melting of the mantle, which was put forward by A. P. Vinogradov, was preferred A. A. Yaroshevskiy pointed out that emanation of magma is not merely a mechanical process, but is accompanied by a change in the composition of the melt. According to A. P. Akimov and others, magma is saturated with radioactive components while moving through the "granitic" layer. The wide variation of the radioactive elements in xenoliths is explained on the basis of the above concept. P. N. Kropotkin pointed out that the "granitic"

layer can in no way be obtained from mantle material. A primary "granitic" layer was formed at an early stage of the Earth's evolution from a silicate-water system. The absence of the "granitic" layer beneath the oceans is explained by continental drift. A secondary "granitic" layer is formed from sediments, the primary "granitic" layer, and partly from the "basaltic" layer melting out in orogenic belts.

Heat flow

Ye. A. Lyubimova, A. A. Borisov, and G. I. Kruglyakova presented the results of a study of heat flow in different types of crust. The heat flow in shields was found to be effected by the mantle. The temperatures at the Moho discontinuity beneath shields are found to be 300-400° C, while those beneath oceans are 200-300° C. A. A. Borisov and G. I. Kruglyakova found, using a different method, that the temperatures at the Moho discontinuity over a large part of the USSR are 300-400° C (lower temperatures of 200-300° C are found in shields and higher at 300-500° C, in plates).

Magnetism and seismology

M. N. Berdichevskiy, A. T. Bondarenko, L. L. Van'yan, E. I. Parkhomenko, V. Ye. Fadeyev, and I. S. Fel'dman reported the results of magnetotelluric soundings. A high conductivity layer is observed in the north-central Pannonian depression at 50 km, in the south Caspian depression at 40-60 km, in the Vilyuyskaya syneclise at 15-25 km, in Baykal rift zone, etc. The origin of this layer is explained as due to the process of dehydration and partial melting, as well as amorphization, or due to chemical reactions or phase transition in the upper mantle. N. P. Lopatina and V. Z. Ryaboy reported the occurence of a discontinuous low velocity layer in the upper mantle in the Baykal region and on Kamchatka. They have compiled a map

of the velocity along the Moho discontinuity for the USSR territory. The upper mantle is characterized by lateral inhomogeneities, but regardless of this fact, the average velocity of seismic waves to a depth of 150-200 km appears to be the same over the entire territory. A. V. Nikolayev and others identified relatively small inhomogeneities in the upper mantle by studying the seismic "turbidity factor". It was found that the "seismic turbidity" of the crust is higher by a factor of 2-4 than that of the upper mantle, whereas the turlidity of the continental crust is higher than that of the oceanic crust. L. P. Vinnik and A. A. Godzikovskaya proposed a new method for the analysis of converted waves from earthquakes (the method of seismically conjugate points). P. W. Kropotkin and B. W. Frolov established the existence of strong compressional horizontal stresses, considerably exceeding hydrostatic pressure, while studying the stress state in the rocks in mines. This excess stress reaches its peak value at a depth of 10-40 km. It is also observed in the Baltic shield, the North American and African ancient platforms, the Paleozoic folded belts of Norway, Spitsbergen, Iceland, the Urals, Sayan, Kazakhstan, Tasmania, and the Cenozoic folded belts of Portugal, Iran, Malaysia, and California.

Physical properties of rocks at high temperatures and pressures.

M. P. Volarovich, Ye. I. Bayuk, A. I. Levykin, and I. S. Tomashevskaya determined velocity-pressure curves for major rock types, at pressures ranging to 15 kbar. The velocity anisotropy for rocks and minerals was established. It was found that the velocity of elastic waves in rocks decreases in the process of plastic deformation. According to the authors, the low velocity layer within the crust (Central Asia, Zakarpat'ye), corresponds to the velocity in schist, not in gabbroic rocks. T. S. Lebedev, V. I. Shapoval and V. A. Korchin (Institute of Geophysics of the Academy of Sciences, Ukrainian SSR) showed that, under P, T conditions in the Ukrainian shield, the velocity of compressional waves in granitic rocks

increases by 8-10% to a depth of 7-10 km. With a further increase in depth (10-15 km), velocity does not change or changes insignificantly. Within the depth interval from 18-20 km, velocity decreases by 2-3%, while at greater depths, it increases again. Thus, in the Ukrainian shield, where granitic rocks lie at depths of 18-20 km, there exist favorable conditons for the occurrance of a low velocity layer.

Sobolev, G. A., V. N. Morozov, N. T. Migunov. Electrotelluric field and strong earthquakes in Kamchatka. IN: AN SSSR. Izvestiya. Fizika Zemli, no. 2, 1972, 73-80.

An analysis is given of an observed anomalous time variation of the electrotelluric field accompanying two strong earthquakes in Kamchatka on 19 December 1968 (M = 6, h = 40-50 km) and 2 January 1969 (M = 5, h = 30 km). Observations of the electrotelluric field were conducted at the Shipunskiy, Semlyachik, Kronoki, and Paratunka stations (see Fig. 1), using an M17/13 galvanometer and lead electrodes spaced 200 m apart in NS-EW directions.

The observed time variations of the electrotelluric field are shown in Figure 2. Prior to the 19 December 1968 earthquake, significant variations up to 300 mV/km were observed at the Shipunskiy station (smallest epicentral distance) and smaller ones at the Semlyachik station. In the period between 19 December and 2 January, less notable variations were observed at all stations. After 2 January, variations were again smooth. Disturbances of E due to the effect of the ionosphere and ocean tides were negligible during that period. Polarization at the electrodes was considered as a stationary process. Temperature variations did not correlate with E variations.

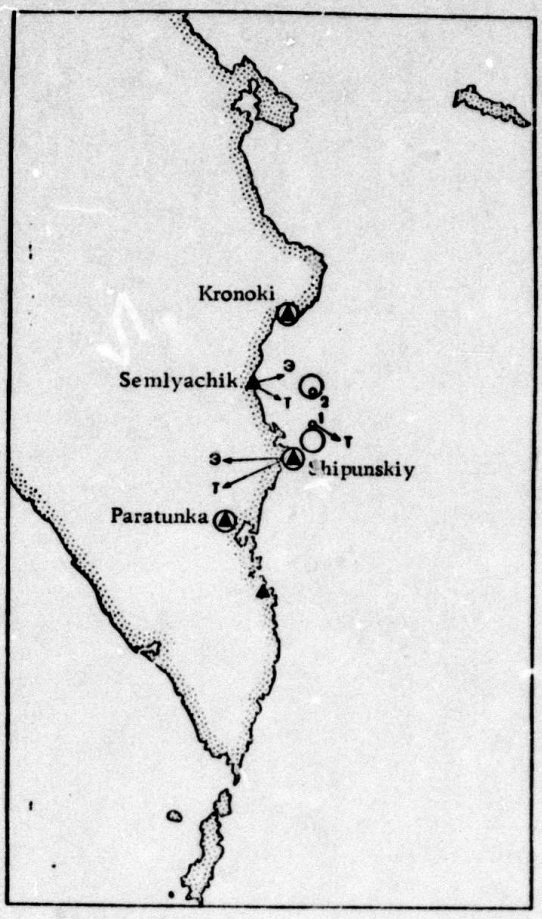

Fig. 1. Location (1) of the Hypothetical Dipole Electric Source prior to the Earthquake of 19 December 1968 and its Field.

T - calculated; E - observed; 2 - location of the hypothetical source prior to the earthquake of 2 January 1969.

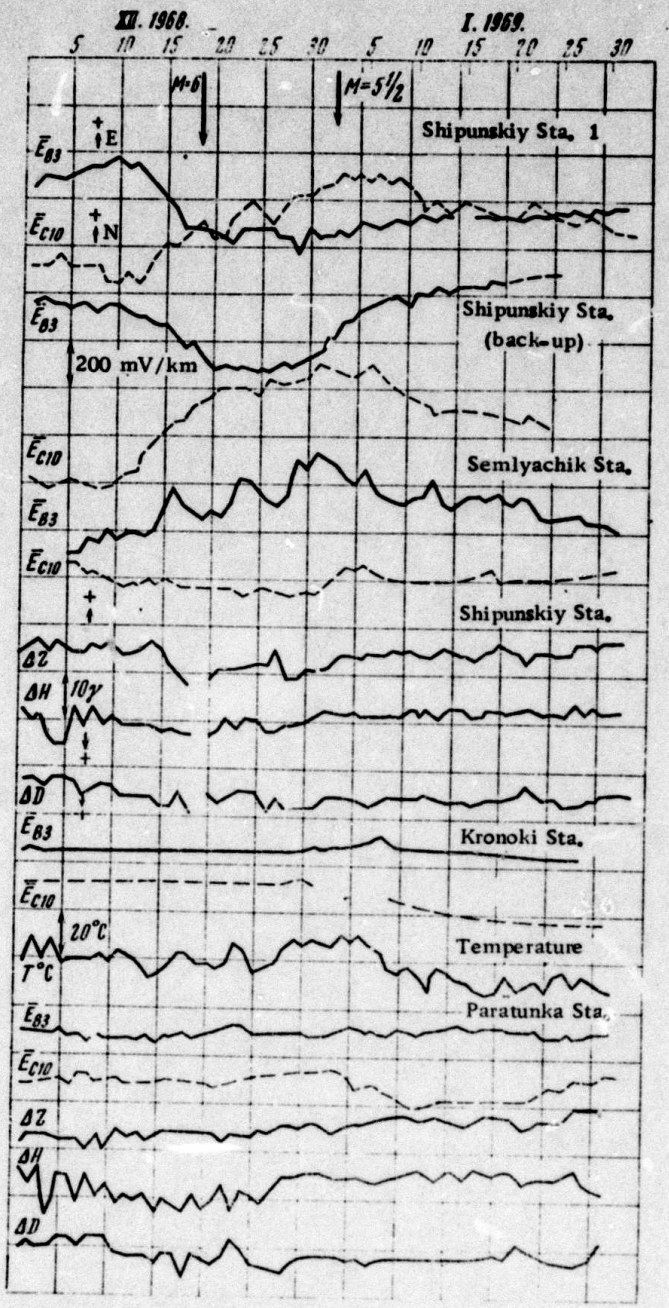

Fig. 2. Variation of the Intensity of Electrotelluric and Geomagnetic Fields in December 1968 - January 1969.

The position of the hypothesized piezoelectric source of the anomalous variation of the electrotelluric field intensity is determined as observed at the Shipunskiy and Semlyachik stations prior to the earthquake of 19 December 1968. The source was assumed to be a horizontal dipole, on the basis of the criterion $\rho < 10\ h$ (h = 5-10 km corresponding to the depth of the "granitic" layer) and prevailing horizontal compressional stresses in Kamchatka. The position of the dipole at a depth of 5-10 km was determined using criteria $G_{12\ exp} = G_{12\ theor}$, where

$$G_{12} = \frac{E_1^2}{E_2^2} = \frac{A_1\cos^2\varphi_1 + B_1\sin^2\varphi_1}{A_1\cos^2\varphi_2 + B_2\sin^2\varphi_2} \qquad (1)$$

The assumed position of the source and the theoretical field induced by it are shown in Figure 1. The possible location of the source lies near the Pacific focal zone. Similar anomalous variations of the electrotelluric field intensity prior to strong earthquakes with epicentral distance less than 150 km were observed at the following seismographic stations in Kamchatka.

Date	Magnitude	Station	Onset of anomaly prior to earthquake (in days)
4 May 1958	7 3/4	Petropavlovsk-Kamchatskiy	15
22 December 1965	5 3/4	-"-	14
4 September 1968	5	Shipunskiy	17
8 June 1969	5 1/2	-"-	16
16 July 1969	5 1/2	Shipunskiy, Paratunka	13
11 February 1969	4 1/2	Shipunskiy, Kronoki	7
17 February 1969	4 1/2	Shipunskiy	4
24 February 1969	4 1/2q	Shipunskiy, Semlyachik, Kronoki	5
22 October 1969	4 1/2	Shipunskiy	6

Yanovskiy, A. K. Use of crosscorrelation functions of seismic traces for coordinating seismic observations. IN: AN SSSR. Sibirskoye otdeleniye. Institut geologii i geofiziki. Diskretnaya korrelyatsiya seysmicheskikh voln (Discrete correlation of seismic waves). Novosibirsk, Izd-vo Nauka, 1971, 50-72.

A statistical model of a wave field recorded during a reflection survey has been constructed. An analysis is given of the relationship existing in such a model among $B_z(\tau)$ - the cross-correlation function, and the distribution of $\Delta t_k = \frac{\Delta x}{V_k}$* time increments on the time distance curves of reflected waves. The use of correlation functions for discrete wave correlation, as well as the determination of static and dynamic corrections in positional wave correlation, is discussed.

The statistical model has the following characteristics: on a set of adjusted records, there exist a large number of incoherent waves with identical waveforms; there exists a dispersion of their apparent velocities and amplitudes around the mean values (of these parameters).

It was found that for such a model, the crosscorrelation function can be considered as an autocorrelation function passed through a low-frequency filter, which results in a decrease of maximum amplitude and apparent frequency, and a narrowing of the signal frequency range. There exists a class of Δt distribution (normal distribution, in particular) which is very favorable from the view point of the utilization of correlation functions in wave correlation. Experimental results give evidence that the distributions found under real conditions either belong to or are similar to the above class.

The mean error in determining the crosscorrelation function does not depend upon the dispersion of Δt distribution. The crosscorrelation function displays an interference effect, so as to suppress uncorrelated waves and resolve (on the τ-axis) wave groups with different mean apparent velocities.

The determination of the mean true offset between traces ($m = M\Delta t_k$) from the maximum of the crosscorrelation function, with filtering is an asymptotically optimum one. For this case, the signal-to-noise ratio does not affect the accuracy of the determination, but only the magnitude of peak value of correlation coefficient.

The problem of the correlation of N traces is reduced to finding the value at which, for a given filtering, the sum of the cross-correlation functions of all possible pairs of traces reaches a maximum.

The experimental values of dispersion of Δt distributions obtained for two different geological regions are in good agreement, Δt_k was significantly correlated along the profiles. The introduction into the records of static corrections determined by crosscorrelation functions proved to be highly efficient.

Voytov, G. I., et al. Some geological-geochemical consequences of the 14 May 1970 Dagestan earthquake. IN: AN SSSR. Doklady, v. 202, no. 3, 1972, 576-579.

The 14 May 1970 Dagestan earthquake with a focal depth of about 30 km (crustal thickness in its epicentral zone is about 30 km) manifested, in addition to geomorphological, the following geochemical effects:

1). The content of hydrogen, helium, carbon dioxide, and methane in samples of air taken from two open faults in the epicenter zone was higher relative to the same content in the atmosphere, as can be seen from the following table:

Table 1

	H_2	He	O_2	N_2	CO_2	CH_4	
1.	0.038	up to 0.001	20.82	78.90	up to 0.1	0.00014	%
2.	0.014	-"-	20.31	79.50	-"-	0.00013	%;

2). The salinity of the water from wells varied significantly, while its overall mineralization and pH value were unchanged. In an oil well 10-15 km from the epicenter, the content of H_2SiO_3, SO_4, J_2, Br_2 and NH_4 decreased, the content of HBO_3, Ca, Mg and Cl increased, while the content of Na + K was unchanged (see Table 2). In another oil well 5-6 km from the epicenter, overall mineralization decreased, while the salinity varied greatly after the main shock (see Table 2). The original salinity level was gradually reestablished.

TABLE 2

Borehole	Date	pH	Overall mineralization gr/l	Salinity, mgr/l										
				H_2SiO_3	HBO_2	Na + K	Ca	Mg	Cl	SO_4	HCO_3	J	Br	NH_4
No. 3	1 Aug 1967	7.6	4.22	12.0	2.5	1807.0	8.0	4.0	1216.5	16.4	2979.0	2.5	13.5	21.6
	20 June 1970	7.3	4.37	1.4	22.75	1807.0	22.04	7.30	1316.1	13.99	2921.2	-	-	-
	12 Aug 1970	7.6	4.53	25.94	2.41	1820.0	25.0	9.12	1347.5	-	256.2	0.85	10.85	1.5
No. 2	6 June 1960	8.0	2.92	59.0	15.8	912.5	6.40	4.26	308.9	905.0	695.4	8.08	1.65	12.0
	12 Aug 1970	8.05	2.37	44.10	0.65	849.8	11.02	5.42	297.9	836.4	496.4	-	4.68	1.5

3) The daily discharge of gas, water and oil from wells over a large area (100-250 km from epicentral zone) varied, either increased or decreased or was reestablished (in an old oil well). The variations observed in oil fields 40-50 and 50-60 km from the epicenter are illustrated.

Tabulevich, V. N. Radiation of microseismic oscillations and intrasound by an area of standing waves. IN: AN SSSR. Izvestiya. Fizika Zemli, no. 6, 1972, 85-89.

A theory of oscillations radiated into water and air by a finite area of standing waves is developed. A mathematical description of oscillations radiated into water is given, considering an oscillating plane piston as the model of a radiator. A numerical example is shown for an area of standing waves with diameter d = 30 km and a microseismic wave period of λ = 6 sec. The radiation directivity was calculated by the formula

(1)

where $J_1(x)$ is a Bessel function of first order. The radiation is found to be sharply vertical with dispersion not exceeding 15%.

For a mathematical description of infrasonic waves radiated into the air, a system of alternating cophasal and antiphasal oscillating halfwave plates was considered as the model of the radiator. Numerical calculations were conducted for a radiator consisting of 10 ocean waves (N = 20), with the total length $N \cdot D_x = 300$ m, wave crest length Dy = 10 km, amplitude A = 5 m, frequency $\omega = 1/20$ Hz and acoustic impendence $\zeta = 43$ CGS. The pressure at distance $r_o = 1000$ km generated by a single halfwave radiator is found to be $p_{eff} = 4.2$ microbar. The radiation pattern in the vertical plane through the middle of the system of halfwave radiators is characterized by zero radiation in the vertical ($\theta = 0^o$) and maximum radiations of $0.985\ p_{eff} = 4.15$ microbar in the horizontal.

B. Recent Selections

Aliyev, A. M., et al. Determination of direction to epicenter by a geometric method. IN: AN AzerSSR. Izvestiya. Seriya nauk o Zemle, no. 2, 1972, 153-155.

Aranovich, Z. I., and I. B. Dubinskiy. An optimum system for seismic observations in Crimea. Seysmicheskiye pribory, no. 6, 1972, 67-69.

Balakhovskiy, M. S., et al. Experimental study of the motions produced by large "walking" excavators, using seismic instruments. Seysmicheskiye pribory, no. 6, 1972, 88-94.

Begushin, G. K. Improvement of the recording quality of seismic processes on photosensitive semiconductor paper. Seysmicheskiye pribory, no. 6, 1972, 110-115.

Belyayevskiy, N. A., and A. G. Rodnikov. The crust in Far East seas and island chains. IN: AN SSSR. Mezhduvedomstvennyy geofizicheskiy komitet. Rezul'taty po mezhdunarodnym geofizicheskim proyektam. Metodika i rezul'taty issledovaniy zemnoy kory i verkhney mantii (Methods of and results from studies of the crust and upper mantle). Moskva, Izd-vo Nauka, 1972, 64-104. (ITS: Verkhnyaya mantiya, no. 8, 1972).

Belyayevskiy, N. A., et al. Nature of seismic layers and interfaces in the crust. IN: AN SSSR. Mezhduvedomstvennyy geofizicheskiy komitet. Rezul'taty po mezhdunarodnym goefizicheskim proyektam. Metodika i rezul'taty issledovaniy zemnoy kory i verkhney mantii (Methods of and results from studies of the crust and upper mantle). Moskva, Izd-vo Nauka, 1972, 7-43. (ITS: Verkhnyaya mantiya, no. 8, 1972).

Borisevich, Ye. S. Balancing galvanometers used in recording strong earthquarkes. Seysmicheskiye pribory, no. 6, 1972, 46-53.

Borisevich, Ye. S. Mirror-equipped frame-type torsional vibration meters. Seysmicheskiye pribory, no. 6, 1972, 14-16.

Bulashevich, Yu. P., et al. Helium in ground water a'ong the Sverdlovsk deep seismic sounding profile. IN: AN SSSR. Doklady, v. 208, no. 4, 1973, 825-828.

Chekunov, A. V. Symposium of the physical properties, composition, and structure of the upper mantle (Moscow). IN: AN UkrSSR. Geofizicheskiy sbornik, no. 50, 1972, 77-80.

Dashkov, G. G. Some problems of frequency selection when recording surface waves. Seysmicheskiye pribory, no. 6, 1972, 82-88.

Fedoseyenko, N. Ye., and A. S. Deniskov. Seismic equipment for parameter measurements in horizontal and vertical boreholes, mines, and outcroppings. Seysmicheskiye pribory, no. 6, 1972, 21-26.

Fedoseyenko, N. Ye., and I. Ya. Goncharuk. Electrical oscillation mixers. Seysmicheskiye pribory, no. 6, 1972, 157-159.

Fotiadi, E. E., and I. K. Tuyezov. Deep structure of the northwestern sector of the Pacific Ocean tectonic belt. Geologiya i geofizika, no. 12, 1972, 6-22.

Fremd, V. M. Possible use of galvanometers for recording strong earthquakes. Seysmicheskiye pribory, no. 6, 1972, 35-46.

Fremd, V. M., et al. APT-1 three-component piezoelectric accelerometer. Seysmicheskiye pribory, no. 6, 1972, 9-14.

Goncharov, V. L. Initial processing system for seismic data. Seysmicheskiye pribory, no. 6, 1972, 94-97.

Gostev, M. A., and L. L. Shul'pin. Seismograph for slow motion. Seysmicheskiye pribory, no. 6, 1972, 5-8.

Kabychenko, N. V. Arrangement for matching a galvanometer with a signal source containing a constant component. Seysmicheskiye pribory, no. 6, 1972, 127-129.

Kabychenko, N. V. Some problems in seismic signal compression. Seysmicheskiye pribory, no. 6, 1972, 129-138.

Kalashnikov, N. G., et al. Dynamic compressibility of calcite group minerals. IN: AN SSSR. Izvestiya. Fizika Zemli, no. 2, 1973, 23-29.

Katrenko, V. G. Method of transmitting seismic data. Seysmicheskiye pribory, no. 6, 1972, 160-166.

Khrychev, B. A. Some results from studies of crustal velocity characteristics along the Temirtau - Kuybyshev deep seismic sounding profile. IN: AN SSSR. Mezhduvedomstvennyy geofizicheskiy komitet. Rezul'taty po mezhdunarodnym geofizicheskim proyektam. Metodika i rezul'taty issledovaniy zemnoy kory i verkhney mantii (Methods of and results from studies of the crust and upper mantle). Moskva, Izd-vo Nauka, 1972, 172-180. (ITS: Verkhnyaya mantiya, no. 8, 1972).

Kirnos, D. P., and M. I. Yaroshevich. Wide-band seismograph with constant magnification in the 2 to 200-second seismic-wave period range. Seysmicheskiye pribory, no. 6, 1972, 3-5.

Kirnos, D. P., et al. RZZ recording unit for "rough" recording of strong distant earthquakes. Seysmicheskiye pribory, no. 6, 1972, 17-21.

Kondorskaya, N. V., and Z. I. Aranovich. Trends in the development of the network of seismological stations in the USSR, from 1956 to 1966. Seysmicheskiye pribory, no. 6, 1972, 58-66

Kuzin, I. P. P- and S-wave velocities in the upper mantle of Kamchatka. IN: AN SSSR. Izvestiya. Fizika Zemli, no. 2, 1973, 3-16.

Kuznetsov, A. A., et al. Device for automatic selection of precise time signals. Seysmicheskiye pribory, no. 6, 1972, 151-157.

Lurmanashvili, O. V. Periodicity of strong Caucasian earthquakes. IN: AN SSSR Izvestiya. Fizika Zemli, no. 2, 1973, 80-86.

Markaryan, R. R. Experimental recording of seismic signals using a minimum number of discrete values. Seysmicheskiye pribory, no. 6, 1972, 80-82.

Mavlyanov, G. A., et al. Possible use of local variation in the geomagnetic field for earthquake prediction. Uzbekskiy geologicheskiy zhurnal, no. 1, 1973, 68-71.

Melamud, A. Ya., and S. A. Negrebetskiy. Seismic delay unit with a band cutoff device. Seysmicheskiye pribory, no. 6, 1972, 138-143.

Melamud, A. Ya., and S. A. Negrebetskiy. Semiconductor seismic correlator. Seysmicheskiye pribory, no. 6, 1972, 144-151.

Nikolayev, A. V. Model of a seismically turbid medium and possibilities for studying small inhomogeneities in the crust. IN: AN SSSR. Mezhduvedomstvennyy geofizicheskiy komitet. Rezul'taty po mezhdunarodnym geofizicheskim proyektam. Metodika i rezul'taty issledovaniy zemnoy kory i verkhney mantii (Methods of and results from studies of the crust and upper mantle). Moskva, Izd-vo Nauka, 1972, 159-171. (ITS: Verkhnyaya mantiya, no. 8, 1972).

Osadchiy, A. P. Optimum matching of a seismometer with an amplifier. Seysmicheskiye pribory, no. 6, 1972, 102-108.

Peshkov, A. B., and F. Sadikov. Some characteristic features in the study of the phase-dispersion velocities of surface waves in individual regions of southeastern Central Asia. Uzbekskiy geologicheskiy zhurnal, no. 1, 1973, 82-86.

Pol'skiy, E. M. Power ratios for thermal recording. Seysmicheskiye pribory, no. 6, 1972, 115-120.

Pustil'nikov, M. P., and A. V. Semenov. Tectonics of the basement of the platform within the confines of the northern Caucasus. Sovetskaya geologiya, no. 2, 1973, 121-129.

Rakhimova, I. Sh. Relationship between the main crustal interfaces in the Ukraine. IN: AN UkrSSR. Dopovidi. Seriya B. Heolohiya, heofizyka, khimiya ta biolohiya, no. 2, 1973, 157-160.

Razinkova, M. I. Relationship between thicknesses of crustal layers within large elements of the geological structure of the USSR. IN: AN SSSR. Mezhduvedomstvennyy geofizicheskiy komitet. Rezul'taty po mezhdunarodnym geofizicheskim proyektam. Metodika i rezul'taty issledovaniy zemnoy kory i verkhney mantii (Methods of and results from studies of the crust and upper mantle). Moskva, Izd-vo Nauka, 1972, 243-249. (ITS: Verkhnyaya mantiya, no. 8, 1972).

Rozenberg, I. M. Recording the initial phase of a random process in a delay mode. Seysmicheskiye pribory, no. 6, 1972, 120-127.

Ryabinin, Yu. N. A possible mechanism for the origination process of deep-seated earthquakes. IN: AN SSSR. Doklady, v. 208, no. 4, 1973, 822-824.

Ryaboy, V. Z., and I. N. Galkin. Absolute amplitude characteristics of signals in deep seismic sounding studies. IN: AN SSSR. Mezhduvedomstvennyy geofizicheskiy komitet. Rezul'taty po mezhdunarodnym geofizicheskim proyektam. Metodika i rezul'taty issledovaniy zemnoy kory i verkhney mantii (Methods of and results from studies of the crust and upper mantle). Moskva, Izd-vo Nauka, 1972, 140-158. (ITS: Verkhnyaya mantiya, no. 8, 1972).

Rykov, A. V. Extending the frequency response of a seismograph through filtering. Seysmicheskiye pribory, no. 6, 1972, 32-34.

Rykov, A. V. Improvement of seismometer stability through feed back near its stability limit. Seysmicheskiye pribory, no. 6, 1972, 26-32.

Sarkisov, Yu. M. Basement relief of the Baltic syneclise and its position in the overall structure of the northwestern Russian Platform. IN: AN SSSR. Mezhduvedomstvennyy geofizicheskiy komitet. Rezul'taty po mezhdunarodnym geofizicheskim proyektam. Metodika i rezul'taty issledovaniy zemnoy kory i verkhney mantii (Methods of and results from studies of the crust and upper mantle). Moskva, Izd-vo Nauka, 1972, 231-237. (ITS: Verkhnyaya mantiya, no. 8, 1972).

Shchukin, Yu. K., and T. B. Dobrev. Characteristics of seismogenic fractures in the crust. IN: AN SSSR. Mezhduvedomstvennyy geofizicheskiy komitet. Rezul'taty po mezhdunarodnym geofizicheskim proyektam. Metodika i rezul'taty issledovaniy zemnoy kory i verkhney mantii (Methods of and results from studies of the crust and upper mantle). Moskva, Izd-vo Nauka, 1972, 181-195. (ITS: Verkhnyaya mantiya, no. 8, 1972).

Shlezinger, A. Ye. The position of mountainous Crimea in the overall structure of the southern USSR. IN: AN SSSR. Mezhduvedomstvennyy geofizicheskiy komitet. Rezul'taty po mezhdunarodnym geofizicheskim proyektam. Metodika i rezul'taty issledovaniy zemnoy kory i verkhney mantii (Methods of and results from studies of the crust and upper mantle). Moskva, Izd-vo Nauka, 1972, 212-230. (ITS: Verkhnyaya mantiya, no. 8, 1972).

Smelyanskaya, T. V. Interpretation of subsequent arrivals of wave fields recorded during deep seismic sounding. IN: AN UkrSSR. Geofizicheskiy sbornik, no. 50, 1972, 50-54.

Sultankhodzhayev, A. N. Hydrogeological criteria for the prediction of strong earthquakes. Uzbekskiy geologicheskiy zhurnal, no. 1, 1973, 9

Tokmakov, V. A. Nomograms for computing seismograph damping. Seysmicheskiye pribory, no. 6, 1972, 97-102.

Tuyezov, I. K., and E. G. Zhil'tsov. Deep structure of Japan, based on seismic data. IN: AN SSSR. Mezhduvedomstvennyy geofizicheskiy komitet. Rezul'taty po mezhdunarodnym geofizicheskim proyektam. Metodika i rezul'taty issledovaniy zemnoy kory i verkhney mantii (Methods of and results from studies of the crust and upper mantle). Moskva, Izd-vo Nauka, 1972, 114-134. (ITS: Verkhnyaya mantiya, no. 8, 1972).

Vashchilov, Yu. Ya., and A. G. Gaynanov. Density discontinuities in the crust and upper mantle. IN: AN SSSR. Mezhduvedomstvennyy geofizicheskiy komitet. Rezul'taty po mezhdunarodnym geofizicheskim proyektam. Metodika i rezul'taty issledovaniy zemnoy kory i verkhney mantii (Methods of and results from studies of the crust and upper mantle). Moskva, Izd-vo Nauka, 1972, 44-52. (ITS: Verkhnyaya mantiya, no. 8, 1972).

Yepinat'yeva, A. M. Determination of the thickness of a refracting layer. IN: AN UkrSSR. Geofizicheskiy sbornik, no. 50, 1972, 3-12.

Zarayskiy, M. P. Correction of the frequency response of a seismograph. Seysmicheskiye pribory, no. 6, 1972, 53-57.

Zhadin, V. V., and A. A. Dergachev. Measurement of crustal Q from microearthquake records. IN: AN SSSR. Izvestiya. Fizika Zemli, no. 2, 1973, 17-22.

Monographs

Galkin, I. N. Postroyeniye seysmicheskoy modeli zemnoy kory (Construction of a seismic model of the Earth's crust). Moskva, Izd-vo Nauka, 1972, 121 p.

Malovitskiy, Ya. P., and Yu. P. Neprochnov, eds. Stroyeniye zapadnoy chasti Chernomorskoy vpadiny (Structure of the western portion of the Black Sea depression). Moskva, Izd-vo Nauka, 1972, 241 p. (SERIES NOTE: AN SSSR. Mezduvedomstvennyy geofizicheskiy komitet. Rezul'taty issledovaniy po mezdunarodnym geofizicheskim proyektam. Verkhnyaya mantiya, no. 10, 1972).

Zharkov, V. N. Vnutreneye stroyeniye Zemli, Luny i planet (Internal structure of the Earth, Moon, and planets). Moskva, Izd-vo Znaniye, 1973, 63 p. (Novoye v zhizni, nauke, tekhnike. Seriya kosmonavtika, astronomiya, no. 2, 1973).

4. Particle Beams

A. Abstracts

Yegorov, N. V., V. I. Il'in, and G. N. Fursey. Device for studying pulsed field emission. PTE, no. 4, 1972, 157-160.

The subject pulsed field emission device consists of a vacuum tube high-voltage square pulse generator and sensitive circuitry for direct recording of weak field emission currents. The generator produces pulses of varying polarity at a single output with regulated duration and amplitude. The amplitude is regulated smoothly from 0 to 20 kv for negative pulses and from 0 to 7 kv for positive pulses by varying the anode voltage of the switch tubes. Positive and negative pulse duration is controlled by varying the starter pulse duration of a two channel generator, providing 220 v positive pulses and 120 v negative pulses for each channel at durations from 10 μsec to 10 msec. The high-voltage negative pulse had a rise of 2 to 3 μsec, a $\leq$ 50 μsec drop and a surge-free peak decaying at a rate of 0.015% per μsec. The high-voltage positive pulse had a 1 msec rise and drop and a peak, with surges, decaying at a rate of 0.005% per msec. The sensitive circuitry can record weak field emission currents of $\sim 10^{-11}$ - 10^{-12} a. Full schematics are given of the pulse generator and the field emission current recording circuit, and the operating characteristics are briefly discussed. The apparatus provides a refinement in measuring high-voltage field emission currents, since it increases the current measuring range by 7 or 8 orders.

Mesyats, G. A., B. M. Koval'chuk, and Yu. F. Potalitsyn. A method of obtaining an electric discharge in gas. Author's certificate, USSR no. 356824, published February 20, 1970. (Otkr izobr , no. 32/72, p. 171) (Translation)

A method is introduced of producing an electric discharge in gas by application of potential to the discharge circuit electrodes, and

discharge initiation by an electron beam. The electron beam should have sufficient energy for the electrons to cross the discharge gap to expand the discharge zone and shorten the discharge build-up time.

Bobylev, V. I., A. M. Kozodayev, N. V. Lazarev, V. S. Skachkov, and Yu. B. Stasevich. High-voltage thyristor generator of powerful pulsed current. PTE, no. 4, 1972, 103-106.

A thyristor pulse generator is described which develops a powerful pulsed current in an inductive load (Fig. 1). The generator

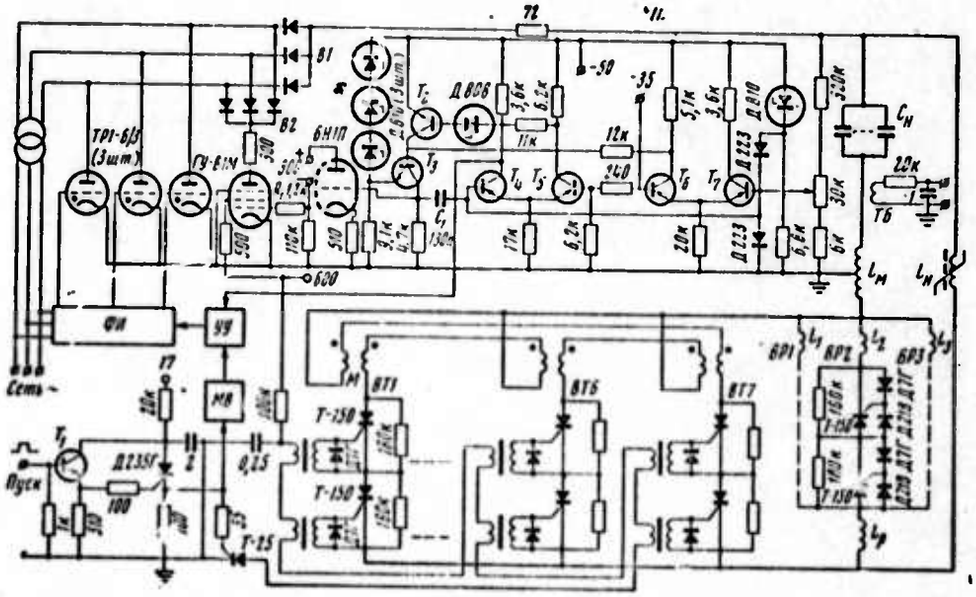

Fig. 1. Pulsed current generator.

Capacitance, C_H, is from 30 condensers. Rectifier groups B_1 and B_2 are assembled in series-parallel connections of diodes D234B. T_1 - MP111B; T_2 and T_3 - P308; T_4 - T_7 - MP26B.

minimizes the difficulties in using high-speed charging circuits for capacitive accumulators. During condenser charging, all points of the winding remained practically below ground potential. The pulsed voltage at the load outputs relative to ground potential was reduced by 50%, in comparison to standard battery condenser voltages, and was applied to the winding outputs (relative to the average ground points) during pulse operation only. Alternate operation of the high-current thyristor and high-speed charge sources of the capacitive accumulator (4.5 mf), along with the regeneration of condenser energy, produced a pulsed current of 20 ka, 0.7 to 1 msec duration, and a frequency of several Hz, and stabilized battery condenser voltages with an accuracy of ±0.01%. The stability of pulsed current amplitude was ±0.03%. Experimental results were in good agreement with theoretical findings.

Varfolomeyev, A. A., V. A. Bazylev, and N. K. Zhevago. Bremsstrahlung spectrum of ultrarelativistic electrons in a dense medium. ZhETF, v. 63, no. 3, 1972, 820-830.

The bremsstrahlung radiation from high energy electrons was investigated in a dense absorbing medium. Variation of the electron multiple scattering constant due to specific energy losses resulted in higher radiation suppression than the usual multiple scattering effect. The feasibility is considered of separating the total loss of ultrarelativistic electrons in the absorbing media into bremsstrahlung and direct electron-positron pair formation. Expressions for the bremmstrahlung spectra are derived with allowance for the virtual quantum absorption, ambient polarization and multiple scattering having a varying constant. Results are plotted in Fig. 1.

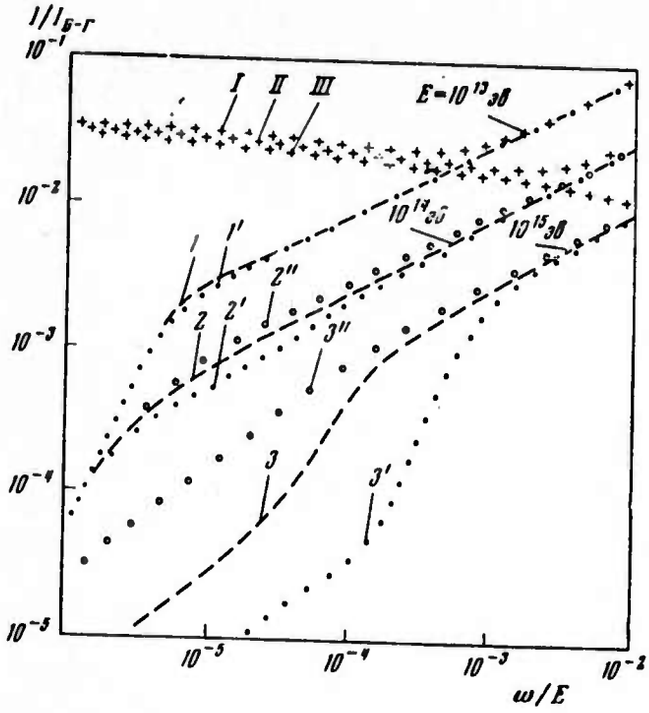

Fig. 1. Bremsstrahlung loss of electrons with various energies in lead.

I - radiation intensity taking into account the effect of the medium
I_{B-G} - radiation intensity according to Bethe-Heitler
ω - quantum radiation energy
E - electron energy.

I, II, III - total electron energy loss from formation of electron-positron pairs and bremsstrahlung.
1, 2, 3 - normal multiple scattering effect along with virtual quantum absorption and medium polarization.
1', 2', 3' - variations in energy and subsequent multiple scattering constant on the coherent length.
2'', 3'' - calculated results.

For electrons with energies not exceeding 10^{14} ev, the ambient polarization effect predominates in the soft quanta region $\omega \lesssim 10^{-3}E^{2/3}$ ev, and the normal multiple scattering effect occurs in the region where $\omega \gtrsim 10^{-3}E^{2/3}$ ev. At an energy of 10^{14} ev, the effects of virtual quantum absorption and scattering constant variation become significant in the frequency region 10^{8} ev $\lesssim \omega \lesssim 10^{-20}E^{2}$ ev, and polarization in the medium affects quantum radiation with

frequencies 10^8 ev $> \omega$. In the hard quantum region $\omega > 10^{-20}E^2$ ev, however, the normal multiple scattering effect predominates. The effect of multiple scattering constant variation at high electron energies on the radiation processes consequently results in extensive suppression of bremsstrahlung in the quantum frequency region, expanding rapidly with increase in electron energy.

Antonov, G. G., V. S. Borodin, A. I. Zaytsev, and F. G. Rutberg. Problems of investigating heavy-current discharge in a high pressure chamber. I. ZhTF, no. 10, 1972, 2121-2126.

Plasma properties were investigated from a heavy-current discharge in a high pressure chamber. The experimental device shown in Fig. 1 was a stainless steel pulse plasmatron designed for 1500 atm. The

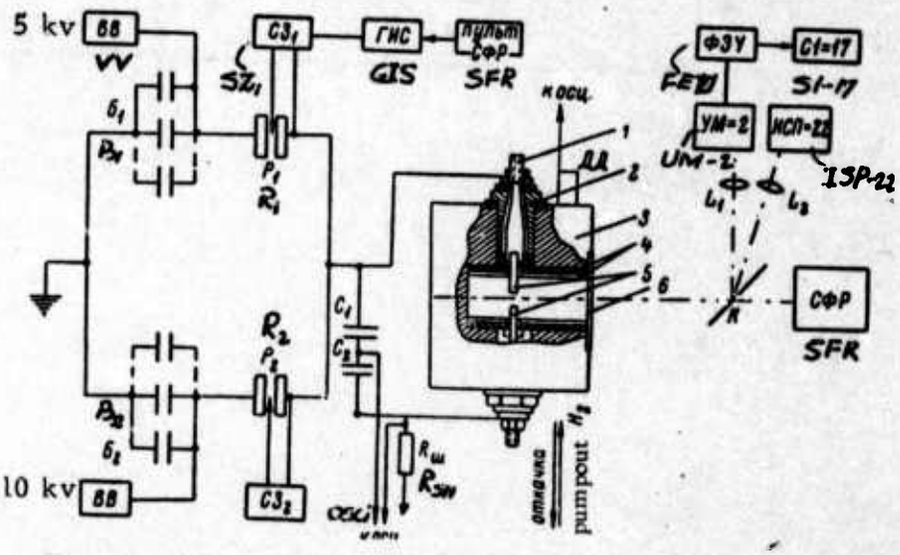

Fig. 1. Block diagram of experimental device.

1 - current lead, 2 - gasket, 3 - plasmatron frame, 4 - insulation, 5 - electrodes, 6 - diaphragm of lenses L_1 and L_2, SZ - trigger circuit, vv - high-voltage rectifier, k - beam splitter.

ID was 50 mm with a 65 mm depth. Electrode (7 mm. dia., tungsten or copper) spacing varied from 15 to 30 mm. Hydrogen was the working medium, and the plasmatron was fed from condenser batteries. The main battery (capacitance $C = 8 \cdot 10^{-3}$ f) had 80 100 μf, 5 kv condensers and the auxiliary battery used 34 μf, 10 kv condensers. The plasmatron was connected to the source through dischargers R_1 and R_2 (Fig. 1) and operation was synchronized by pulse generators. A noninductive coaxial shunt with a resistance $R_{SH} = 4 \cdot 10^{-4}$ ohm was used to measure the current. Overall inductance and active resistance of the batteries and input circuit were $1 \cdot 5 \times 10^{-6}$ h and 10^{-3} ohm, respectively. Voltage, current, temperature and electron density were measured as well as the geometry and intensity of discharge, and discharge chamber pressure.

Fig. 2 shows typical discharge voltage and current oscillograms

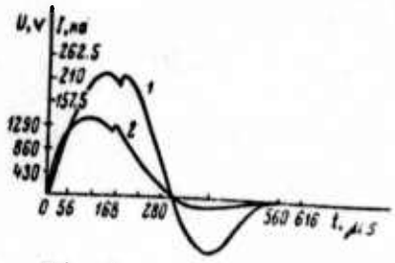

Fig. 2. Discharge current and voltage oscillograms.

1 - I = 270 ka; 2 - U = 1420V; p = 6 atm. Working gas - H_2.

with limiting values of 1800 v and 350 ka. The nonrectangular radial intensity distribution characteristic of the discharge column indicates that the plasma did not radiate like a black body. Measurements based on recombination and bremsstrahlung spectra reveal that the electron density varied in the range $(2 \text{ to } 4) \cdot 10^{19}$ cm^3 in the maximum current region. The electron density was determined under the assumption that the discharge column average temperature was $(0.6 \text{ to } 1) \cdot 10^5$ °K. At such temperatures and densities, the absorption coefficient in H_2 in the visible region did not exceed (0.5~3)/cm. Streak camera pictures indicate that the discharge was stable with an average or optical column diameter of 0.5 - 0.6 cm. A constriction was noted 10-20 μsec

after the discharge initiation with a diameter of 0.3-0.4 cm (Fig. 4).

Fig. 3. Streak camera picture of the discharge.
I = 270 ka, U = 1420 v, p = 6 atm.
a - 6; b - 20; c - 150 μsec.

The constriction remained for at least 180 μsec but did not cause discharge destabilization.

Chogovadze, M. Ye. Quasilinear relaxation of a monoenergetic relativistic electron beam in an external magnetic field. ZhTF, no. 10, 1972, 2022-2028.

The quasilinear relaxation of linear oscillations of a monoenergetic relativistic electron beam were investigated in a confined plasma in the presence of an external magnetic field. The author considers a system consisting of a plasma-filled, metal waveguide of radius R, through which the monoenergetic relativistic electron beam passes with a velocity U along the waveguide axis. Dispersion equations are formulated for the axisymmetrical modes of electromagnetic waves in the system, and the residual magnetic fields are discussed for dense ($\omega_{Lo} >> \Omega$) and rare ($\Omega >> \omega_{Lo}$) plasma (ω_{Lo} - Langmuir frequency of plasma electrons, Ω - Larmor frequency). It is noted that the quasilinear relaxation of a monoenergetic relativistic electron beam in a confined plasma in the presence and absence of an external magnetic field is significantly inhomogeneous, and the beam decays at a velocity characterized by Maxwellian scattering with an anisotropic temperature.

In a weak magnetic field, $\Omega\gamma^{-1} < \mathrm{Re}\,\delta_k$ [$\gamma = (1 - u^2/c^2)^{-1/2}$, $\mathrm{Re}\,\delta_k$ - instability increment], conditions and results are similar to those of a plasma with no magnetic field. The steady-state oscillation energy in such cases is about $(n_1/2n_e)^{1/3}$ of the initial beam energy. In a strong magnetic field, $\Omega\gamma^{-1} > \mathrm{Re}\,\delta_k$, conditions exist for hydrodynamic beam instability and at certain conditions [$(k^2/k_\parallel^2)(\gamma^4\beta_u) > (\Omega^2\gamma^{-2}/(\mathrm{Re}\,\delta_k)^2) > 1$], the quasilinear relaxation time, the temperature and the steady-state oscillation energy in the dense as well as rare plasmas are strongly dependent on the external magnetic field. The steady-state energy of quasilinear oscillation relaxation in a dense plasma differs from that in a rare plasma only by a numerical factor.

Kolomenskiy, A. A., and I. I. Logachev.
Problems on the theory of ion acceleration
by electron beam scanning. IN: 2-go Vses.
soveshch. po uskoritelyam zaryazhen. chastits,
1970. T. 1. Moskva, nauka, 1972, 204-206.
(RZhElektr, 12/72, no. 12A383)(Translation)

Particle dynamics are discussed during scanning by electron beams charged with ions. The collective ion accelerator containing the electron beam scanner consists of an electron gun and focusing and deflecting systems. Electron beam scanning was done by magnetic or electrical rotating systems, with parameters selected from optimum accelerating conditions. Computer calculations show that ion motion during angular beam displacement, within 30° limits occurred in a near-parallel forward scanning direction, accompanied by a negligible thermal ion velocity effect on the motion characteristics. At an 8 ka electron beam current, the maximum ion acceleration energy would be 200 Mev.

Lavrovskiy, V. A., I. F. Kharchenko, and Ye. G. Shustin. Single-mode interaction of a plasma-beam discharge in a turbulent regime. ZhETF P, v. 16, no. 11, 1972, 602-606.

Transient characteristics in a high frequency beam-plasma system are analysed. The characteristics were measured during a time interva much shorter than the normal time of discharge parameter variations. Measurements were made in a plasma-beam discharge in hydrogen during steady injection of a 1 kev electron beam at currents of 20 to 40 ma. Distribution functions were determined during the application of a 2.5×10^{-7} sec duration sawtooth voltage on an analyzer with a delay potential. The time structure of HF oscillations was fixed at a time interval equal to 10^{-7} sec. The measurement circuit operated in a single triggering regime at random times. A typical statistically analyzed oscillogram of E(t) is given in Fig. 1.

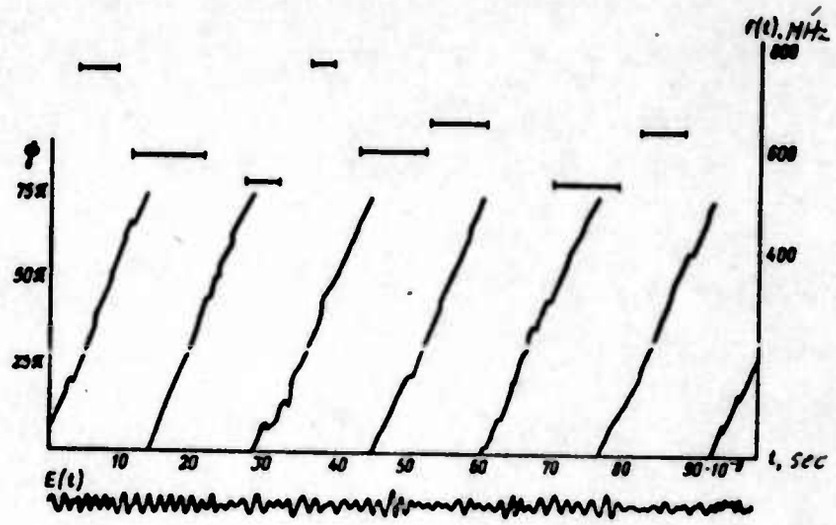

Fig. 1. Typical oscillogram of HF field E(t), running phase of oscillation $\psi(t)$, and instantaneous frequency of quasi-harmonic inclusions f(t).

Quasi-harmonic inclusions and sharp oscillation phase changes are evident in the $\psi(t)$ curve. The f(t) curve indicates that oscillations mainly occur in four frequency zones: 530; 580-590; 630-640; and 750-760 MHz, which apparently alternate randomly with time. The duration of the quasi-harmonic inclusions is short: $(5\text{-}10)\times10^{-9}$ sec. Frequency retuning is usually followed by phase discontinuities of 70 to 180°.

Addition of the duration of separate frequency components yields values characterizing the probability distributions of the frequency excitations. Electron beam interactions with plasma appear to be coherent, although the average spectra indicate the interactions to be stochastic. The average characteristic of HF oscillations and beam conditions conceal the natural interaction characteristics. The author suggests that the rapid retuning frequency oscillations, resulting in the stochasticity of the system average characteristics, is due to the oscillation instability of separate frequencies owing to low frequency oscillations; the relation of various normal modes; or the excitation of satellite spectra from periodic oscillations of bunches in the potential well of an excited wave.

Levin, V. M., V. V. Rumyantsev, K. P. Rybas, and B. N. Telepayev. Electron gun for obtaining intense electron beams. IN: Tr. 2-go Vses. soveshch. po uskoritelyam zaryazhen. chastits, 1970. T. 1. Moskva, Nauka, 1972, 92-94. (RZhElektr, 12/72, no. 12A385) (Translation)

Standard Pierce optics permits the generation of an electron beam with a perveance of $\leq 3\times10^{-6}$ $A/B^{3/2}$. Reducing of the anode aperture

by grid methods can increase the perveance value significantly. A compressed porous nickel-oxide cathode with a spherical emitting surface and a 50 mm diameter was developed. At a temperature of 970° C, the emission current density in a space charge regime was 110 a/cm^2; the cathode heating power up to this temperature was 500 w. The electron gun reached a maximum perveance of 11×10^{-6} A/B$^{3/2}$ even at a 200 kv voltage and a 1 ka current. The authors conclude that it is feasible to produce a dual-electrode gun with a gridded anode at currents to 4 ka, a pulse duration to 0.1 msec, a duty cycle of $2 \cdot 10^{-6}$, and voltages to 3000 kv.

Yakushev, V. P., and A. N. Serbinov. Stable operating conditions for high-voltage accelerator tubes. IN: Tr. 2-go vses. soveshch. po uskoritelyam zaryazhen. chastits, 1970. T. 1. Moskva, Nauka, 1972, 86-88. (RZhElektr, 12/72, no. 12A380) (Translation)

The volt-ampere characteristics of high-voltage accelerating tubes were analyzed. A method for calculating stability limits was verified using an inclined-field, 200 kv tube. The tube has four accelerator gaps, a 480 mm active section length, and 20 mm diameter electrode apertures. The optimistic stability limit was 49 kv, the pessimistic limit was 109 kv, and the experimental limit was 75 kv. The stability limits were determined for individual tube sections. Stability diagrams are given for EG-1 and EG-2.5 accelerator tubes.

Meskhi, G. O., and B. N. Yablokov. Electron gun with a cold emission cathode. IN: Tr. 2-go Vses. soveshch. po uskoritelyam zaryazhen. chastits, 1970. T. 1. Moskva, Nauka, 1972, 90-92. (RZhElektr, 12/72, no. 12A364) (Translation)

An equivalent electron gun circuit for generating nanosecond pulses is analyzed. Glycerin was used as an insulating medium in the ESU-1 accelerator, designed for voltages up to 3 Mv and 30 ka pulsed currents. The high-voltage insulator served as an impedance match from the glycerin-filled coaxial line to a vacuum coaxial line. The use of a dielectric with high permittivity and a sufficiently high susceptance avoids insulator sectioning and simplified the design. The proposed electron gun structure permits controlled spacing between the cathode and anode, and varying of the number of tungsten needle cathodes.

Grishayev, I. A., A. N. Dovbnya, and V. V. Petrenko. A method for obtaining bunches of charged particles in linear accelerators. Author's certificate, USSR, no. 322138, published March 27, 1972. (RZhElektr, 12/72, no. 12A397 P) (Translation)

A method was developed for generating charged particle bunches in a linear accelerator using an HF transverse field with a frequency identical to that of the accelerated field. After passing through the HF field, the particle bunch is injected into a longitudinal magnetic field to reduce the phase spread. Bunch magnitude and length are selected so that the particle path difference at the magnetic field outlet is equal to the bunch initial length.

Kazanskiy, L. N., A. A. Kolomenskiy, G. O. Meskhi, and B. N. Yablokov. A heavy-current direct-action electron pulse accelerator. IN: 2-go Vses soveshch. po uskoritelyam zaryazhen. chastits, 1970. T. 1. Moskva, nauka, 1972, 95-97. (RZhElektr, 12/72, no. 12A384) (Translation)

A model electron pulse accelerator (ESU-O) at 600-800 kev was built to test the principles of the ESU-1 accelerator at FIAN. Model line wave impedance was the same as the ESU-1 at 7 ohms. The external line was commutated by a spark gap, filled with nitrogen at 7 atm. The ESU-O model was used for testing various types of spark gaps, pulse distortions, pulse transformers and electron gun designs. The electron source was 1 to 5 tungsten needles, having a 0.1 mm tip radius and fabricated by electrolytic polishing of 2-3 mm diameter wires. Model parameters were: beam energy at outlet-0.8 Mev, pulsed beam current - 20 ka, pulse duration - 35 nsec and single pulse operating mode.

Bondarenko, B. V., V. I. Makukha, and A. S. Gaydarov. Investigating knife-edge field emitters of disc-like form. RiE, no. 12, 1972, 2634-2637.

Field emission from tantalum, niobium and copper disc-shaped knife-edge cathodes was tested. The 50 μ foil discs were electrochemically etched. The cathodes were shaped by HF current hardening in vacuum under the simultaneous effect of an electric field with reverse polarity (high positive voltage to the disc-cathode, negative voltage to the anode).

The discs were heated to 600° C at pressures of 3-- 5×10^{-6} torr during this stage.

Surface-processed specimens were placed in test diodes (Fig. 1) to examine field emission currents. Residual gas was maintained at 2×10^{-7} torr after evacuating and gettering.

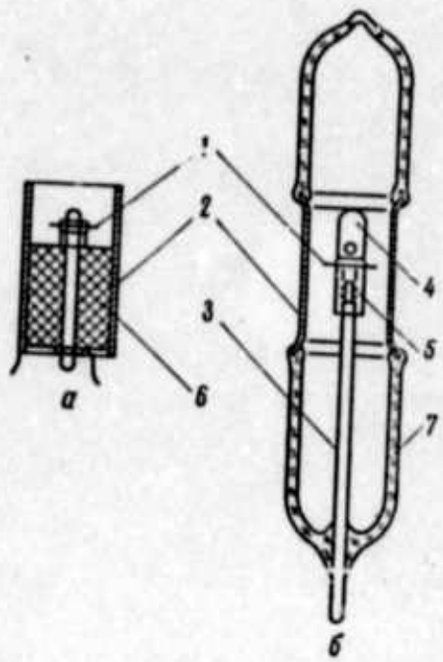

Fig. 1. Test diodes. a - ceramic b - Kovar-sealed anode. 1 - cathode, 2 - anode, 3 - molybdenum inlet, 4 - shaped bolt, 5 - coupling, 6 - ceramic material, 7 - cylinder.

The volt-ampere characteristics i(u) of the knife-edge field emitters are plotted in Fig. 2 using the customary coordinates, $\lg (i/u^2)$ vs. $(10^4/u)$. Disc diameter was 13 mm, and electrode spacing was 0.5 mm. A steady-state mode current of 100 μa was generated at voltages of 5 kv (tantalum), 6 kv (niobium), and 7 kv (copper).

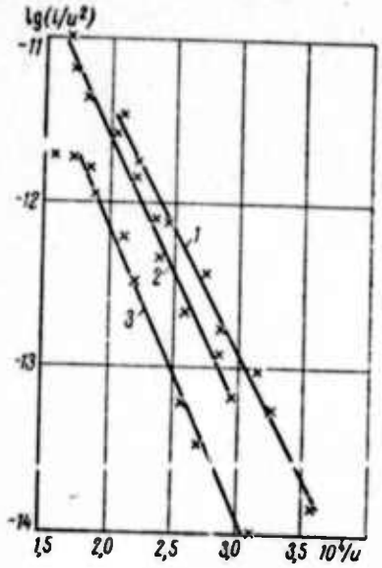

Fig. 2. Volt-ampere characteristics of knife-edge field emitter current. 1 - tantalum, 2 - niobium, 3 - copper.

The cathode field emission was unstable with time and nonuniform along edge boundaries for all three cathodes; this was particularly evident in the copper cathode, which underwent a current drop from 100 to 20 μa, after a 5 minute operating period. Fig. 3 shows emission effects on two of the three tested metals.

Results indicate that flattening of the edge curvature did not occur but many microhardness or field emission centers developed. The edge curvature dispersion should be minimized, by using single crystal materials for the edges or reducing nonuniform recrystallization, to generate substantial field emission currents from tantalum and niobium emitters. Owing to its low strength and high work function, copper is an unsatisfactory material for disc emitter cathodes.

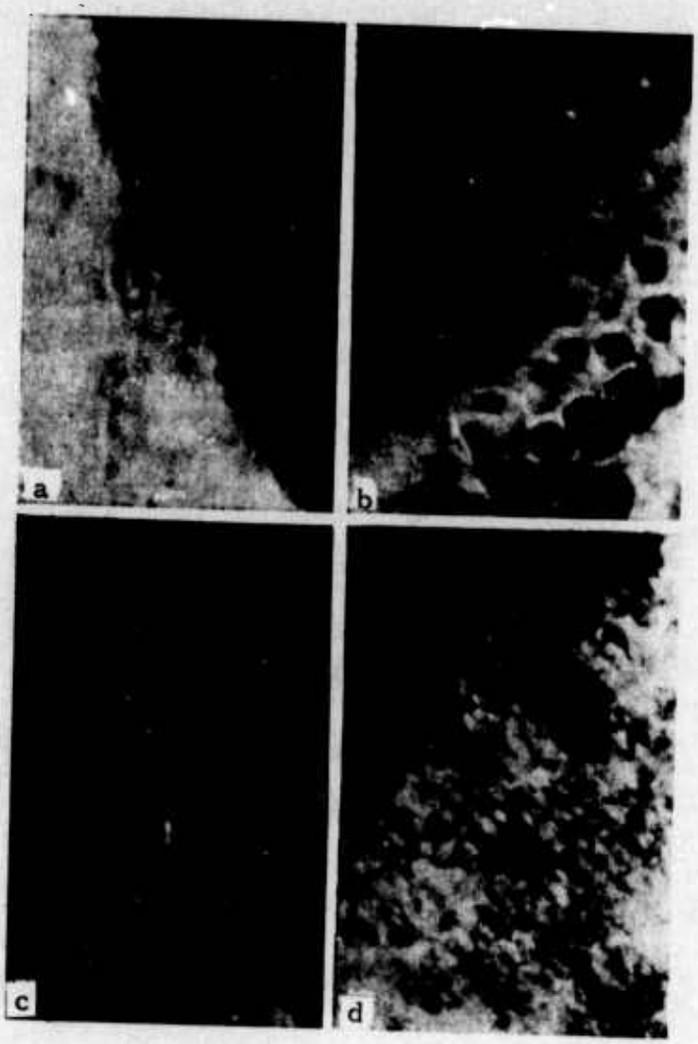

Fig. 3. Knife-edge emitters after etching (x200).
a, c, d - tantalum; b - niobium.

Lazarenko, B. R., and N. I. Lazarenko.
Plasmoids - a powerful technological factor. EOM, no. 5, 1972, 3-8.

Plasma generation from short electric pulses is reviewed. Three cases of electric spark discharge are considered: 1) the electrode geometrical axes are collinear; 2) the axes are at an angle; and 3) the axes are parallel. Fig. 1 shows an exterior view of a discharge in the first

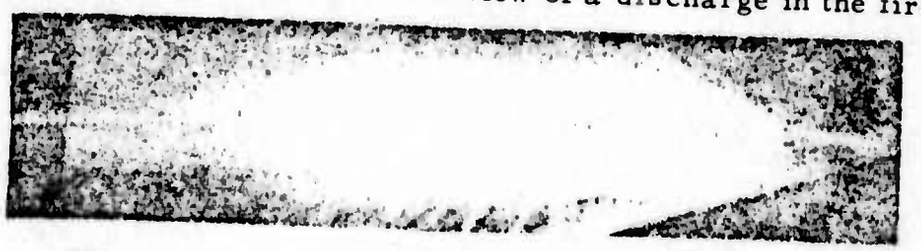

Fig. 1. Scan of a spark discharge between electrodes with collinear geometrical axes. Pulse duration = 100 μsec, current = 2000 a.

case, whose features are:

a) the direction of the electrode material vapor jet coincides with that of electron beam motion and has a common geometrical axis.

b) the beam moves in a straight line, impacts a solid metal surface (anode), and penetrates it without changing the axis of motion.

c) the plasma generated from the spark discharge is confined by the interelectrode gap and touches the electrode surface at both ends. The discharge channel and metal vapor jet for the second case is shown in Fig. 2.

Fig. 2. Scan of a spark discharge between electrodes with geometrical axes at 90° angles. Maximum current = 2000 a.

Distinctive features are:

a) The electron beam movement axis is a curved line.

b) The trajectory of the electrode material vapor jet did not coincide with that of the discharge channel. The observed flares of electrode material vapors had no part in conducting current.

c) The discharge plasma could partially deviate from the discharge channel trajectory.

d) The electron beam touched the electrode surfaces at both ends during the full pulse duration.

The third case (parallel electrodes) of an electric discharge results in plasmoids or toroidal energy bunches moving at a high velocity (Fig. 3). The authors cite the early experimental work of Bostik (Problemy)

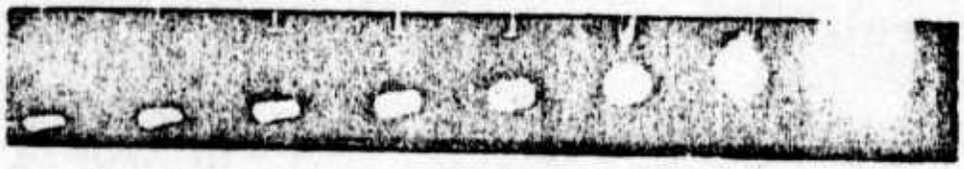

Fig. 3. Photo sequence of energy bunch emission from a plasmoid generator. Speed = 5000 frames/sec.

Vsovremennoy fiziki, 1958, no. 3) using two parallel electrodes. When a current pulse of 0.5 μsec duration and a few thousand amperes amplitude was excited, plasmoids were generated moving at a velocity of 190 km/sec. Plasmoid properties are summarized, including the capacity of freely passing through magnetic fields, surviving mutual collisions, and behaving as an independent electrical system. They can be stretched into cylinders, twisted into coils, formed into loops, and be interlaced. Plasmoids are very effective in technological processing, especially when the treated specimens are not components of the electric circuit.

Grishayev, I. A., V. D. Krasnikov, and T. F. Nikitina. Method of phasing the accelerating sections of a linear accelerator. Author's certificate, USSR, no. 328531, published April 3, 1972. (RZhElektr, 12/72, no. 12A395 P)(Translation)

A method is suggested for phasing the accelerating sections of a linear accelerator by using a phase inverter. To increase phasing accuracy, an alternating phase change of the accelerating section voltage is made using an auxiliary phase inverter. After detection, the accelerating voltage pulses at the phasing section outlet are compared on the basis of amplitude. The phase of the accelerating section voltage is regulated by the resulting difference signal.

Abu-Asali, Ye., B. A. Al'terkop, and A. A. Rukhadze. Non-linear ion oscillations in plasma, excited by current. ZhETF, v. 63, no. 4, 1972, 1293-1299.

The work continues that of two of the authors (Al'terkop and Rukhadze, ZhETF, v. 62, 1972, 989 and 1760) on the nonlinear oscillation development stage of the audio component in an ion-acoustic instability spectrum of a dense non-isothermal ($T_e >> T_i$) current-carrying plasma. The authors investigated shortwave ion Langmuir oscillation instabilities for conditions of: 1) a rarified weak-collision plasma, when the oscillation buildup is due to the electron Cerenkov effect; and 2) frequent oscillations, when the instability is caused by inverse conductivity and plasma electron diffusion.

Equations are derived for the ion-acoustic instability theory of a non-isothermal current-carrying plasma. The time evolution of the amplitude of a linear unstable wave is studied up to the saturation stage. It is shown that under the conditions considered, the nonlinear shift in excitation wave frequency is an efficient mechanism for restricting amplitude growth.

Voronkov, R. M., V. A. Danilichev, B. Yu. Bogdanovich, and V. F. Gass. Experimental study of field-emission gun parameters. IN: Tr. 2-go vses. soveshch. po uskoritelyam zaryazhen. chastits, Moskva, Nauka, v. 1, 1970, 126-127. (RZhElektr, 12/72, no. 12A355) (Translation)

A field-emission gun is described and gun measurement parameters are given. The gun is intended for the injection of 30 to 40° phase length and 300 to 400 kev electron bunches into an accelerator section at a constant phase velocity equal to the speed of light, and an SHF field intensity of ~100 kv/cm. The resonator is designed for a 16.5 cm wavelength. The tungsten-wire emission cathode is fixed in the resonator such that a direct current will heat it to 1000°-- 2000° C. The 6 to 10 μ radius of curvature points were prepared by electrochemical etching in a 10% KOH solution. A curve of variations is given for the focused magnetic field intensity. A relationship is formulated for beam current and average electron energy as a function of input SHF power.

Persiantsev, I. G., V. D. Pismennyy, A. T. Rakhimov, and A. N. Starostin. Radial distribution of fast electrons in a Z-pinch. ZhETF P, v. 16, no. 2, 1972, 68-72.

The mechanism of charged particle acceleration in powerful pulsed discharges in a rarified gas was investigated based on the radial distribution of fast electrons in a Z-pinch. The experimental device parameters similar to the setup described by Koval'skiy (ZhETF, 38, 1960, 1439), were: C = 60 μf; Vo = 40 kv; I_{max} = 500 ka; and pulse duration = ~ 20 μsec. The working gas was hydrogen at a pressure of 3×10^{-2} torr, purified through a palladium filter. The alundum chamber ID was 20 cm, and chamber length was 80 cm. The anode was a 1.5 mm thick copper electrode with a central diameter of 80 mm. A 1 mm thick plexiglass shield, covered with a thin terphenyl film and protected against plasma emission and electrons below 100 kev by a 45 μ thick aluminum foil, was placed near the anode. Shield luminescence was simultaneously recorded and photographed. Results were:

1. generation of fast electrons (above 100 kev) was observed only after a series of preliminary discharges and not at all at the least indication of gas contamination; this generation lasted for 60 to 150 nsec, and begins and ended in all emission zones simultaneously (within ~10 nsec).

2. The fast electron distribution along the discharge chamber cross-section was characterized by a large diversity for each discharge; it occupied an area of from a fraction to several cm^2, and usually had approximately the same intensity within the limits of each distinctly defined injection zone.

Photographs and microphotograms of a perforated anode are shown in Figs. 1 and 2, respectively. A theoretical explanation of the experimentally observed phenomenon is presented. Theoretical and experimental results are in good agreement.

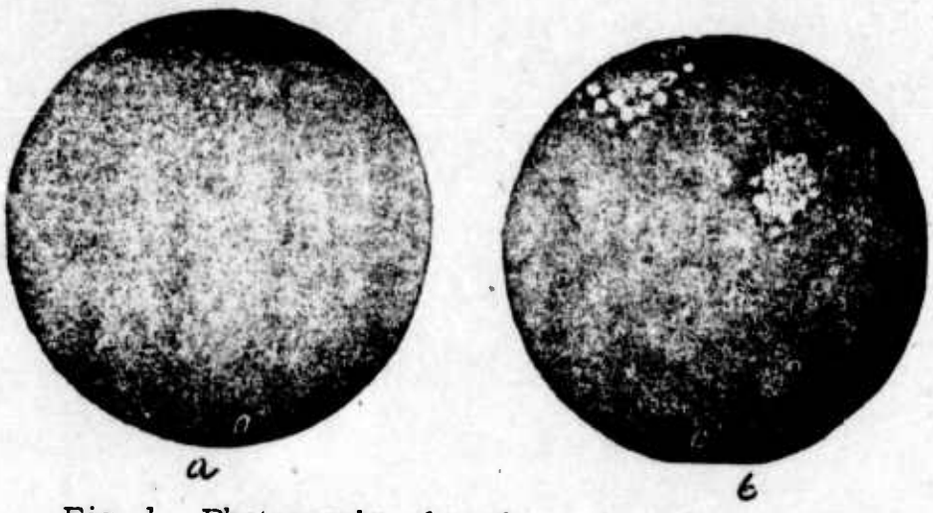

Fig. 1. Photographs of perforated anode in a fast electron beam.

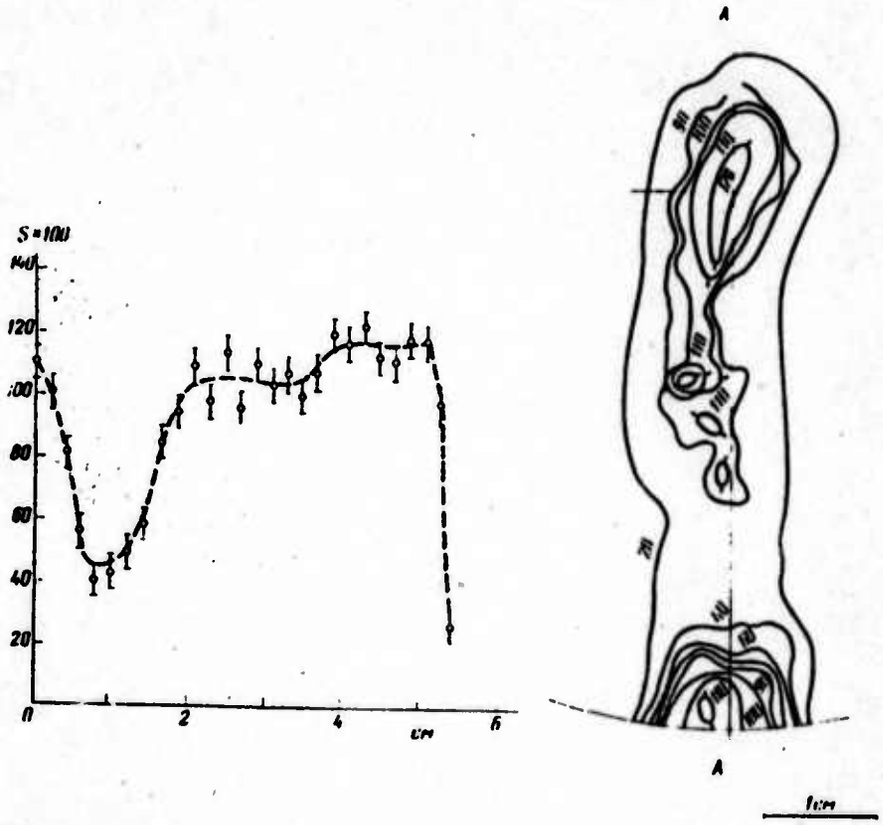

Fig. 2. Microphotograms along A-A and isolines of even darkening for (a) and (b) conditions of Fig. 1.

Danilov, V. N. Quasi-one-dimensional solution to equations for a high-current electron beam. ZhPMTF, no. 4, 1972, 47-56.

Based on a one-dimensional solution to equations for an axisymmetrical double-flow beam, adiabatic approximations are derived which describe the effect of a weakly-inhomogeneous magnetic field on a steady-state quasi-neutral beam. Tubular and beam configurations are discussed, which are confined near the axis at critical current and above. Results show that in strong external fields at the cathode, $B_k \sim 1.7\ (\varkappa/a)$ koe x cm, and high currents $J \sim (R_k/a)\ 8.5$ ka (where $\varkappa$ - relativistic factor, a - beam thickness, R_k - cathode radius), the beam takes on a tubular form with a thickness $a << R_k$. During smooth extraction from the external field, the beam structure changes only slightly compensated by self-fields, commensurate with B_k. By decreasing the current $J \sim 8.5\ \varkappa$ ka, it is possible to generate a drifting beam, in which practically all the linear energy density, $\varkappa^2 (R/a)$ joule/cm, results from lateral oscillations and compares with the heavy-current beam energy density. Beam drift is destroyed at fields substantially lower than $1.7\ (\varkappa/a)$ koe. Beam passage through a diaphragm increases the oscillating energy. Further external field gains in low-current beams make it feasible to adiabatically convert forward and rotational energy into oscillating energy. At a weak external field $B_k \sim 1.7\ (\varkappa/B_k)$ koe x cm, the beam is narrow and tubular with a low oscillation energy, if passed through the diaphragm at a narrow angle to the external field. The cold beam radius significantly increases with withdrawal from the external field. The external field required to localize the laminar beam at a radius R is $1.7\ (\varkappa/R)$ koe x cm and the total current is $\varkappa M 8.5$ ka, proportional to the number of laminations M.

A high current is vital to produce the conditions discussed. A decrease of the relativistic factor $\varkappa$ and a proportional change of current does not affect the beam structure.

Ginzburg, V. L. Electron accelerator with laser undulator as an x-ray source. KSpF, no. 2, 1972, 40-44.

The problem of generating powerful, directed, polarized and monochromatic x-radiation using laser undulators is analyzed. A Doppler formula is given supporting the feasibility of x-ray generation in undulators by accelerated high energy electrons (20-50 Mev). The beam is modulated by laser radiation and the frequency is converted in a manner similar to light scattering on moving electrons. Expressions are formulated for the total radiation energy and the amplitude of electron oscillations by applying simple formulas derived for standard undulators to the study of a laser undulator. Compared to an electric or a magnetic undulator, the laser amplitude is double and the radiation intensity is 4 times greater. Results are similar for laser undulator calculations using the method of light scattering on moving electrons. It is shown that x-ray radiation in high and low energy accelerators can be generated only by sharply increasing the current intensity in the low energy beam. At a high energy accelerator current of $\sim 10^{-4}$ a, the low energy accelerator current should be on the order of 1a. The use of heavy-current accelerators is suggested, making it feasible to generate pulsed current densities up to 10^{8} a/cm^{2}. A related article by Ginzburg appeared earlier (Feb. 1973 Report, 118).

Zav'yalov, M. A. Breakdown conditions in powerful plasma sources of electrons. EOM, no. 4, 1972, 56-61.

Causes of breakdown in powerful plasma sources of electrons are analyzed, such as: increased neutral gas pressure in the gun region; flow breakdown of the operating gas from the gas-discharge source; discharge

formation in metal vapors, impinging on the accelerating gap during materials treatment; and subsiding of a portion of the electron beam in the gun anode. The experimental device (Fig. 1) consisted of a "duo-plasmotron" gas-discharge plasma source, insulator-mounted in the

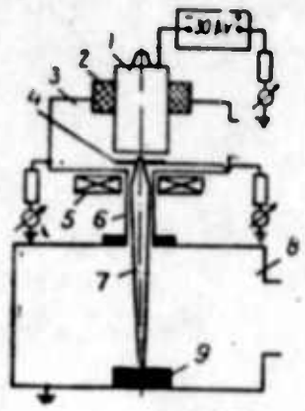

Fig. 1. Experimental sketch.

1 - gas discharge source, 2 - insulator, 3 - intermediate chamber, 4 - accelerating electrode (gun anode), 5 - magnetic lens, 6 - beam guide, 7 - electron beam, 8 - processing chamber, 9 - receiving electrode.

intermediate gap and with a negative potential of 30 kv with respect to the grounded accelerator electrode - anode gun. The exit hole diameter of the gas-discharge source housing was 1.5 - 2 mm; the housing comprised a cylindrical steel electrode, which served as the anode for the duo-plasmatron. The intermediate electrode and cathode were installed in the housing to maintain a gas discharge with the required parameters. Argon pressure was varied from 4×10^{-2} to 1 torr and the discharge current from 0.1 to 12 a. The magnetic lens focuses the electron beam, which passes through the beamguide into the processing chamber, where it is picked up by the receiving electrode.

Total beam length is ~1 m, and the beam diameter close to the electrode ~1 cm. Test pressures in both chambers were varied from 1×10^{-5} to 3×10^{-2} torr by admitting air or argon through an orifice.

Based on a model device, fundamental parameters were estimated for various metals (Fe, Cu, Ni, Ta, Ti) at 30 kv and a power density of $Q_o = 10^3$ w/cm^2 (Table 1). Verification tests were made using a

Table 1

Fundamental process parameters at a specific power of $Q_o = 10^3$ w/cm^2.

Element	Z,e	$\rho \cdot 10^{22}$, cm^3	T°, °K	p(T°), Torr	$n_e \cdot 10^{-16}$, cm^{-3}	α_{eff}, cm^{-1}
Ni	7,6	3,99	~2000	90	45	180
Fe	7,9	4,71	~2600	43	16,5	78
Cu	7,7	4,06	~2200	28	12,7	52
Ti	6,8	5,97	~2600	7,4	2,8	17
Ta	7,7	7,41	~4900	10	2,2	16

plasma electron source with an extracting system design similar to the model used for calculations. The results were found to be in good agreement with calculations. The tests show that a plasma gun, developed with various extracting systems and an electron beam formation power to 90 kw, could work without gas evacuation from the intermediate chamber and under conditions of melting and evaporation of tungsten and niobium, assuming the processing chamber pressure does not exceed $(1-5) \cdot 10^{-4}$ torr, and the beam loss at the anode does not lead to discharge formation in the anode metal vapors. The allowable electric field intensity in the acceleration gap of the plasma electron gun under operating conditions is 100 kw/cm. During high pressure gas tests, no appreciable deformation and destruction was observed in the system from ion bombardment of the source housing (made of standard steel and water-cooled). The author concludes that the feasibility of plasma electron source operation at pressures to 10^{-3} torr probably will lower the demands placed on vacuum systems, thereby simplifying the design problems of processing assemblies.

B. Recent Selections

Aseyev, G. G., G. G. Kuznetsova, N. S. Repalov, B. G. Safronov, and N. A. Khizhnyak. Parametric instability of an electron beam in a spatially-periodic electric field. IN: Fizika plazmy i problemy upravleniya termoyadernogo sinteza. Resp. mezhved. sb., no. 3, 1972, 202-208. (RZhF, 11/72, no. 11G248)

Avilov, E. A., N. V. Belkin, A. V. Dudin, A. P. Zykov, M. A. Kanunov, and A. A. Razin. Stable pulsed high pressure discharger. PTE, no. 1, 1973, 137-139.

Bakuto, I. A., A. I. Bushik, and I. G. Nekrashevich. Distribution in intensity of the spectral line of ions in pulsed discharge plasma. ZhPS, vol. 18, no. 3, 1973, 396-399.

Bogdankevich, L. S., and A. A. Rukhadze. Problems of heavy-current relativistic electron beams. Priroda, no. 2, 1973, 46-49.

Bondarenko, B. V. Effect of cathode sputtering on the stability of electron emission and useful life of field emitters. RiE, no. 3, 1973, 659-661.

Bredikhin, M. Yu., A. M. Il'chenko, A. I. Maslov, A. I. Skibenko, Ye. I. Skibenko, and V. B. Yuferov. Study of a dense plasma, formed by an electron beam in a magnetic trap. IN: Fiz. plasmy i probl. upravl. termoyader. sinteza. Resp. mezhved. sb., no. 3, 1972, 147-161. (RZhF, 11/72, no. 11G237)

Bredikhin, M. Yu., A. I. Maslov, Ye. I. Skibenko, and V. B. Yuferov. Investigating electron heating of a dense beam-plasma discharge in strong magnetic fields. UFZh, no. 2, 1973, 315-317.

Charnaya, F. A. Some absolute data on pulsed discharge emission in the vacuum ultraviolet. ZhPS, v. 18, no. 2, 1973, 187-189.

Demirkhanov, R. A., A. K. Gevorkov, A. F. Popov, and O. A. Kolmakov. Investigating absorption and radiation of waves excited by an electron beam in an inhomogeneous magnetically-active plasma. ZhTF, no. 2, 1973, 294-301.

Fal'kovskiy, N. I. Coaxial shunt for measuring high pulsed currents. PTE, no. 1, 1973, 147-149.

Kikvidze, R. R., V. G. Koteteshvili, and A. A. Rukhadze. Interaction of an electron beam with a solid-state plasma. FTT, no. 2, 1973, 622-623.

Kikvidze, R. R., and A. A. Rukhadze. Theory of oscillation and stability of a semiconducting plasma with small number of carriers in a strong electric field. IN: Trudy Fizicheskogo instituta AN SSSR, no. 61, 1972, 3-41.

Korenev, I. L., and L. A. Yudin. Resistive instability of a relativistic ring in a waveguide. IN: Trudy radiotekhnicheskogo instituta AN SSSR, no. 9, 1972, 144-152. (RZhElektr, 2/73, no. 2A401)

Koval'chuk, B. M., V. V. Kremnev, G. A. Mesyats, and Ya. Ya. Yurike. Development of a nanosecond surface discharge on dielectric with a large dielectric constant in gas. ZhPMTF, no. 1, 1973, 48-55.

Kovpik, O. F., Yu. Ye. Kolyada, Ye. A. Kornilov, Ye. V. Lifshits, and S. A. Nekrashevich. Effect of external high-frequency modulation of an electron beam on ion heating during its interaction with plasma. IN: Fiz. plazmy i probl. upravl. termoyader. sinteza. Resp. mezhved. sb., no. 3, 1972, 15-23. (RZhF, 11/72, no. 11G284)

Kozlov, N. P., L. V. Leskov, Yu. S. Protasov, and V. I. Khvesyuk. Plasma focus as a dense plasma source. TVT, no. 1, 1973, 191-193.

Krivoruchko, S. M., and Ye. A. Kornilov. Excitation and interaction of low-frequency oscillations during beam instability. IN: Fiz. plazmy i probl. upravl. termoyader. sinteza. Resp. mezhved. sb., no. 3, 1972, 208-213. (RZhF, 11/72, no. 11G247)

Kurilko, V. I. Mechanism of beam instability development in plasma. DAN SSSR, v. 208, no. 5, 1973, 1059-1061.

Lutsenko, Ye. I., Ya. B. Faynberg, V. A. Vasil'chuk, and N. P. Shepelev. Interaction of an intense electron beam with homogeneous and nonhomogeneous plasma. IN: Fiz. plazmy i probl. upravl. termoyader. sinteza. Resp. mezhved. sb., no. 3, 1972, 5-15. (RZhF, 11/72, no. 11G249)

Mikhaylova, R. Investigating air breakdown by powerful radiation. IN: Izv. in-ta elektron. Bulg. AN, no. 5, 1971, 55-62. (RZhF, 11/72, no. 11G142).

Nekrashevich, I. G., A. I. Bushik. On measuring plasma emission from an electric discharge. ZhPS, v. 18, no. 2, 1973, 190-193.

Pavlov, V. G., A. A. Rabinovich, V. N. Shrednik. Detecting point drawing by an electric field. ZhETF P, v. 17, no. 5, 1972, 247-250.

Pavlovskaya, N. G., T. V. Kudryavtseva, N. A. Dron', G. N. Sloyeva, and L. V. Tsvetkov. Miniature tube with a cold cathode for obtaining nanosecond fast-electron pulses. PTE, no. 1, 1973, 22-24.

Pustovalov, V. V., and V. P. Silin. Nonlinear theory of wave interaction in plasma. IN: Trudy fizicheskogo instituta AN SSSR, no. 61, 1972, 42-281.

Razrabotka i prakticheskoye primeneniye elektronnykh uskoriteley. (Development and practical application of electron accelerators). IN: Tezisy dokl. Vses. konf., Tomsk, 5-7 sent., 1972 goda. Tomsk, Tomskiy universitet, 1972, 218 p. (RZhElektr, 2/72, no. 2A393 K).

Rukhadze, A. A., and M. Ye. Chogovadze. Interaction of a monoenergetic nonrelativistic electron beam with surface potential oscillations of plasma. ZhTF, no. 2, 1973, 256-265.

Skoblik, I. P., I. M. Zolototrubov, and Yu. M. Novikov. Effect of initial gaseous states in a coaxial accelerator on plasma parameters. ZhTF, no. 2, 1973, 281-286.

Volovik, V. D., V. I. Kobizskoy, V. V. Petrenko, G. F. Popov, and G. L. Fursov. Ionization luminescence of air due to relativistic electrons. Atomnaya energiya, v. 34, no. 2, 1973, 130-131.

Yerokhin, N. S., and S. S. Moiseyev. Problems of linear and nonlinear theory of wave transformation in heterogeneous media. UFN, v. 109, no. 2, 1973, 225-258.

Zykov, V. G., V. I. Karpukhin, Yu. F. Lonin, N. I. Rudnev, and V. T. Tolok. Investigating the possibility of electron injection in heliotron-type closed magnetic traps. ZhTF, no. 2, 1973, 287-293.

5. Material Sciences

A. Abstracts

Fremel', T. V., R. V. Torner, L. M. Luk'yanova, and L. A. Flekser. Failure of high-pressure polyethylene in an [insulator] element. MP, no. 5, 1972, 935-936.

Cracking of cable insulation made of high-pressure polyethylene was studied experimentally, to determine the service life of polyethylene products. Ring-shaped specimens were subjected to 100-140 kg/cm^2 bending stresses. Failure of these prestressed specimens occurred at 20-80° C in a surface-active medium under conditions of stress relaxation. Micrographs of the cracked surface revealed a cracking dependence on crack formation conditions. Many cold drawing areas were observed on the cracked surface after accelerated testing of a specimen having a service life of several hours. One-year service life specimens exhibited cracking patterns typical of the brittle fracture of amorphous plastics, with sharply-defined mirror-like and roughness areas. The mirror-like area expanded with increased life-time and covered the entire crack surface after 5-6 years. It was concluded that cracking of a polymer manufactured article in service, under conditions of relaxation of an initially small stress, features slow crack propagation, with complete elimination of rapid cracking (roughness areas). Electron micrographs of crack surface replicas and raster micrographs revealed surface layer deformation concurrent with brittle fractures and micronecks uniformly distributed over the entire smooth area of a crack surface. Crack propagation from the middle to the end of growth consequently proceeds according to the same mechanism: a material orientation in a crack front and disruption of micronecks joining the crack edges. The micronecks were not observed on a crack surface formed under near-equilibrium conditions in 5-6 year service life specimens.

Korolev, V. P., M. V. Nikulin, V. N. Uvarov, and G. Ye. Chernenko. Measuring heat-insulating materials ablation using loaded-shell strain data. MP, no. 5, 1972, 824-828.

A simple and practical method is described for determining ablation and the load-carrying layer boundary of a loaded shell subjected to erosion and thermal decomposition. The method is based on strain measurements and loads applied to the shell surface. Application of the method does not violate the structural integrity and gives ablation characteristics data of increased accuracy. The strains ϵ_1 and ϵ_2 in the axial and circular directions and the angle of shear are measured by strain gauge. Pressure sensors and dynamometers measured applied stresses T_1 and T_2 in axial and circular directions and the shear tensor S. Thermal stresses T_{1T} and T_{2T} are calculated using the elasticity coefficients B_{jk} and shell coefficients of thermal expansion without thermal shear ($S_T = O$). The rigidity matrix C of a statically defined and symmetrically loaded shell at a time τ is given by

$$C=\frac{T+T_T}{E}. \tag{1}$$

where T, T_T, and E are the applied loads, thermal stresses, and strain matrices. The relationship $\Delta\delta = \delta_o - \delta_\tau$ defines the ablation layer thickness, where δ_o and δ_τ are the initial and running shell wall thicknesses. For a cylindrical shell of n orthotropic layers

$$\delta(\tau)=\frac{T+T_T}{EB}, \tag{2}$$

where B is the elastic coefficient matrix; and for a single-layer orthotropic

shell

$$\delta(\tau) = \frac{pR + T_{2\tau}}{B_{22}\varepsilon_2 + B_{12}\varepsilon_1}, \tag{3}$$

The method was verified experimentally using cylindrical fiberglass reinforced plastic models in high-velocity, high-temperature (1800-2300° K) gas flow. Model characteristics and gas flow parameters are tabulated. Temperatures were measured at variou depths in the wall cross-section. The experimental data (Fig. 1) show that initially shell rigidity, hence δ_τ, decreases sharply,

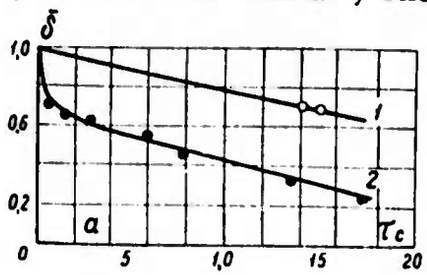

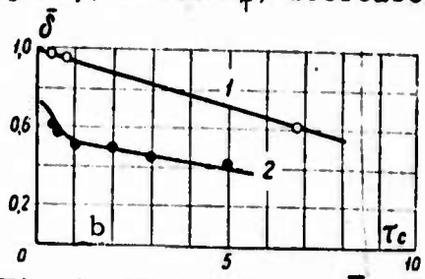

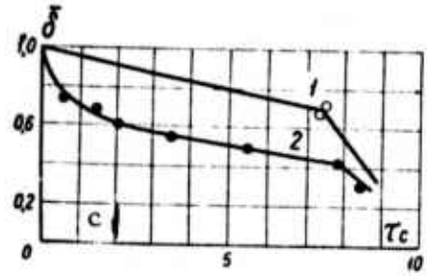

Fig. 1. Experimental $\bar{\delta} = \delta/\delta_o$ data for (a) single-layer shell, (b) a shell with carbonized surface layer, and (c) double-layer shell. All shells are of glass-reinforced plastics. Curve 1 - $\bar{\delta}_w$, 2 - $\bar{\delta}_c$.

and the destruction process subsequently stabilizes rapidly in $\Delta\tau < 1$ sec. The theoretical position of the load-carrying layer boundary coincides satisfactorily with the direct measurement and thermal state measurement data. The described method is recommended for evaluating the destruction characteristics of thermal insulation coatings.

Ovsyannikov, V. M. Effective cross-section method of calculating radiation and absorption selectivity of a hot gas. ZhPMTF, no. 5, 1972, 76-83.

A rapid method of computing radiation transfer in a selectively radiating and absorbing hot gas is given, based on the effective cross-sections S, σ, ϵ which are characteristic of the gas absorption spectrum. Machine time is saved by substituting S and σ or S, σ, and ϵ for the absorption cross-section σ_λ in formulas of the radiation flux q (r) and divergence div q (r) in a space point with an r coordinate (Fig. 1a) or in a two-dimensional layer point (Fig. 1b), respectively. The method of effective cross-sections

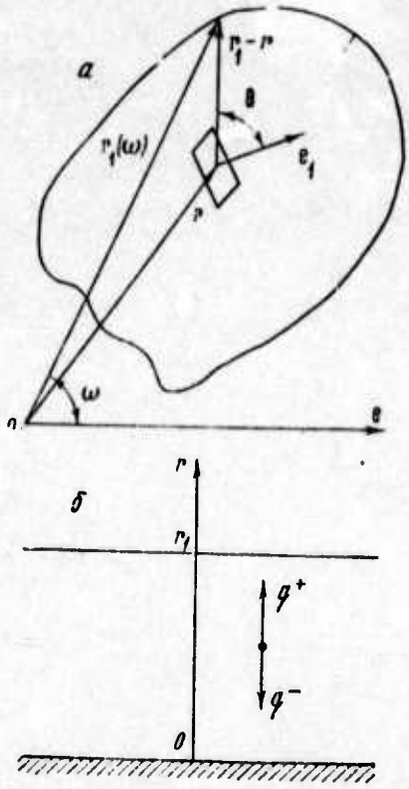

Fig. 1. Diagram of radiation transfer in a three-dimensional space (a) and in a two-dimensional layer (b): ω- solid angle, θ - angle between ray direction and the normal e_1 to a given area; $r_1(\omega)$ - a point at the radiating volume boundary.

consists of two integration steps: (1) integration over λ of the S, σ, and ϵ expressions, and (2) integration from r to $r_1(\omega)$ of the substituted expressions for the radiation flux field. Integration over λ by the exact method must be done in small steps, because σ_λ is a complex function which therefore requires greater machine computation time. Integral formulas are given for calculating S, σ, ϵ, q (r), and div q (r) in a homogeneous gas-filled space and S^*, σ^*, ϵ^*, q^+ (r), q^- (r), and div q (r) in a two-dimensional homogeneous gas layer, where q^+ (r) and q^- (r) are unidirectional fluxes, and

$$q(r) = q^+(r) - q^-(r) \qquad (1).$$

These formulas can be applied to the case of a multicomponent gas mixture, if $x_k \varphi_k$ (T) is substituted for ψ_k, where x_k (k = 1, ..., $\varkappa$) is molar concentration of the $\varkappa$ components. Examples are given of numerical calculations of radiation transfer in a shock layer of hypersonic air flow around a sphere with high-velocity gas injection through the surface. The q^- (r) data calculated by the effective cross-sections method in the first and second approximations are compared to precisely calculated q^- (r) data for the given temperature profile in the shock layer (Fig. 2) with air as the

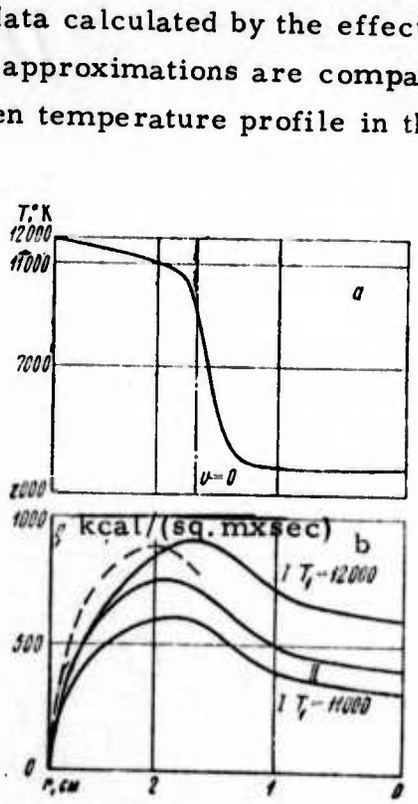

Fig. 2. a- temperature profile in shock layer. Air is to the left and injected gas to the right of the v = o line; b - q^- (r) versus r plots: broken line - exact data, solid lines - data computed by the effective cross-section method, I and II - first and second approximations.

injected gas. A comparison is also made for an injected gas other than air. Temperature profiles calculated by the same method in the first and second approximations are shown. Machine time for the cited examples was reduced by a factor of 120 in comparison to exact solution time requirements. The accuracy of $q^-(r)$ computations was 15-25%.

Boyko, A. N., V. M. Yeroshenko, V. P. Motulevich, and L. A. Yaskin. Temperature state of a porous plate cooled by strong blowing under conditions of radiative-convective heating. I-FZh, v. 23, no. 5, 1972, 792-800.

The internal cooling of a porous, finite thickness plate with surface radiation flow was analyzed using initial equations describing the heat tranfer in the wall and the cooling liquid in the form

$$\lambda_w \frac{d^2T_w}{dx^2} = \alpha_v (T_w - T_g) \tag{1}$$

$$-\lambda_w \frac{dT_w}{dx} = \rho v c (T_g - T_{g\infty}). \tag{2}$$

where λ- thermal conductivity coefficient, T_w - plate surface temperature, T_g - coolant temperature, α_w - volumetric coefficient of internal heat transfer, ρ - density, v - velocity and c - isobaric heat capacity. By simple tranformations of the (1) and (2) equations, the generalized equations of energy for a porous material are written in the dimensionless form

$$\frac{d^2\theta_w}{d\xi^2} - \frac{\mathrm{Nu}}{\mathrm{Pe}} \cdot \frac{l}{d} \cdot \frac{d\theta_w}{d\xi} - \mathrm{Nu}\,\frac{\lambda_g}{\lambda_w}\left(\frac{l}{d}\right)^2 \theta_w = 0. \tag{3}$$

where $\theta_w = \frac{T_w - T_{g\infty}}{T_{g0} - T_{g\infty}}$, the unknown quantity of temperature excess at the

wall outlet, Nu - Nusselt number, Pe - Peclet number, d - particle diameter, l - plate thickness, and ξ is a dimensionless coordinate. The boundary conditions of Eq. (3), necessary for measuring the temperature field, are derived and a solution to a boundary - value problem for this equation is found. Based on the solution, an expression for the temperature excess at the porous wall outlet is formulated an analyzed for various blowing, heating and plate parameters. The experimental setup and procedures used to verify the theoretical results are described, and the findings on the temperature excess are presented in a graph. The agreement of the results was satisfactory. The experimental and theoretical data indicate that when strong blowing is used the temperature variation between a porous material and the coolant may be substantial, which should be considered when calculating thermal regimes for certain equipments.

Galkin, V. S., M. N. Kogan, and O. G. Fridlender. Gas flow around an intensively heated sphere at low Reynolds numbers. PMM, no. 5, 1972, 880-885.

The problem of gas flow around a uniformly heated (cooled) sphere at Reynolds numbers $R_\infty \ll 1$ is solved allowing for the Barnett thermal stresses, under the assumptions that the effect of gravitational convection is negligible and the gas is monatomic and composed of Maxwellian molecules. The adiabatic constant is 5/3 and the Prandtl number is 2/3. Using the authors' earlier formulated (MZhiG, no. 3, 1970) dimensionless conservation (state, energy and angular momentum) equations and boundary conditions, the slow motion ($M_\infty \ll 1$) of gas around the uniformly heated (cooled) bodies is described. The equations and boundary conditions using a spherical coordinate system and certain conditions and assumptions, were revised to describe the gas flow. The problem was reduced to the solution of a boundary-value problem for a system of ordinary

linear differential equations. Numerical integration was simplified by introducing new variables. Using an expression for the variable part of the stress tensor and the derived equations, the effect of the local thermal stresses on the force F acting on the sphere is analysed. It is shown that this effect is equal to zero and the force F is an integral over the sphere surface owing to the pressure and viscous stresses. The numerical results indicate that the thermal stresses affect the velocity field only slightly, but at high temperatures F decreases rapidly. Graphs are given of numerical results, both with and without allowance for thermal stresses.

Kleyner, M. K. A method for solving the heat transfer problem in heating of large bodies in a moving layer. I-FZh, v. 23, no. 5, 1972, 926-927.

Heat transfer problems in the heating of large bodies in a moving layer are classed as complex boundary value problems. In addition to the usual boundary conditions of the third kind, a coupling equation for the temperatures of the gases and heated bodies is given.

$$W(X)\frac{dt_r(X)}{dX} = -Q(X) + \frac{dW}{dX}[t_r^0 - t_r(X)] + \mathrm{Bi}[t_r(X) - t(1, X)] + \mathrm{Bi}_1[t_r(X) - t_{окр}]. \quad (1)$$

where W(X) is a given differentiable function, dependent on the ratio of gas and heated bodies water equivalents; and Q(X) is a function dependent on the heat release variation in the gas phase. (The remaining values are defined by the author in I-FZh, v. 18, no. 2, 1970).

The solution method, similar to the Tikhonov method, is based on solving the third boundary-value for arbitrary $t_r(X)$, and substituting this solution in Eq. (1), to derive an integro-differential equation for $t_r(X)$. Numerical realization of the method revealed computational difficulties in the domain of small W(X) values, close to the point at which the free term and the kernel of the integral equation have singularities. When W(X) changes linearly, the solutions can be obtained by the method of perturbations in the form of infinite sums. To determine unknown coefficients, a system of recurrence equations is derived which can be solved by the cited method of integro-differential equations. The application of both methods is feasible for almost the entire domain of W(X) variations.

Shestaka, I. S. Coefficient of meteor ablation and maximum brightness. Astronomicheskiy vestnik, v. 6, no. 3, 1972, 186-194.

A statistical analysis is presented of data from baseline photographic observations in Odessa of bright meteors. Meteor velocity v and drag dv/dt, and instant (I) and integral (E) meteor luminous fluxes were determined for meteor trail image points; and the ablation coefficient σ for these points and the mean σ of each meteor were calculated. The mean log σ value of the meteors was found to be -11.39 ± 0.05. The log σ of various meteor showers is also shown. Plots of the mean log σ values of the Odessa meteors versus the principal parameters of meteoroids falling through the atmosphere (Fig 1) show that σ decreases with increasing v, but is apparently independent of the mass m, zenith angle Z_R of the meteor radiant, and atmospheric density ρ.

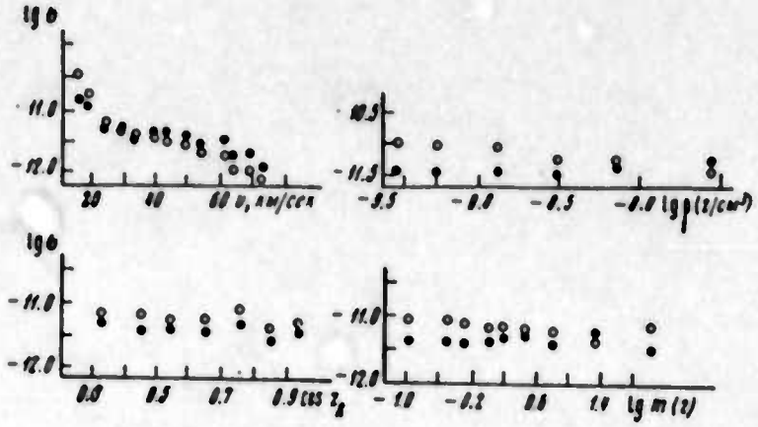

Fig. 1. Ablation coefficient versus meteor parameters: light circles are observed mean log σ, cm^{-2}. sec^2, dark circles are log σ values adjusted to a reference meteor.

The observed log σ of all meteors, sporadic meteors, and Perseids also depend on the integral E_{ie} from the meteorite appearance until its disappearance. The E_{ie} dependence of σ is attributed to the v effect, since the m-dependence of σ is negligible. When meteor log σ data are adjusted to a reference meteor with the parameters

$$\lg v_\infty = 6.477,\ \lg m_\infty = 0.77,\ \lg \cos Z_R = -0.20, \tag{1}$$

and log ρ_{max} at maximum brightness = -8.00, a decrease in log σ is observed with an increase in ρ_{max} (Fig. 1). The weak ρ_{max} dependence and a more pronounced v-dependence of log σ may be due to a decrease of the heat transfer coefficient from an increased barrier effect of the ablated molecules, or to the rise in the effective heat of ablation.

The observed absolute magnitude of maximum meteor brightness, M_{max} of all the bright Odessa meteorites was calculated to be lower than theoretical M_{max} values. This finding indicates a changing ablation pattern during the flight of large meteoroids which break up into bright meteors. The observed M_{max} increased sharply with meteoroid acceleration and increases in their mass, but only insignificantly with an increase in cos Z_R.

Murav'yev, A. I., I. V. Chernyshevich, and S. L. Fofanov. Method for solving Stefan problems. IAN B, seryya fizika energetychnykh navuk, no. 4, 1972, 108-112.

A method is introduced to solve a one-dimensional, single-phase boundary value problem for a moving boundary in the process of material destruction. This problem arises in calculations of the temperature field in heat-insulating coatings on flying vehicle nose sections, heat transfer in combustion of solid rocket propellants, and heating of electrodes in plasma devices. The method is based on the assumptions that the time function $x = S(\tau)$ describing the boundary motion is known, and heat flux transfer occurs within the destruction region. A partial differential equation of heat conduction with boundary conditions describes the destruction and ablation phase of the problem. The Stefan condition at the boundary is

$$q(\tau) = \rho\varkappa \frac{dS}{d\tau} - \lambda \frac{\partial t(0, \tau)}{\partial x} . \qquad (1)$$

where $dS/d\tau$ is the velocity of the coordinate system motion in a positive direction along the Ox axis, ρ is the material density, $\varkappa$ is the total heat of fusion and vaporization, and λ is the coefficient of thermal conductivity. By applying a Laplace transform and a Euler formula to the partial differential equation, an integral equation and a formula are derived for the time function $g(\tau)$ of the heat flux and the temperature distribution field $t(x, \tau)$, respectively. When the temperature function of the thermal properties is known, $\lambda(t)$ is introduced into the original differential equation and the problem becomes self-similar. If $v(\tau) = dS/d\tau$ is the boundary motion velocity, the ablation rate is $S(\tau) = \beta\sqrt{a(T_0)\tau}$, where β is a dimensionless factor and a is the diffusivity. The ablation rate $v(\tau)$ decreases and burnup increases with time, as shown by calculated $v(\tau)$ and $S(\tau)$ plots. For a graphite with constant thermal properties, $t(x, \tau)$ and $g(\tau)$ in the combustion region are

plotted (Figs. 1 and 2)

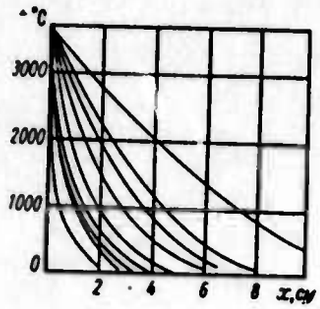

Fig. 1. Temperature distribution in a hot plate versus burning duration. T curves correspond to 1, 3, 4, 6, 9, 15, 25, 36, and 100 sec. from left to right.

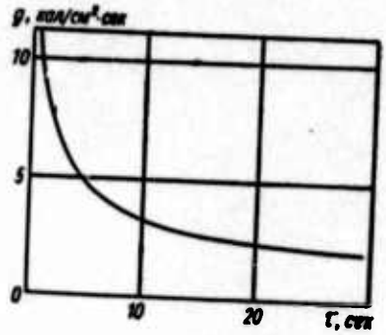

Fig. 2. Total heat flux distribution required for destruction and ablation and transferred to a solid body.

The authors conclude that the method for solution of a one-dimensional boundary value problem, as applied to solids with unsteady thermal conductivity and a moving boundary, can be extended to three-dimensional problems for semi-finite parallelopipeds, cylinders, or spheres with one or two moving boundaries.

Konkin, A. A., and N. F. Konnova. Carbon fibers. Zhurnal Vsesoyuznogo Khimicheskogo obshchestva, no. 6, 1972, 632-639.

This is a review of the 1953-1971 literature (about 20% of the citations are from Soviet sources) on the preparation, properties, and applications of carbon fibers. Preparation of carbon fibers from poly (acrylonitrile) (PAN) and raw hydrated cellulose fibers is emphasized as the only process presently used for manufacturing various types of carbon fibers.

Soviet scientists have confirmed the formation of intermolecular bonds as one of the PAN cyclization mechanisms in the thermal oxidation process (at 200-300° C). Other Soviet scientists have studied PAN carbonization at 900-1500° C in an inert gas atmosphere and established that weight loss is greatest at 280-420° C. Another Soviet research team has produced evidence that the original fibrous structure of PAN remains unchanged at least in the early stage of the carbonization process, and consequently affects carbon fiber properties. Carbonization of hydrated cellulose was also studied by Soviet scientists. Earlier studies established that levoglucosan is one of the most important thermal decomposition products. A. S. Fialkov et al found that a two-dimensional ordering phase appears at 300-400° C and a three-dimensional ordering appears at 900° C. Konkin et al recommend the use of nitrogen, cellulose decomposition products, carbohydrates, coal etc. as protective media for cellulose carbonization.

The authors also reviewed studies on preparation of carbon fibers from other synthetic fibers, e.g. PVC, saran, polyamide and polyester, but high-quality carbon fibers from these raw fibers have not yet been produced. Non-Soviet data are cited on the preparation of glassy carbon fibers from petroleum and coal tars, as well as phenolic resins. The latter are considered to be promising raw materials. High heat- and chemical resistance, especially the extremely high ablation resistance, of carbon fibers are emphasized. Comparison of the mechanical characteristics of carbon fiber-reinforced epoxy resins and the most common structural materials show that the resins are superior in strength-to-density ratios and rigidity.

Shveykin, G. P., and V. D. Lyubimov. Review of 13th session of the AN SSSR scientific council on the problem of physicochemical fundamentals for manufacturing new heat-resistant materials. NM, no. 11. 1972, 2058-2059.

The subject scientific council session was held May 23-27 1972 at Pervoural'sk. General topics of the 170 papers presented, 115 by Ural scientists, were refractory materials, oxygen-free compounds, oxides and coatings. Reports were presented on the synthesis and properties of dense sintered ceramics, mullite, ZrO_2 and HfO_2-base solid solutions, periclase, periclase-chromite composites, boron and aluminum nitride-base compounds and others. Studies of the Eastern Institute of Refractories are cited on the synthesis of such materials as mullite spinels and fire-resistant concrete. Progress is mentioned of research on oxidation of carbides, nitrides, and their alloys, synthesis and properties of silicides, germanides, and aluminides of transition metals, ZrO_2-rare earths solid solutions, cermets, and other lamellar compounds, oxycarbides, oxynitrides, carbonitride and carboborides. The preparation and properties of protective heat-resistant coatings were the subjects of over 26 papers. Widespread utilization of the new materials will contribute to the rapid development of energy, rocket, MHD generator, fuel cell and other technologies.

Trunin, I. I., V. I. Kumanin, and R. B. Bogomol'naya. Study of failure characteristics of heat-resistant steel. MiTOM, no. 10, 1972, 46-50.

Tensile strength test data are presented for type EP 44 heat-resistant bracing steel containing (in%): c - 0.22; Cr - 1.45, Mo - 1.03, V - 0.9,

Nb - 0.15, Ni - 0.15, B - 0.0026, and Ce - 0.06. The test specimens were heat treated by two different procedures to obtain the same metal in the brittle and plastic states. At 565° C, the total creep deformation of the plastic state was more than double that of the brittle state. Specimen failure characteristics were studied after wear tests, by measuring microhardness, density, and porosity characteristics at 0-10 mm. distances from the fracture. The data show that creep failure resulted from micropore concentration in a small volume of metal and the formation of a main crack after the micropore concentration attained a certain critical value. The greater the stress or the shorter the time-to-rupture, the greater was the micropore localization. Conversely the lower the steel creep deformability, the greater was the volume of defective (porous) metal and the lower the metal densi y.

Vvedenskiy, V. L. Jump in heat capacity of liquid He^3 at 2.65×10^{-3}°K. ZhETF P, v. 16, no. 6, 1972, 358-360.

The author discusses the origin of a 1.8-fold slope change kink of the pressure-time curve P(t), which Osheroff, et al (Phys. Rev. Lett, 28, 1972, 885) detected at ~0.0027° K in the process of cooling He^3 to 0.001° K. The Osheroff interpretation of the kink as the manifestation of a new solid phase is discarded in favor of the hypothesis that the observed transition occurs in liquid He^3 having a short thermal relaxation time. Calculations show that the transition time is ~2 sec within the 10^{-5}° K interval studied, which coincides with the liquid phase relaxation time. This hypothesis and the assumption of thermal insulation of a solid during a fast process led to the conclusion that the kink on the P(t) curve, and consequently the T(t) curve, is correlated with a jump in the heat capacity of liquid He^3. This conclusion is supported by calculations based on literature data. It was established, allowing for the additional heat capacity C of the solid-liquid He^3 boundary, that the 1.8-fold kink corresponds to a jump in heat capacity of $C_-/C_+ \cong 2.4$ at a 2.65×10^{-3}° K transition temperature. A solid He^3

slow warming process is described on the basis of the proposed interpretation of the transition point. The warming rate changes rapidly due to the jump in liquid heat capacity. This change is reflected in pressure recordings. The jump in warming rate of the slow process, as recorded by a platinum thermometer, indicates that the "mantle" on solid He^3 at the jump is much thinner than on the chamber wall. Peshkov (ZHETF, v. 48, 1965, 997 and UFZh, v. 94, 1968, 607) observed a jump in liquid He^3 heat capacity at zero pressure and 0.003° K. An earlier, theoretical study reported a superfluid transition jump of $C_-/C_+ = 1.7$ or 2.06.

Vvedenskiy, V. L., and V. P. Peshkov.
Vapor pressure of He^3 and He^4 mixtures in the temperature interval 0.7 to 1.3° K.
ZhETF, v. 63, no. 4, 1972, 1363-1370.

Experimental data are presented on vapor pressure P of He^3-He^4 mixtures at 0.7-1.3° K temperatures for 32.2 to 98.6% He^3 concentrations in the vapor phase and up to 5% He^3 concentrations in the liquid phase. The accuracy of the low pressure readings was 3 μ, adequate for the detection of minute kinks on the gas mass-pressure isotherms. The special manometric tube geometry allowed P measurements down to 0.3 torr. He^3 concentration in the liquid mixture was maintained constant, within a 2% accuracy, in a 23.7 cm^3 liquid volume. Experimental P data are tabulated (Table 1) for specific temperatures and He^3 concentrations x. A 0.3 P_3/P_4 versus 1/T curve was plotted from Table 1 and literature data for x near 100%. The interpolation formula

$$P = P_4 \Big/ \left[x_{4\pi} + \frac{P_4}{P_3} \exp\left(-0.7 x_{4\pi} \frac{P_3}{P_4}\right) \right]. \qquad (1)$$

(where P_3 and P_4 are the pressures of pure He^3 and He^4 and $x_{4\pi}$ is the He^4

molar concentration in vapor) was derived to describe the vapor-pressure curve of the liquid-vapor phase diagram of the He^3-He^4 mixtures. The vapor pressur

Table 1. Vapor pressure over a He^3-He^4 liquid mixture for varying He^3 content in the vapor phase.

T, °K	P, torr	T, °K	P, torr
$x = 33,2\%$		$x = 95,44\%$	
0,984	0,176±0,006	0,906	1,11±0,07
1,117	0,512±0,005	$x = 97,60\%$	
1,153	0,660±0,007	0,886	1,57±0,07
1,301	1,845±0,015	0,923	1,93±0,07
$x = 66,8\%$		0,963	2,75±0,07
0,978	0,337±0,01	$x = 96,59\%$	
1,085	0,78±0,03	0,869	2,22±0,07
1,104	0,88±0,02	0,915	3,17±0,23
$x = 91,3\%$		$x = 98,55\%$	
0,914	0,485±0,04	0,908	3,11±0,17
0,943	0,83±0,015	1,036	6,90±0,15
1,007	1,37±0,13	1,065	7,6±0,4
1,128	3,60±0,20		

curves (Fig. 1) calculated from the formula (1) agree well with the experimental data up to 1.8° K. Using the tabulated P data measured over liquids containing 0.98-4.79% He^3, the temperature dependence of the Henry law constant a in the 0.7-2.0° K range was expressed by

$$a = 4{,}75(1/T - 0{,}17) \qquad (2)$$

The a versus 1/T plot is in good agreement with the data for high temperatures and literature data interpolated for a 10% He^3 concentration. Eqs. (1) and (2) were used to compile tables of 1000 P_x/P_3 values as functions of T = 0.6-2.0° K and 0-1 He^3 molar concentrations. The parameters Δ and m^* of the

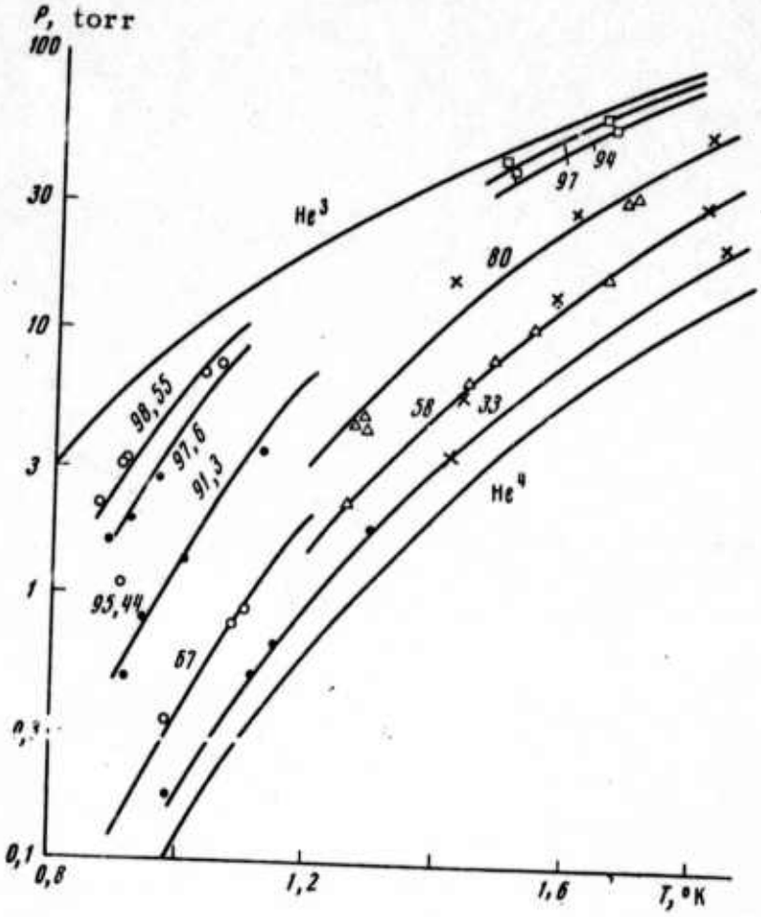

Fig. 1. Pressure versus temperature plot for various gas phase compositions: ●, o - authors' data; ▲ - literature data, 58 and 78% He^3; x - idem, 35.4, 57.6, and 82.4% He^3; □ - idem, 94 and 97% He^3. Solid lines are calculated from (1).

excitation spectrum in dilute He^3 solutions in He^4 were calculated to be

$$\Delta = -2{,}65 \pm 0{,}1^\circ, \quad m^* / m_3 = 2{,}8 \pm 0{,}2. \tag{3}$$

The Δ value in (3) coincides with values from the literature for He^3 concentration < 4% and in the 0.6-1.0° K range. The averaged m^*/m_3 value in (3) is higher than the literature values for T < 0.6° K.

Klyachko, V. Method for increasing fatigue strength of metals. Ekonomicheskaya gazeta, no. 44, October 1972, p. 22.

The discovery is reported of a low stress state on contact surface edges in a loaded composite body. The discovery was made by K. Chobanyan of the Institute of Mechanics, AN ArmSSR, from a mathematical analysis of the load-induced stresses in structural points composed of disparate elements joined by welding, or sealing. Results show that the mechanical properties of such structures depend on the shape of the joined structural elements and the material elasticity.

Chobanyan proved that structural members can be reinforced by transferring surface stress concentrations into bulk materials. Reinforcement is made by optimizing the configuration of adjacent structural members and carefully selecting structural components materials based on elasticity. The findings have application in the increase of fatigue strength of structures, e.g., bridges, TV towers, welded vessel structures and reservoirs.

Khomenko, A. A., Yu. Ye. Smirnov, V. P. Sosedov, and V. I. Kasatochkin. Thermal transformation of interatomic bonds in glassy carbon. DAN SSSR, v. 206, no. 5, 1972, 1112-1114.

An x-ray diffraction analysis of glassy carbon formed at varying temperatures in the 1500-3000° C range was made to determine the effect of the heat-treatment temperature on the interatomic bonds. X-ray

diffraction spectra of heat-treated specimens were used to compute radial distribution functions of electron density (Fig. 1).

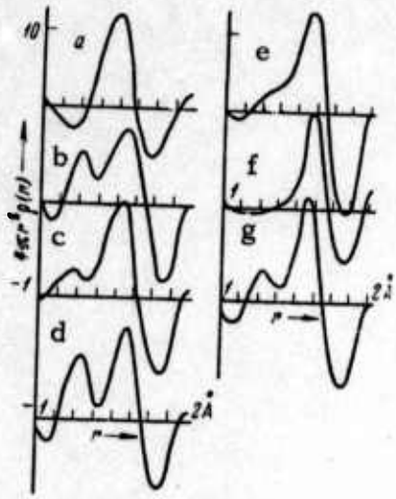

Fig. 1. Radial distribution function for various heat treatment temperatures of glassy carbon: a - 1,500, b - 1,800, c - 2,000, d - 2,600, e - 2,700, f - 2,800, and g - 3,000° C.

Analysis of the Fig. 1 data and similar data of Khomenko, Smirnov, et al (DAN SSSR, v. 206, no. 4, 1972) for a specimen pretreated at 1,800° C indicated the formation at 1,500-1,800° C of small regions of C chains with $(-C \equiv C-)_n$ and $(=C = C=)_n$ bonds, which co-exist with diamond-like formations up to 2,600° C (the 1.28 Å peak in Fig. 1 b, c, and d). The stability of these formations is explained by the high-pressure generated by very strong local strains due to heat-treatment. In the specimens pretreated at 2700 and 2800° C, the 1.28 Å peak almost disappears completely, owing to heterogeneous graphitization by the vapor phase. The peak reappears in specimens treated at 3,000° C. The curve of radial distribution of electron density confirmed the assumption that continuous chemical destruction and synthesis occurs in carbonaceous materials over the temperature range studied. At high temperatures, the vapor phase actively interferes with these processes. The experimental data also confirmed the view of one of the authors (Kasatochkin) that glassy carbon is an amorphous nongraphitizable

polymer composed of sp^3, sp^2, and sp hybrid state C atoms in varying ratios and with diamond, graphite, and carbyne-type interatomic bonds. The structure of glassy carbon formed at $T > 1500^{\circ}$ C can be visualized as a polymeric assembly of small formations of trigonal (graphite-like) carbon atoms arranged in aromatic layers which are interconnected through even smaller fragments of C chains and tetrahedral carbon microformations.

Savitskiy, Ye. M., and I. F. Zudin. Review of the 26th session on problems of structure and high temperature strength of metallic materials. IVUZ Metally, no. 5, 1972, 215-216.

The subject session was held from April 3 to 6, 1972 at the Baykov Institute of Metallurgy in Moscow. Most of the 50 papers presented at the 26th session on metallic materials are reviewed briefly in several subject groupings. On the subject of physico-chemical criteria of heat-resistance, new physical criteria (I. N. Frantsevich and M. D. Smolin) and the feasibility of computing melting points of new refractory compounds (Ye. M. Savitskiy and V. B. Gribulya) were reported. In the group of papers on the relationship between heat-resistance and electronic structure, D. A. Prokoshkin and Ye. V. Vasil'yev showed that diffusion is the strength-controlling mechanism at a temperature above 0.5 T_m, and V. K. Grigorovich concluded that the heat-resistance of Fe-Al, Fe-Si, Fe-Co, Ni-Cr, and Ni-Co alloys depends on the electron density of the matrix, the structure, and the thermodynamic stability of reinforcing phases.

The role of crystal structure defects in deformation and failure was studied, among others, by V. S. Ivanova and V. A. Yermishkin, who concluded that dislocations formed during creep are the creep-resistance controlling factor in body-centered cubic single crystals, e.g., tungsten; and

by N. N. Rykalin and M. Kh. Shorshorov, who examined material deformation near a free surface. Crystal size was examined by V. D. Sadovskiy et al, who established that a high deformation rate in high-temperature thermo-mechanical treatment can prevent recrystallization; and by I. L. Mirkin, who determined that the creep-resistance of a steel with 1% Cr-Mo-V increases ten-fold when the intercrystalline distance is decreased from 850 to 550 Å at 550°.

The effect of alloying was treated by: I. R. Kryanin and L. P. Trusov, who assumed that the maximum relaxation stability of 1.5-2 and 12% Cr-containing steels is achieved in the presence of NbC, VC, or the intermetallic Laves phase; L. N. Zimina, who established the positive effect of Nb on Ni-Cr-Fe, Ni-Cr-Mo-W-Ti, and Ni-Cr-Mo-W-Al-Co alloys; N. N. Morgunova, who confirmed the beneficial effect of Mo alloying with W, Ta, Re, Os, and Zr(0.1-0.2%); and L. I. Pryakhina et al, who achieved a five-fold increase in W strength by alloying with Ta and Mo.

The thermal stability of composite Ni materials strengthened with W and Mo fibers was discussed by B. S. Natapov and F. P. Banas, as well as V. Ye. Panin and Ye. F. Dudarev.

Surface protective coatings were studied by V. P. Prosvirin and by Yu. I. Kozuba. The latter measured the creep rate and long-term strength of Si, Ti, and Cr-coated Mo, TsM-2A alloy, and Nb loaded in the air for 10-100 h at 1,200°.

B. Recent Selections

i. Crack Propagation

Desov, A. Ye., K. N. Kim, and L. I. Soynova. Method of registering the dynamics of crack formation from hardening of synthetic stone materials. Otkr izobr, no. 6, 1973, no. 365641.

Fedorchenko, V. G., Ye. A. Vasil'yev, and V. A. Eksanov. Chemical composition and tendency to crack formation of cast iron. IVUZ Mashinostroyeniye, no. 2, 1973, 105-108.

Finkel', V. M., Yu. A. Brusentsov, V. Ye. Sereda, and Yu. I. Tyalin. Diffraction of bending and tension pulses in a crack. FTT, no. 2, 1973, 463-469.

Gur'yev, A. V., and T. B. Alkhimenkov. Application of a microhardness method in studying heterogenity of plastic deformation in a brittle failure zone of metals. ZL, no. 2, 1973, 197-199.

Kal'yanov, V. N., and O. B. Braylovskiy. Coefficient of thermal expansion and crack formation in a wear-resistant weld metal. Svarochnoye proizvodstvo, no. 10, 1972, 13-14. (LZhS, 6/73, no. 19035)

Kit, G. S., and Yu. S. Frenchko. Effect of thermal penetration factor of arc-shaped cracks on the local thermoelasticity state. FiKhOM, no. 1, 1973, 75-80.

Makhutov, N. N., and S. V. Serensen. Displacement and elastoplastic deformation of a crack edge from tension. IN: Sb. Mekhanika sploshnoy sredy i rodstvennaya problema analiza, Moskva, Izd-vo Nauka, 1972, 305-310. (RZhMekh, 2/73, no. 2V549)

Panasyuk, V. V., and M. D. Dmitrakh. Kinetics of internal oval crack propagation in a brittle solid. Visnyk L'viv. politekhn. in-tu no. 66, 1972, 27-37, 58. (RZhMekh, 2/73, no. 2V550)

Panasyuk, V. V., and L. T. Berezhitskiy. Application of fracture mechanics to calculations of composite materials strength. IN: Sb. XIII Mezhdunarodnogo kongressa po teoreticheskoy i prikladnoy mekhanike, 1972, Moskva, Izd-vo Nauka, 1972, 87. (RZhMekh, 2/73, no. 2V1097)

Panasyuk, V. V., S. Ye. Kovchik, and N. S. Kogut. Use of a cylindrical specimen with an annular crack to measure brittle crack resistance of materials. FiKhOM, no. 1, 1973, 69-75.

Poberezhnyy, O. V. Three-dimensional problem of thermoelasticity for a body with a thermally-insulated internal circular crack. FiKhOM, no. 1, 1973, 118-120.

Regel', V. R., and A. I. Slutsker. All-Union conference on micro-analysis of polymer fracturing. (Leningrad, 14-16 June 1972). MP, no. 1, 1973, 185-186.

Rusinko, K. N., and S. I. Artykova. Failure of solids in a nonuniform stress state. Problemy prochnosti, no. 2, 1973, 43-47.

Shishkanov, V. M. Analysis of concrete crack resistance. IN: Tr. Moskovskogo instituta inzhenernogo zhelezno-dorozhnogo transporta, no. 414, 1972, 195-203. (RZhMekh, 2/73, no. 2V1203)

Sokolova, T. V., Ye. Ya. Litovskiy, T. B. Buzovkina, and S. S. Bartenev. Analysis of microstructural parameters effect on thermal conductivity of porous ceramic materials. NM, no. 2, 1973, 296-300.

Vitvitskiy, P. M., V. V. Panasyuk, and S. Ya. Yarema. Plastic deformation in the vicinity of cracks and fracture criteria (review). Problemy prochnosti, no. 2, 1973, 3-18.

Yarema, S. Ya., and A. I. Zboromirskiy. Effect of method of applying a concentrated force on the stress state in the crack terminus of a plate. FiKhOM, no. 1, 1973, 61-69.

Zhuravl'ov, V. I., and A. D. Oleksiyev. Brittle fracture of a solid crack from variable shear. DAN UkrSSR, Ser. A, no. 3, 1973, 238-243.

ii. High Pressure Research

Buynovski, V., S. Porovski, and A. I. Laysaar. Device for optical studies at high pressures and nitrogen temperatures. PTE, no. 1, 1973, 224-228.

Cisowski, J., and W. Zdanowicz. Electrical properties of Cd_3As_2 under high pressure. APP, A, v. A43, no. 2, 1973, 295-299.

Kalashnikov, Ya. A. Chemical reactions under high pressures. Zhurnal Vsesoyuznogo khimicheskogo obshchestva im. Mendeleyeva, v. 18, no. 1, 1973, 61-72.

Mustafayev, R. A., and V. V. Kurepin. Dynamic method of measuring heat capacity of liquids at high pressures and temperatures. TVT, no. 1, 1973, 144-149.

Rabinovich, V. A., L. A. Tokina, and V. M. Berezin. Determining compressibility of krypton and xenon at temperatures of 300 to 720° K and pressures to 400 bar. TVT, no. 1, 1973, 64-69.

Rozanov, B. V., V. N. Sumarokov, R. Ye. Murashko, G. S. Bobrovnichiy, and Yu. D. Klebanov. Device for developing high pressures. Otkr izobr, no. 5, 1973, no. 364863.

Timofeyeva, N. V., G. Z. Vinogradova, Ye. M. Feklichev, V. N. Apollonov, Ya. A. Kalashnikov, S. A. Dembovskiy, and V. Ye. Svintitskikh. High pressure and temperature study of As-S and As-Se vitreous systems. IN: Sb. Sovremennyye problemy fiziki khimii, Moskva, Izd-vo Moskovskiy universitet, v. 6, 1972, 234-259. (RZhKh, 4/73, no. 4B768)

Zharov, A. A. Chemical transformations under combined effects of high pressure and shear strain. Zhurnal Vsesoyuznogo khimicheskogo obshchestva im. Mendeleyeva, v. 18, no. 1, 1973, 73-79.

iii. High Temperature Research

Aleksandrova, G. N., and M. G. Maslennikova. Heat-resistant concrete with phosphate binders. Beton i zhelezobeton, no. 10, 1972, 24-26. (RZhKh, 5/73, no. 5M92)

Aleynikov, G. D., and S. S. Gul'bin. Short-duration creep of steel under a complex stress state and high temperature. IN: Sbornik nauchnykh trudov Fakul'teta prikladnoy matematiki i mekhaniki Voronezhskogo universiteta, no. 2, 1971, 124-127. (RZhMekh, 2/73, no. 2V1166)

Andreyev, A. A., V. A. Alekseyev, A. L. Manukyan, and L. N. Shumilova. Metal transition conductivity of Se-Te alloys at high temperatures. FTT, no. 2, 1973, 382-384.

Arsen'yev, P. A., and K. E. Binert. Spectral properties of Er^{3+} ions in a $GdAlO_3$ lattice. NM, no. 2, 1973, 327-329.

Avduyevskiy, V. S., G. A. Glebov, and V. K. Koshkin. Calculating the thermodynamic transfer properties of CO_2. TVT, no. 1, 1973, 51-58.

Avgustinik, A. I., S. S. Ordan'yan, R. Ya. Serbezova, and V. N. Fishchev. Mechanical and elastic properties of ZrB_2-ZrO_2-W cermets. Ogneupory, no. 3, 1973, 52-55.

Boganov, A. G., I. I. Cheremisin, V. S. Rudenko, and B. P. Baranov. Failure of quartz single crystals from heating to high temperatures in vacuum. NM, no. 2, 1973, 323-324.

Bondar', S. A., V. I. Strelov, M. M. Kulakov, S. S. Strel'chenko, A. D. Molodykh, and A. Ye. Aleksanov. High-temperature attachment to a mass spectrometer for study of vaporization. ZL, no. 2, 1973, 237-238.

Bondarenko, V. P., and Ye. N. Fomichev. High temperature study of material thermodynamic properties in the condensation phase. IN: Sb. Ukrainskaya respublikanskaya nauchno-tekhnicheskaya konferentsiya, posvyashch. 50-letiyu metrologicheskoy sluzhby USSR, 1972, Khar'kov, 1972, 66. (RZhMetrolog, 2/73, no. 2.32.1010)

Bykov, I. I., L. A. Kozdoba, and F. A. Krivoshey. Electrical modelling of thermophysical properties of stone castings in solid and molten states. FiKhOM, no. 1, 1973, 59-63.

Chekhovskiy, V. Ya., V. D. Tarasov, and L. A. Reshetov. Experimental study of Al_2O_3 enthalpy in the 1400 to 2313° K temperature interval. IN: Sb. Ukrainskaya respublikanskaya nauchno-tekhnicheskaya konferentsiya, posvyashch. 50-letiyu metrologicheskoy sluzhby USSR, 1972, Khar'kov, 1972, 68-69. (RZhMetrolog, 2/73, no. 2.32.972)

Gorenko, V. G., and P. P. Luzan. Effect of microstructure on elastic and strength properties of cast iron at high temperatures. IN: Sb. Liteynyye svoystva splavov, Kiyev, 1972, 218-222. (RZhMekh, 2/73, no. 2V1168)

Gotsulyak, Ye. A., V. I. Gulyayev, and V. K. Chibiryakov. Differential equations for thermoelastic state of shells under surface thermal impact. PM, no. 2, 1973, 32-41.

Ignatova, T. S., V. N. Yamov, N. M. Permikina, V. P. Mar'yevich, P. S. Mamykin, and G. V. Mashukova. Sintering of Al_2O_3-Cr cermet composites and selection of processing methods for parts manufacture. IN: Tr. Vostochnogo instituta ogneuporov, no. 13, 1972, 239-247. (RZhKh, 5/73, no. 5M46)

Kandyba, V. V., V. Ye. Finkel'shteyn, G. L. Iosel'son, and G. P. Pushkarev. Attaining and measuring high temperatures. IN: Sb. Ukrainskaya respublikanskaya nauchno-tekhnicheskaya konferentsiya, posvyashch. 50-letiyu metrologicheskoy sluzhby USSR, 1972, Khar'kov, 1972, 235-237. (RZhMetrolog, 2/73, no. 2.32.1011)

Karpinos, D. M., V. M. Grosheva, Yu. L. Pilipovskiy, and Ye. P. Mikhashchuk. Effect of mullite single-crystal whiskers on heat resistance of aluminum oxide parts. Ogneupory, no. 2, 1973, 56-57.

Kirillov, V. N., I. V. Sobolev, V. A. Yefimov, and S. D. Garanina. Thermophysical properties of glass fiber plastics with silicon fillers. Plasticheskiye massy, no. 2, 1973, 54-57.

Klyachko, L. A., A. N. Zolotko, Ya. I. Vovchuk, and V. G. Shevchuk. Kinetics of boric anhydride vaporization. IN: Sb. 11-ya Vsesoyuznaya konferentsiya po voprosam ispareniya, goreniya i gazovoy dinamiki dispersnykh sistem, 1972, Odessa, 1972, 32. (RZhMekh, 2/73, no. 2B1073)

Kovpak, V. I., and A. N. Olisov. Characteristics of high temperature creep of nickel alloys. Problemy prochnosti, no. 2, 1973, 48-52.

Kuritnyk, I. P., B. I. Stadnyk, and V. I. Lakh. Effect of high temperature vacuum heating on electrophysical properties of niobium single crystals. FiKhOM, no. 1, 1973, 98-99.

Lukin, Ye. S., and A. Ya. Soyuzova. Synthesis, sintering and properties of strontium hafnate. Ogneupory, no. 3, 1973, 40-45.

Masalov, Ya. F. Effectiveness of removing large concentrations of thermal energy during porous evaporation of alkaline metals. IN: Sb. Teplofizicheskiye svoystva i gazodinamika vysokotemperaturnykh sred, Moskva, Izd-vo Nauka, 1972, 106-108. (RZhMekh, 2/73, no. 2B881)

Mel'nik, M. T., N. G. Ilyukha, and V. L. Bernshteyn. Highly refractive cement in a $BaO-Al_2O_3ZrO_2$ system. Visnyk Kharkiv. politekhn. in-tu, no. 70, tekhnol. neorgan. rechovin, no. 4, 1972, 64-65. (RZhKh, 3/73, no. 3M204)

Mel'nik, M. T., and Yu. S. Koval'ov. Highly refractive alumo-zirconic strontium cement. Visnyk Kharkiv. politekhn. in-tu, no. 70, tekhnol. neorgan. rechovin, no. 4, 1972, 65-67. (RZhKh, 3/73, no. 3M191)

Moskatov, K. A. Heat treatment of polymer materials. Plasticheskiye massy, no. 3, 1973, 35-37.

Patzek, Z. Sintering method of preparing dense magnesium oxide. PNR patent no. 62795, published 5/10/71. (RZhKh, 5/73, no. 5M65 P)

Peletskiy, V. E., and V. P. Druzhinin. Integral hemispherical level of titanium blackness at high temperatures. TVT, no. 1, 1973, 212-213.

Popolitov, V. I., and A. N. Lobachev. High temperature and pressure interactions of $Sb-Te-I-R-H_2O$ systems (R = solvent). NM, no. 2, 1973, 210-212.

Samoylov, S. M., and V. N. Monastyrskiy. Effect of heat treatment on properties of ethylene copolymers with vinyltriethoxysilane. Plasticheskiye massy, no. 2, 1973, 23-25.

Shevchenko, A. V., L. M. Lopato, K. G. Akinin, A. Ye. Kushchevskiy, and S. T. Baskakov. High temperature material. Otkr izobr, no. 5, 1973, no. 364577.

Sheyndlin, A. Ye., I. S. Belevich, and I. G. Kozhevnikov. High temperature enthalpy and heat capacity of niobium carbide materials. TVT, no. 1, 1973, 88-92.

Shitova, E. V., S. K. Rakov, Ye. I. Zorin, and P. V. Pavlov. Apparatus for preparing silicon dioxide and nitride films in a low-energy gas discharge plasma. IN: Sb. Elektronnaya tekhnika, Tekhnol., organiz. proizvodstva i oborudovaniya, no. 3(51), 1972, 88-94. (RZhKh, 4/73, no. 4L79)

Shorshorov, M. Kh., V. P. Alekhin, G. G. Aliyev, and S. S. Dryunin. Electron microscopic analysis of the dislocation structure of surface and internal layers of silicon single crystals during the initial stage of deformation. FiKhOM, no. 1, 1973, 71-75.

Shvarev, K. M., B. A. Baum, and P. V. Gel'd. Integral emissivity of silicon alloys with iron, cobalt and nickel at temperatures from 900 to 1750° C. TVT, no. 1, 1973, 78-83.

Slyusar', N. P., A. D. Krivorotenko, Ye. N. Fomichev, A. A. Kalashnik, and V. P. Bondarenko. Experimental study of titanium oxide enthalpy at 500 to 2000° K. TVT, no. 1, 1973, 213-215.

Tarnovskiy, V. I., A. G. Zhigalin, and A. G. Krivolapov. Calculating creep parameters of metals at high temperatures based on the strength curve. IN: Sbornik trudov mashinostroitel'nogo fakul'teta Omskogo politekhnicheskogo instituta, Omsk, 1971, 45-51. (RZhMekh, 2/73, no. 2V1161)

Uglov, A. A. Seminar on the physics and chemistry of materials processing using concentrated energy flux. (25 April 1972). FiKhOM, no. 1, 1973, 158-159.

Uvarov, V. V., and V. N. Samokhvalov. Heat and mass transfer during liquid evaporation from capillary-porous bodies immersed in hot air flow. IVUZ Mashinostroyeniye, no. 2, 1973, 68-72.

Vertogradskiy, V. A., and V. Ya. Chekhovskoy. Thermophysical properties of rhenium at high temperatures. TVT, no. 1, 1973, 84-87.

Vishnevskiy, I. I., Ye. I. Aksel'rod, N. D. Tal'yanskaya, and I. L. Boyarina. High-temperature creep of corundum and effective coefficients of diffusion. NM, no. 2, 1973, 291-295.

Yanchur, V. P., R. A. Andriyevskiy, V. P. Kalinin, and R. N. Lyubel'skaya. Interaction of zirconium-niobium alloys with nitrogen. FiKhOM, no. 1, 1973, 124-129.

Yeron'yan, M. A., R. G. Avarbe, and T. A. Nikol'skaya. Determining the temperature of congruent fusion of zirconium nitride. ZhPK, no. 2, 1973, 428.

Zelenyuk, Ye. Ye., V. V. Krivenyuk, and L. A. Sosnovskiy. Creep and long term strength of molybdenum with a borosilicide coating in vacuum at 1000 to 1400° C. Problemy prochnosti, no. 2, 1973, 53-56.

Zenzin, Yu. A., I. V. Kalganova, and N. A. Blanutsa. Heating of fine particles in plasma jets. IN: Sb. Teplo- i massoperenos v telakh i sistemakh pri razlichnykh granichnykh usloviyakh, no. 1, 1971, 56-60. (LZhS, 5/73, no. 14358)

iv. Miscellaneous Material Properties

Anisimov, S. I., and A. Kh. Rakhmatulina. Vaporization kinetics of solids in vacuum. IN: Sb. XII Mezhdunarodnyy kongress po teoreticheskoy i prikladnoy mekhanike, 1972, Moskva, Izd-vo Nauka, 1972, 28. (RZhMekh, 2/73, no. 2B270)

Belyakov, V. K. Oxidation resistance of aromatic polyamides and polypyromellitic imides. Vysokomolekulyarnyye soyedineniya, Kratkiye soobshcheniya, no. 2, 1973, 99-101.

Boyarskaya, Yu. S. Deformirovaniye kristallov pri ispytaniyakh na mikrotverdost' (Crystal deformation during hardness tests). Kishinev, Izd-vo Shtiintsa, 1972, 235 p. (KL, 5/73, no. 3466)

Deryagin, B. V., E. I. Yevko, V. I. Kisin, V. M. Luk'yanovich, Ya. I. Rabinovich, N. V. Churayev, and R. V. Baranova. Electronographic analysis of modified water. DAN SSSR, v. 208, no. 3, 1973, 603-

Dolgopolov, V. T., and L. Ya. Margolin. Surface impedance of bismuth in high amplitude electromagnetic waves. ZhETF P, v. 17, no. 5, 1973, 233-236.

Karakozova, Ye. I., Ya. M. Paushkin, L. V. Karmilova, and N. S. Yenikolopyan. Inhibition of polyethylene and polyethylene-terephthalate using boric polyether and alkali additives. IAN Kh, no. 2, 1973, 325-329.

Kats, M. S., V. R. Regel', T. P. Sanfirova, and A I. Slutsker. Kinetics of polymer microhardness. MP, no. 1, 1973, 22-28.

Konyushaya, Yu. Neptunium and plutonium "bond points" (preparation of heptavalent neptunium and plutonium). Rabochaya gazeta, 16 March 1973, p. 3.

Korshak, V. V., M. M. Teplyakov, and V. A. Sergeyev. Method of synthesizing polyphenylene polymers by polycyclic condensation of diacetyl aromatic compounds. DAN SSSR, v. 208, no. 6, 1973, 1360-1363.

Lidorenko, N. S., L. T. Kreshchishina, and E. L. Nagayev. N-shaped volt-ampere characteristic of a conductor near the metal-to-insulator anomalous transition point. FTT, no. 2, 1973, 613-614.

Listrov, A. T., and S. P. Levitskiy. Flow stability of a nematic liquid crystal layer in an inclined plane. IN: Tr. NII matematicheskogo Voronezhskogo universiteta, no. 6, 1972, 149-152. (RZhMekh, 2/73, no. 2B1275)

Metals with specified properties (new method of smelting iron alloys). Sovetskaya Rossiya, 21 Feb. 1973, p. 4.

New clay refractory material. Pravda, 14 March 1973, p. 2.

Novozhilov, V. V. Trends in the phenomenological approach to the problem of destruction. IN: Sb. XIII Mezhdunarodnyy kongress po teoreticheskoy i prikladnoy mekhanike, 1972, Moskva, Izd-vo Nauka, 1972, 8-10. (RZhMekh, 2/73, no. 2V544)

Ravvin, I. S. Experimental observation of the electroacoustic magnetic effect in CdS. ZhETF P, v. 17, no. 3, 1973, 144-147.

Rodin, V. I., V. A. Zaytsev, B. V. Gromov, V. M. Gelis, and V. G. Kazak. Silicon dioxide interaction with hydrogen fluoride. IN: Tr. Moskovskogo khimiko-tekhnologicheskogo instituta im. Mendeleyeva no. 71, 1972, 80-82. (RZhKh, 4/73, no. 4B1004)

Sandulova, A. V., V. V. Gospodarevskiy, I. A. Petrushko, and T. A. Moskovets. Mechanical properties of indium antimonide crystals prepared from the gas phase. FiKhOM, no. 1, 1973, 41-43.

Savitskiy, Ye. M. Single crystals of refractory and rare metals. VAN, no. 1, 1973, 68-76.

Sirota, N. N., A. A. Drozd, and V. I. Gostishchev. Measurement of electrical and thermal conductivity of metals in a strong magnetic field. IN: Sb. Teplofizicheskiye svoystva veshchestv pri nizkikh temperaturakh, Moskva, 1972, 149-158. (RZhMetrolog, 2/73, no. 2.32.973)

Tsiskarishvili, P. D., G. Sh. Papava, L. A. Beridze, N. A. Maysuradze, S. V. Vinogradova, and V. V. Korshak. Physical structure dependence of polyarylate properties, prepared from polycyclic bis-phenols. AN GruzSSR, Soobshcheniya, v. 68, no. 3, 1972, 597-600.

Vinogradov, Ye. L., Yu. V. Nikitin, B. I. Shapiro, and T. G. Shlyakhova. Rheological properties of shock resistant polystyrenes. AN LatvSSR, Riga, 1972, 6 p. (RZhMekh, 2/73, no. 2V1259 DEP)

Yastrebkov, A. A., and V. M. Lakeyenkov. Preparation and structure of refractory metal bi-crystals. PTE, no. 1, 1973, 235-236.

Zhuravlev, V. A., I. Ye. Kurov, and A. F. Shurov. On the problem of destruction of solids. IN: Uchenyye zapiski Gor'kovskogo universiteta no. 148, 1972, 108-127. (LZhS, 8/73, no. 24839)

v. Superconductivity

Agranovich, V. M., and Yu. Ye. Lozovik. Semiconductor-to-metal transition from the effect of electrostatic imaging. ZhETF P, v. 17, no. 1, 1973, 209-212.

Agranovich, V. M., A. G. Mal'shukov, and M. A. Mekhtiyev. Exciton and molecular spectra of organometallic compounds. IAN Fiz, no. 2, 1973, 324-328.

Baranov, I. A., V. F. Vasil'chenko, G. A. Kupchinova, and N. F. Kupchinov. Effect of intrinsic magnetization of winding material on field distribution in a superconducting solenoid. PTE, no. 1, 1973, 222-224.

Bobrov, V. S., and E. Yu. Gutmanas. Temperature dependence of variations in the plastic deformation rate of lead in superconducting junctions. ZhETF P, v. 17, no. 3, 1973, 137-140.

Bogomolov, V. N., and N. A. Klushin. Moessbauer effect and tin and gallium superconductivity in a porous glass. FTT, no. 2, 1973, 514-518.

Bondarev, B. I., V. V. Kushin, B. P. Murin, L. Yu. Solov'yev, and A. P. Fedotov. Focusing superconducting solenoids in high energy proton linear accelerators. AE, v. 34, no. 2, 1973, 131-133.

Didenko, A. N., and Yu. G. Shteyn. Stability specifications for parameters of travelling wave superconducting resonators. RiE, no. 3, 1973, 624-625.

Dubrovskaya, L. B., and I. I. Matveyenko. Electron structure and physical properties of transition metal carbides and nitrides with an NaCl structure. IN: Sb. Elektronnyye stroyeniye i fizicheskiye svoystva tverdogo tela, Kiyev, Izd-vo Naukova dumka, part 2, 1972, 67-76. (RZhKh, 4/73, no. 4B543)

Formozov, B. N. Critical parameters of superconducting films. IN: Sb. Elektronnaya tekhnika. Elektron. SVCH, no. 9, 1972, 24-28. (RZhRadiot, 2/73, no. 2Ye323)

Genkin, V. M. Raman scattering in superconductors. IN: Sb. VI Vsesoyuznaya konferentsiya po nelineynoy optike, Minsk, 1972, 227. (RZhRadiot, 2/73, no. 2Ye322)

Grinev, G. G., V. I. Kurochkin, I. F. Vatulin, V. A. Yadroshnikov, A. G. Demishev, and V. V. Permyakov. The SM-72 apparatus for generating a strong magnetic field. PTE, no. 1, 1973, 277.

Kadykova, G. N. Structure and properties of Ti-Nb superconducting alloys. MiTOM, no. 2, 1973, 28-32.

Kaplunov, M. G., D. N. Fedutin, M. L. Khidekel', I. F. Shchegolev, E. B. Yagubskiy, and R. B. Lyubovskiy. Study of potential organic superconductors. II. Comparative effect of cation geometry and electron polarity on the conductivity of 7,7,8,8-tetracyanoquinic dimethane ion-radical complexes. Zhurnal obshchey khimii, v. 42, no. 10, 1972, 2295-2301. (RZhKh, 5/73, no. 5B565)

Kvet, K. Cryoconductors and superconductors. Energetika (CSSR), v. 22, no. 9, 1972,393-398. (RZhRadiot, 2/73, no. 2Ye304)

Landau, I. L. Paramagnetic effects in type I superconductors. ZhETF, v. 64, no. 2, 1973, 557-567.

Lazarev, B. G., V. S. Kogan, I. S. Martynov, and A. L. Seryugin. Electron microscopic analysis of wire structures made from the type 60T superconducting alloy. FMM, no. 1, 1973, 221-224.

Lorkovskiy, Kh. D. Ferrocene polymers. Vysokomolekulyarnyye soyedineniya, no. 2, 1973, 314-326.

Ovchinnikov, Yu. N. Fluctuating shifts of transition temperature in thin superconducting films. ZhETF, v. 64, no. 2, 1973, 719-724.

Ryabov, B. A., A. B. Ryabov, A. M. Petrov, and V. A. Gorshkov. Synthesis of superconducting suspensions with maximum lift. IVUZ Priboro, no. 12, 1972, 75-80.

Takacs, S., and I. Hlasnik. Current distribution in a homogeneous type II superconducting cylinder. APP (A), v. A43, no. 2, 1973, 233-236

Valuyeva, N. A., I. V. Petrusevich, and L. A. Nisel'son. Preparing niobium germanides by combined oxygen reduction of higher chlorides. NM, no. 12, 1972, 2083-2088.

Vatulin, I. F., V. I. Grineva, A. N. Melyus, S. I. Milyutin, and V. V. Permyakov. Apparatus for generating a strong magnetic field at room temperatures. PTE, no. 1, 1973, 276.

Yefetov, K. B. Mixed state structure of type II superconducting films in a perpendicular magnetic field. FTT, no. 2, 1973, 647-649.

Zabrodin, V. A., I. S. Krainskiy, V. B. Nazarov, and L. N. Gal'perin. Suppression of sidebands from specimen rotation in a high resolution NMR spectrometer with a superconducting magnet. PTE, no. 1, 1973, 220-221.

vi. Epitaxial Films

Aleksandrov, L. N., V. M. Zaletin, E. A. Krivorotov, and Yu. G. Sidorov. Chemical decoration and narrow-angle shadowing study of GaAs epitaxial film surface growth. PSS(a), v. 15, 1973, 367-370.

Aleksandrova, G. A., V. A. Vil'kotskiy, B. V. Kornilov, L. V. Marchukov, and I. M. Skvortsov. Correlation between electron mobility and cathode luminescence spectra in gallium arsenide epitaxial layers. FTP, no. 2, 1973, 270-274.

Azimov, S. A., M. M. Mirzabayev, K. Rasulov, and M. N. Tursunov. Dislocation formation in the base region of multilayer structures from epitaxial and diffusion processing. IAN Uzb, Seriya fiz-mat nauk, no. 1, 1973, 76-77.

Bulatov, O. S., A. V. Cherepovskaya, and V. A. Antonov. Effects of anisotropy during selective growth of GaAs layers. NM, no. 2, 1973, 186-189.

Buyko, L. D., P. P. Goydenko, and V. M. Koleshko. Control of epitaxial and dielectric film thickness in spectrophotometers. PTE, no. 1, 1973, 266-267.

Deryagin, B. V., and D. V. Fedoseyev. Diamond whisker and isometric crystals. Novoye v zhizni, nauke, tekhnike, Seriya khimiya, no. 2, 1973, 33-39.

Ibid. Growth of diamond films. Novoye v zhizni, nauke, tekhnike, Seriya khimiya, no. 2, 1973, 24-32.

Ismailov, I., A. Sadiyev, M. Amonov, V. Dubrov, and S. Vakhidova. Electroluminescence of epitaxial p-n structures from $In_{1-x}Ga_xP$ solid solutions. FTP, no. 2, 1973, 415-417.

Kal'nin, A. A., N. A. Smirnova, and Yu. M. Tayrov. Liquid phase epitaxial growth of SiC layers. NM, no. 2, 1973, 319-320.

Koshkin, L. I. Crystallization kinetics of epitaxial ferrite films. IN: Nauchnyye trudy. Kuybyshevskiy gosudarstvennyy pedogogicheskiy institut, no. 104, 1972, 3-15. (RZhKh, 4/73, no. 4B830)

Ksendzov, Ya. M., L. M. Sapozhnikova, and S. A. Semenkovich. Preparing cobalt epitaxial films. NM, no. 2, 1973, 317-318.

Lavrent'yeva, L. G., M. D. Vilisova, I. V. Ivonin, L. M. Krasil'nikova F. A. Kuznetsov, Yu. M. Rumyantsev, and M. P. Yakubenya. Study of transition layers in epitaxial gallium arsenide. Micromorphology and electron distribution in layers as a function of growth rate in an iodide system. IVUZ Fiz, no. 2, 1973, 63-69.

Muszunski, Z. Optimum kinetics and epitaxial growth conditions for gallium arsenide from the liquid phase. Electron technol., v. 5, no. 1, 1972, 23-33. (RZhKh, 5/73, no. 5L98)

Okunev, V. D., and V. I. Gaman. Effect of natural recombination radiation on photo emf development in GaAs p-n junctions. RiE, no. 2, 1973, 138-

Problemy epitaksii poluprovodnikovykh plenok (Problems in semiconductor film epitaxy). Novosibirsk, Izd-vo Nauka, 1972, 226 p. (RBL, 12/72, no. 515)

Sytenko, T. N., V. I. Lyashenko, I. P. Tyagul'skiy, and V. Ya. Shapoval. Low temperature surface properties of p-type gallium arsenide epitaxial films. FTP, no. 2, 1973, 365-370.

Vedenev, A. P. Complex dielectric constant of single crystal Mg-Mn ferrite epitaxial films. IN: Nauchnyye trudy. Kuybyshevskiy gosudarstvennyy pedagogicheskiy institut, no. 104, 1972, 108-113. (RZhKh, 5/73, no. 5B567)

Zotov, V. V., M. I. Ovsyannikov, Yu. A. Romanov, and V. N. Shabanov. Properties of silicon epitaxial varicaps prepared by vacuum sublimation. IN: Uchenyye zapiski Gor'kovskogo universiteta, no. 148, 1972, 87-91. (LZhS, 8/73, no. 25834)

6. Miscellaneous Interest

A. Abstracts

Monin, A. An era of marine science (Soviet and East European Cooperation and Plans in Oceanography Discussed by Director of USSR's Institute of Oceanology). Literaturnaya gazeta, 9 May 1973, p. 13, cols. 6-8.

The Director of the USSR's Institute of Oceanology, A. S. Monin, discusses Soviet and East European cooperation in ocean research in a recent issue of Literaturnaya Gazeta. According to Monin, the Board of Representatives from five member countries of the Council of Mutual Economic Assistance (Bulgaria, East Germany, Poland, Rumania, and the Soviet Union) met recently in Gdynia, Poland. The Board of Representatives was appointed last year to resolve one of the points agreed to in the "General Program of Socialist Economic Integration", specifically, the resolution on "The Study of the Chemical, Physical, Biological, and Other Processes of the Major Areas of the World Ocean". The Board is also responsible for overseeing the activities of the International Coordinating Center which has been set up within the framework of the Institute of Oceanology of the USSR. Some representative institutions involved in the joint oceanographic research programs are: the Center for Scientific Research and Planning for the Fishing Industry (Bulgaria); the Institute of Marine Science (East Germany); the Institute of Ocean Fisheries (Poland); the Institute of Marine Research (Rumania); the State Oceanographic Institute of the USSR Hydrometeorological Service; and others.

Monin describes various joint research areas in general terms, citing global-scale air-sea interface studies, fish farming research, undersea mining, sedimentation, crustal origin, etc. Plans are presently under way for joint oceanographic cruises by the above countries in the Atlantic Ocean and the Baltic and Black Seas. The research programs are to be coordinated

by the International Coordinating Center. It is mentioned that the Soviet R/V Akademik Kurchatov and the East German R/V Alexander Humboldt will participate together in a program begun last year by Soviet, Polish, and East German scientists aboard the R/V Albrecht Penck (East Germany). Last year's program involved a month-long study of pollution levels in the Baltic Sea.

In concluding his article, Monin touches on "man-in-the-sea" research, stating that manned submersibles are the most effective research technique available to modern oceanography. Joint Soviet and East European man-in-the-sea research will be concentrated at an international oceanological research facility to be established probably at Varna, Bulgaria. This site was selected because the Black Sea is warmest in this area and the coast zone is highly suitable. The facility will be permanently staffed by specialists and divers from the five participating countries.

B. Recent Selections

Aliyev, Yu. M., and O. M. Gradov. Parametric excitation of surface waves in an inhomogeneous confined plasma. ZhTF, no. 2, 1973, 439-440.

Avaliani, D. I., and T. Sh. Zoidze. Light scattering in turbulent pulsations of a liquid. AN GruzSSR, Soobshcheniya, v. 69, no. 1, 1973, 125-127.

Bondarenko, I. M., A. A. Zagorodnikov, V. S. Loshchilov, and K. B. Chelyshev. Relationship of sea state parameters to spatial spectrum of aerial photographs and radar images of the sea surface. Okeanologiya, no. 6, 1972, 1099-1106.

Dolgopolov, V. V. Nonlinear standing Langmuir monochromatic waves in plasma. IN: Sb. Fizika plazmy i problemy upravleniya termoyadernogo sinteza, no. 3, 1972, 37-40. (RZhF, 11/72, no. 11G190)

Dymov, B. P., O. M. Kapliy, D. Yu. Stupin, and V. N. Tezikov. Pulsed source of a continuous spectrum for flash-photolysis. PTE, no. 1, 1973, 181.

Dzhuvarly, Ch. M., G. V. Vechkhayzer, and P. V. Leonov. Rotational temperature in an electric discharge confined by dielectric surfaces. ZhFKh, no. 2, 1973, 303-308.

Frolov, V. S. Elektronno-vychislitel'naya tekhnika v voyennom dele (Computers in military affairs). Moskva, Izd-vo DOSAAF, 1972, 126 p. (RBL, 12/72, no. 744)

Gavrilov, F. V., A. S. Myasnikov, G. G. Zhadan, G. S. Orlova, and M. V. Strokin. Results of flight tests of an ion engine model with cesium-on-tungsten surface ionization. Kosmicheskiye issledovaniya, no. 1, 1973, 140-144.

Kapitsa, P. L. Method of generating high temperature plasma. Otkr izobr, no. 6, 1973, no. 333889.

Kapitsa, P. L. Device for generating high temperature plasma. Otkr izobr, no. 6, 1973, no. 333890.

Korolyuk, A. P., and V. F. Roy. "Giant" oscillations of an electro-acoustic current. ZhETF P, v. 17, no. 4, 1973, 184-186.

Laser power launching of antimissile missiles. IN: Sb. Elektronnaya tekhnika, Nauchno-tekhnicheskiy sbornik. Elektronnaya SVCh, no. 9, 1972, 132-133. (RZhRadiot, 2/73, no. 2Ye212)(U. S. sources)

Rocket meridian (Launch of Soviet meteorological rockets from Kerguelen Island). Izvestiya, 7 March 1973, p. 4.

Pistrov, A. T., and S. P. Levitskiy. On the Squire theorem for a nematic liquid crystal layer flowing in an inclined plane. IN: Tr. NII Matematicheskogo Voronezhskogo universiteta, no. 6, 1972, 88-96. (RZhMekh, 2/73, no. 2B1274)

Polovin, R. V., and V. V. Rozhkov. Mathematical problems of stochastic processes in a plasma. IN: Sb. Fizika plazmy i problemy upravleniya termoyadernogo sinteza, no. 3, 1972, 67-69. (RZhF, 11/72, no. 11G200)

Popov, D. I. Threshold signals of a selection system for moving targets with amplitude limiting. Radiotekhnika, no. 2, 1973, 90-91.

Sonic Sun? (Sound-type waves in photographs of solar radiation). Komsomol'skaya pra[illegible], 3 March 1973, p. 4.

Tsivilev, M. P., et al. Chto nado znat' o vedenii spasatel'nykh i neotlozhnykh avariyno-vosstanovitel'nykh rabot v ochage yadernogo porazheniya (Na azerbaydzhanskom yazyke) (What one should know about rescue and emergency operations at the site of a nuclear explosion) (in Azerbaydzhani). Leningrad, Izd-vo Sudostroyeniye, 1972, 272 p. (RBL, 12/72, no. 975)

Velikhov, Ye. P., A. A. Vedenov, A. D. Bogdanets, V. S. Golubev, E. G. Kasharskiy, A. A. Kiselev, F. G. Rutberg, and V. V. Chernukha. Feasibility of generating megagauss magnetic fields using high pressure compressed gas linings. ZhTF, no. 2, 1973, 429-438.

Vinogradov, A. Lunokhod-2: a laboratory in the Sea of Tranquillity. Pravda, 11 February 1973, p. 3.

Vodyanitskiy, A. A., and N. S. Repalov. Three-dimensional echoes and nonlinear interactions in plasma. IN: Sb. Fizika plazmy i problemy upravleniya termoyadernogo sinteza, no. 3, 1972, 47-63. (RZhF, 11/72, no. 11G199)

Zakharov, A. I., I. G. Persiantsev, V. D. Pis'mennyy, A. V. Rodin, and A. N. Starostin. Theory of streamer breakdown. ZhPMTF, no. 1, 1973, 56-65.

7. SOURCE ABBREVIATIONS

AiT	-	Avtomatika i telemekhanika
APP	-	Acta physica polonica
DAN ArmSSR	-	Akademiya nauk Armyanskoy SSR. Doklady
DAN AzSSR	-	Akademiya nauk Azerbaydzhanskoy SSR. Doklady
DAN BSSR	-	Akademiya nauk Belorusskoy SSR. Doklady
DAN SSSR	-	Akademiya nauk SSSR. Doklady
DAN TadSSR	-	Akademiya nauk Tadzhikskoy SSR. Doklady
DAN UkrSSR	-	Akademiya nauk Ukrainskoy SSR. Dopovidi
DAN UzbSSR	-	Akademiya nauk Uzbekskoy SSR. Doklady
DBAN	-	Bulgarska akademiya na naukite. Doklady
EOM	-	Elektronnaya obrabotka materialov
FAiO	-	Akademiya nauk SSSR. Izvestiya. Fizika atmosfery i okeana
FGiV	-	Fizika goreniya i vzryva
FiKhOM	-	Fizika i khimiya obrabotka materialov
F-KhMM	-	Fiziko-khimicheskaya mekhanika materialov
FMiM	-	Fizika metallov i metallovedeniye
FTP	-	Fizika i tekhnika poluprovodnikov
FTT	-	Fizika tverdogo tela
FZh	-	Fiziologicheskiy zhurnal
GiA	-	Geomagnetizm i aeronomiya
GiK	-	Geodeziya i kartografiya
IAN Arm	-	Akademiya nauk Armyanskoy SSR. Izvestiya. Fizika
IAN Az	-	Akademiya nauk Azerbaydzhanskoy SSR. Izvestiya. Seriya fiziko-tekhnicheskikh i matematicheskikh nauk

IAN B	-	Akademiya nauk Belorusskoy SSR. Izvestiya. Seriya fiziko-matematicheskikh nauk
IAN Biol	-	Akademiya nauk SSSR. Izvestiya. Seriya biologicheskaya
IAN Energ	-	Akademiya nauk SSSR. Izvestiya. Energetika i transport
IAN Est	-	Akademiya nauk Estonskoy SSR. Izvestiya. Fizika matematika
IAN Fiz	-	Akademiya nauk SSSR. Izvestiya. Seriya fizicheskaya
IAN Fizika zemli	-	Akademiya nauk SSSR. Izvestiya. Fizika zemli
IAN Kh	-	Akademiya nauk SSSR. Izvestiya. Seriya khimicheskaya
IAN Lat	-	Akademiya nauk Latviyskoy SSR. Izvestiya
IAN Met	-	Akademiya nauk SSSR. Izvestiya. Metally
IAN Mold	-	Akademiya nauk Moldavskoy SSR. Izvestiya. Seriya fiziko-tekhnicheskikh i matematicheskikh nauk
IAN SO SSSR	-	Akademiya nauk SSSR. Sibirskoye otdeleniye. Izvestiya
IAN Tadzh	-	Akademiya nauk Tadzhiksoy SSR. Izvestiya. Otdeleniye fiziko-matematicheskikh i geologo-khimicheskikh nauk
IAN TK	-	Akademiya nauk SSSR. Izvestiya. Tekhnicheskaya kibernetika
IAN Turk	-	Akademiya nauk Turkmenskoy SSR. Izvestiya. Seriya fiziko-tekhnicheskikh, khimicheskikh, i geologicheskikh nauk
IAN Uzb	-	Akademiya nauk Uzbekskoy SSR. Izvestiya. Seriya fiziko-matematicheskikh nauk
IBAN	-	Bulgarska akademiya na naukite. Fizicheski institut. Izvestiya na fizicheskaya institut s ANEB
I-FZh	-	Inzhenerno-fizicheskiy zhurnal

IiR	-	Izobretatel' i ratsionalizator
ILEI	-	Leningradskiy elektrotekhnicheskiy institut. Izvestiya
IT	-	Izmeritel'naya tekhnika
IVUZ Avia	-	Izvestiya vysshikh uchebnykh zavedeniy. Aviatsionnaya tekhnika
IVUZ Cher	-	Izvestiya vysshikh uchebnykh zavedeniy. Chernaya metallurgiya
IVUZ Energ	-	Izvestiya vysshikh uchebnykh zavedeniy. Energetika
IVUZ Fiz	-	Izvestiya vysshikh uchebnykh zavedeniy. Fizika
IVUZ Geod	-	Izvestiya vysshikh uchebnykh zavedeniy. Geodeziya i aerofotos"yemka
IVUZ Geol	-	Izvestiya vysshikh uchebnykh zavedeniy. Geologiya i razvedka
IVUZ Gorn	-	Izvestiya vysshikh uchebnykh zavedeniy. Gornyy zhurnal
IVUZ Mash	-	Izvestiya vysshikh uchebnykh zavedeniy. Mashinostroyeniye
IVUZ Priboro	-	Izvestiya vysshikh uchebnykh zavedeniy. Priborostroyeniye
IVUZ Radioelektr	-	Izvestiya vysshikh uchebnykh zavedeniy. Radioelektronika
IVUZ Radiofiz	-	Izvestiya vysshikh uchebnykh zavedeniy. Radiofizika
IVUZ Stroi	-	Izvestiya vysshikh uchebnykh zavedeniy. Stroitel'stvo i arkhitektura
KhVE	-	Khimiya vysokikh energiy
KiK	-	Kinetika i kataliz
KL	-	Knizhnaya letopis'
Kristall	-	Kristallografiya
KSpF	-	Kratkiye soobshcheniya po fizike

LZhS	-	Letopis' zhurnal'nykh statey
MiTOM	-	Metallovedeniye i termicheskaya obrabotka materialov
MP	-	Mekhanika polimerov
MTT	-	Akademiya nauk SSSR. Izvestiya. Mekhanika tverdogo tela
MZhiG	-	Akademiya nauk SSSR. Izvestiya. Mekhanika zhidkosti i gaza
NK	-	Novyye knigi
NM	-	Akademiya nauk SSSR. Izvestiya. Neorganicheskiye materialy
NTO SSSR	-	Nauchno-tekhnicheskiye obshchestva SSSR
OiS	-	Optika i spektroskopiya
OMP	-	Optiko-mekhanicheskaya promyshlennost'
Otkr izobr	-	Otkrytiya, izobreteniya, promyshlennyye obraztsy, tovarnyye znaki
PF	-	Postepy fizyki
Phys abs	-	Physics abstracts
PM	-	Prikladnaya mekhanika
PMM	-	Prikladnaya matematika i mekhanika
PSS	-	Physica status solidi
PSU	-	Pribory i sistemy upravleniya
PTE	-	Pribory i tekhnika eksperimenta
Radiotekh	-	Radiotekhnika
RiE	-	Radiotekhnika i elektronika
RZhAvtom	-	Referativnyy zhurnal. Avtomatika, telemekhanika i vychislitel'naya tekhnika
RZhElektr	-	Referativnyy zhurnal. Elektronika i yeye primeneniye

RZhF	-	Referativnyy zhurnal. Fizika
RZhFoto	-	Referativnyy zhurnal. Fotokinotekhnika
RZhGeod	-	Referativnyy zhurnal. Geodeziya i aeros"-yemka
RZhGeofiz	-	Referativnyy zhurnal. Geofizika
RZhInf	-	Referativnyy zhurnal. Informatics
RZhKh	-	Referativnyy zhurnal. Khimiya
RZhMekh	-	Referativnyy zhurnal. Mekhanika
RZhMetrolog	-	Referativnyy zhurnal. Metrologiya i izmeritel'naya tekhnika
RZhRadiot	-	Referativnyy zhurnal. Radiotekhnika
SovSciRev	-	Soviet science review
TiEKh	-	Teoreticheskaya i eksperimental'naya khimiya
TKiT	-	Tekhnika kino i televideniya
TMF	-	Teoreticheskaya i matematicheskaya fizika
TVT	-	Teplofizika vysokikh temperatur
UFN	-	Uspekhi fizicheskikh nauk
UFZh	-	Ukrainskiy fizicheskiy zhurnal
UMS	-	Ustalost' metallov i splavov
UNF	-	Uspekhi nauchnoy fotografii
VAN	-	Akademiya nauk SSSR. Vestnik
VAN BSSR	-	Akademiya nauk Belorusskoy SSR. Vestnik
VAN KazSSR	-	Akademiya nauk Kazakhskoy SSR. Vestnik
VBU	-	Belorusskiy universitet. Vestnik
VNDKh SSSR	-	VNDKh SSSR. Informatsionnyy byulleten'
VLU	-	Leningradskiy universitet. Vestnik. Fizika, khimiya
VMU	-	Moskovskiy universitet. Vestnik. Seriya fizika, astronomiya

ZhETF	-	Zhurnal eksperimental'noy i teoreticheskoy fiziki
ZhETF P	-	Pis'ma v Zhurnal eksperimental'noy i teoreticheskoy fiziki
ZhFKh	-	Zhurnal fizicheskoy khimii
ZhNIPFiK	-	Zhurnal nauchnoy i prikladnoy fotografii i kinematografii
ZhNKh	-	Zhurnal neorganicheskoy khimii
ZhPK	-	Zhurnal prikladnoy khimii
ZhPMTF	-	Zhurnal prikladnoy mekhaniki i tekhnicheskoy fiziki
ZhPS	-	Zhurnal prikladnoy spektroskopii
ZhTF	-	Zhurnal tekhnicheskoy fiziki
ZhVMMF	-	Zhurnal vychislitel'noy matematiki i matematicheskoy fiziki
ZL	-	Zavodskaya laboratoriya

8. AUTHOR INDEX